Stochastic model predictive control of a set of electric vehicle charging stations for demand response service provision

Kovačević, Marko

University of Zagreb

FACULTY OF ELECTRICAL ENGINEERING AND COMPUTING

Marko Kovačević

STOCHASTIC MODEL PREDICTIVE CONTROL OF A SET OF ELECTRIC VEHICLE CHARGING STATIONS FOR DEMAND RESPONSE SERVICE PROVISION

DOCTORAL THESIS

Zagreb, 2023.

University of Zagreb

FACULTY OF ELECTRICAL ENGINEERING AND COMPUTING

Marko Kovačević

STOCHASTIC MODEL PREDICTIVE CONTROL OF A SET OF ELECTRIC VEHICLE CHARGING STATIONS FOR DEMAND RESPONSE SERVICE PROVISION

DOCTORAL THESIS

Supervisor: Professor Mario Vašak, PhD

Zagreb, 2023

Sveučilište u Zagrebu

FAKULTET ELEKTROTEHNIKE I RAČUNARSTVA

Marko Kovačević

STOHASTIČKO MODELSKO PREDIKTIVNO UPRAVLJANJE SKUPOM PUNIONICA ELEKTRIČNIH VOZILA ZA PRUŽANJE USLUGE ODZIVA POTROŠNJE

DOKTORSKI RAD

Mentor: Prof. dr. sc. Mario Vašak

Zagreb, 2023.

Doctoral thesis is made at the University of Zagreb Faculty of Electrical Engineering and Computing, Department of Control and Computer Engineering

Mentor: Professor Mario Vašak, PhD

Doctoral thesis contains 83 pages

Thesis no.: _____

About the Supervisor

Mario Vašak was born in Bjelovar in 1980. He received his BSc and PhD degrees in electrical engineering from University of Zagreb Faculty of Electrical Engineering and Computing (UNIZGFER), Croatia, in 2003 and 2007, respectively. He is currently a full professor at the Department of Control and Computer Engineering, UNIZGFER and he is heading its Laboratory for Renewable Energy Systems (LARES). His research interests are in the domain of dynamic systems predictive control with applications to systems from the low-carbon energy sector: wind turbines, energy-efficient buildings, microgrids, water distribution systems and electrified railway transport. He is the main inventor of the US patent for fault-tolerant control of wind turbine generators. He designed the concept of hierarchical and modular energy management in buildings with integrated microgrids for enabling their economically optimal interoperation. He had a leading or collaborator role on several research projects funded by the European Union or Croatian national funds related to implementation of this concept and its verification from the level of consumption control in individual buildings to the level of coordination of infrastructure and buildings in the smart city environment. He is the author or co-author of more than 25 papers in international scientific journals and overall of more than 200 internationally reviewed papers.

Prof. Vašak is a member of professional associations IEEE and the Croatian Society for Communications, Computing, Electronics, Measurements and Control (KoREMA). He has received more than 10 different acknowledgements and awards for his scientific and professional achievements. The following ones are highlighted: 2022 Fran Bošnjaković prize awarded by University of Zagreb, 2019 Prize for Science of UNIZGFER, 2008 Croatian state annual prize for young scientists in the field of technical sciences, Vera Johanides Award of the Croatian Academy of Engineering, Josip Lončar Silver Plaque of UNIZGFER, Končar Award for Doctoral Thesis with application in industry, and Top Scholarship for Top Students 2002.

O mentoru

Mario Vašak rođen je u Bjelovaru 1980. godine. Diplomirao je i doktorirao u polju elektrotehnike na Sveučilištu u Zagrebu Fakultetu elektrotehnike i računarstva (FER), 2003. odnosno 2007. godine. Trenutno je redoviti profesor na Zavodu za automatiku i računalno inženjerstvo na FERu gdje vodi Laboratorij za sustave obnovljivih izvora energije (LARES). Njegovi istraživački interesi su u domeni prediktivnog upravljanja dinamičkim sustavima s primjenama na sustave iz niskougljičnog energetskog sektora: vjetroagregate, energetski učinkovite zgrade, mikromreže, vodoopskrbne sustave i elektrificirani željeznički promet. Glavni je izumitelj US patenta za upravljanje vjetroagregatima otporno na kvarove generatora. Osmislio je koncept hijerarhijskog i modularnog gospodarenja energijom u zgradama s integriranim mikromrežama za omogućavanje njihova ekonomski optimalnog međudjelovanja. Vodio je ili surađivao na nekoliko istraživačkih projekata financiranih sredstvima Europske unije ili nacionalnim sredstvima vezanih uz implementaciju navedenog koncepta te njegovu provjeru od razine upravljanja potrošnjom u pojedinim zgradama do razine koordinacije sustava distribucije električne energije i vode u okruženju naprednog (pametnog) grada. Autor je više od 25 radova u međunarodnim znanstvenim časopisima te ukupno više od 200 međunarodno recenziranih radova.

Prof. Vašak član je stručnih udruga IEEE i Hrvatskog društva za komunikacije, računarstvo, elektroniku, mjerenja i upravljanje (KoREMA). Primio je više od 10 različitih priznanja i nagrada za svoj znanstveni i stručni rad. Među ostalima ističu se: Nagrada Fran Bošnjaković Sveučilišta u Zagrebu 2022. godine, Nagrada za znanost FERa za 2019. godinu, Godišnja državna nagrada znanstvenim novacima u području tehničkih znanosti za 2008. godinu, Vera Johanides nagrada Akademije tehničkih znanosti Hrvatske, srebrna plaketa "Josip Lončar" FERa, nagrada koncerna Končar za doktorsku disertaciju s primjenom u industriji te Top stipendija za top studente 2002.

Acknowledgements

My belief is that we were put into this world of wonders and beauty with a special ability to appreciate them, in some cases to have the fun of taking a hand in developing them, and also in being able to help other people instead of overreaching them and, through it all, to enjoy life – that is, to be happy.

Robert Baden-Powell

The journey begun a long time ago. The first to cherish my curiosity were mom Iva and dad Iver. Especially through student days, they gave me joy-full time exploring my profession, which I am thankful for.

Through all my education, many teachers, professors and mentors supported me. In the elementary school the first mentor in my scientific career was my teacher Anica Kroflin who introduced the beauty of mathematics to me. She was followed by Mirjana Perišić, Radojko Orlić, Suzana Fajdetić, Rajka Klicper and Sanja Ilčić who watered my curiosity and supported me on the beginning of my scientific and engineering journey. During high school, my math and engineering skills were developed under the supervision of Buga Mikšić in XV. Gymnasium and Damir Hržina and Ivan Romštajn from Zagreb Observatory.

Thanks to my mentors, although in nonscientific fields, Boris, Davorina and Eko, who gave me significant confidence and self-esteem. They taught me to pursue my ideas and passionately fight obstacles.

To my wingmen Mikić, Malenica and Štambuk during numerous flights into dreaming of what is possible and what could be our next project.

To prof. Zdenko Kovačević who recognised potential in my master thesis which seeded in me the idea of academic career.

Special thanks to my supervisor prof. Mario Vašak for the support. He always found time for my questions and every time had a passionate idea or suggestion. Thank you professor for the passion about all your research and transferring it on me.

To Nikola, Branimir, Hrvoje, Anita and Vinko for the countless hours of discussions, advises and motivation. Maybe more important, for making our LARES warm and happy environment. Thanks to the rest of the department for making these four years a wonderful experience.

And to my Julija, there are no words to thank for all the patience, support, understanding and love.

Abstract

Stochastic model predictive control of a set of electric vehicle charging stations for demand response service provision

Charging electric vehicles (EVs), whose number is increasing, is a great challenge for the power grid due to the charging load variability. Coordinated charging and schedule optimisation with seized demand response opportunities are well-known conceptual solutions to that. Still, there are two challenges for the implementation. The first is to adequately predict availability and parameters of electric vehicles which is crucial for determining the charging schedule and the demand response potential. The second challenge is charging schedule optimisation that addresses the uncertainty ensuring the feasibility and economic benefits.

This thesis proposes a method to represent a population of electric vehicles that on the one hand enables prediction via machine learning and on the other it enables an accurate optimisation of the charging schedule and demand response ability. The method essence is to use five discrete-time signals spanned over a prediction horizon period which are related to envelopes of feasible charging power and charging states for the EV population on that horizon. A robust conversion of any sequence of these signals into individual EVs data is also introduced. It enables to pose and solve the optimisation problem of charging scheduling with included demand response for a predicted population in the introduced representation.

The aggregated representation is a foundation of the proposed charging scheduling framework that includes day-ahead flexibility analysis based on historical data, short-term forecasting of EV arrivals and finally stochastic model predictive control of EV charging. The historical dataset is transformed to the aggregated representation, and it is analysed and used for training of two gradient boosting models for the short-term prediction. Day-ahead flexibility analysis based on chance-constraints enables the aggregator to influence the certainty of fulfilling contracted flexibility.

Keywords: electric vehicles, EV aggregator, demand response, tertiary frequency regulation, stochastic model predictive control, linear optimisation, chance-constraints, aggregated EV representation, Light gradient boosting machine, Extreme gradient boosting

Sažetak

Stohastičko modelsko prediktivno upravljanje skupom punionica električnih vozila za pružanje usluge odziva potrošnje

Izvorno, proizvodna strana elektroenergetske mreže uglavnom je bila upravljiva i igrala je ključnu ulogu u održavanju ravnoteže sustava. No, s elektrifikacijom naših života i promjenama u navikama, raste potrošnja sustava i povećava se njena varijabilnost. Primjer toga su brzi punjači elektičnih vozila snage od 50 ili 100 kW koji se koriste za vozila u vrlo kratkom vremenskom roku. S druge strane, proizvodnja postaje neupravljiva i sve varijabilnija zbog upotrebe solarne energije i energije vjetra, koje su snažno ovisne o vremenskim uvjetima. Svi ovi trendovi predstavljaju značajan izazov za elektroenergetsku mrežu.

Rastući broj električnih vozila (EV) bez koordiniranog rasporeda punjenja predstavlja prijetnju elektroenergetskim mrežama, uzrokujući nagle promjene opterećenja i dodatne troškove balansiranja sustava. Koordinirano punjenje EV-a ne samo da rješava ove probleme, već donosi dodatnu vrijednost elektroenergetskoj mreži putem pomoćnih usluga implementirajući odziv potrošnje (OP). Analiza podataka pokazuje da je prosječno vrijeme mirovanja EV-a (kada je priključeno, ali se ne puni) na javnoj punionici oko 4 sata, dok je u slučaju privatne punionice čak i duže. Ova činjenica nudi priliku za pružanje pomoćnih usluga, poput tercijarne regulacije frekvencije, bez ikakvog utjecaja na vlasnike EV-a. Naravno, nužno je prikupiti informacije o preferencijama vlasnika EV-a kako bi se izbjeglo njihovo nezadovoljstvo. Na temelju ovih informacija, agregator koji upravlja parkiralištem opremljenim punjačima EV-a može optimizirati raspored punjenja, što je ključno za učinkovit OP.

Fleksibilnost električnih vozila i njihov potencijalni doprinos različitim aspektima OP teško je kvantificirati. Autori istražuju fleksibilnost električnih vozila u smislu prijenosa opterećenja iz jednog intervala u drugi. Fleksibilnost se također izražava kao snaga koja se može smanjiti u određenom vremenskom razdoblju. Također se predlaže kvantitativna mjera, ali samo za izravnavanje opterećenja. Za potpunu implementaciju OP putem rasporeda punjenja potrebna je i analiza potencijala i metode određivanja rasporeda u stvarnom vremenu.

U ovom radu pretpostavlja se da agregator posjeduje informacije o svakom EV-u spojenom na punjač, uključujući relativni kapacitet baterije (koliko energije nedostaje do potpune napunjenosti), traženo konačno stanje napunjenosti, nominalnu maksimalnu snagu punjenja i predviđeno vrijeme odlaska EV-a. Ovi podaci mogu se prikupiti putem unosa vlasnika EV-a na parkirnom automatu, putem mobilne aplikacije ili putem buduće komunikacijske infrastrukture između vozila i mreže (punjača). S obzirom na pretpostavku

da će vlasnici vozila prilikom priključivanja na punjač dati ove informacije, jedino što nedostaje agregatoru su podaci za buduća vozila koja će doći na parkiralište kako bi imao potpuni opis zadataka punjenja i time definirani optimizacijski problem za određivanje rasporeda punjenja. Dva su ključna izazova za implementaciju koordiniranog punjenja električnih vozila koje je preduvjet za OP. Prvo je potrebno predvidjeti dolaske električnih vozila kako bi se optimizacijski problem mogao definirati. Drugi izazov je definirati sam problem optimizacije i riješiti ga.

Kao rješenje navedenih izazova, u ovome se radu predlaže cjeloviti koncept. Koncept se sastoji od tri koraka. Prvi korak je pronaći optimalni kapacitet regulacije frekvencije za ugovor s operatorom elektroenergetske mreže jedan dan unaprijed, a dobiva se rješavanjem optimizacijskog problema za prosječnu populaciju električnih vozila za određeni dan u tjednu, na temelju povijesnih podataka. Drugi i treći korak su dio modelskog prediktivnog upravljanja rasporedom punjenja u stvarnom vremenu. Drugi korak je predviđanje dolazaka električnih vozila, a treći korak je dobivanje optimalne energije punjenja za svako električno vozilo, priključeno na punjač, za naredni diskretni period.

Ključni element u ovim koracima je novouvedena agregirana reprezentacija populacija EV-a koja se sastoji od dva algoritma. Prvi transformira pojedinačne podatke o EV-ima u agregirani prikaz, a drugi čini suprotno, transformira agregirani prikaz natrag u pojedinačne podatke o EV-ima. Pojedinačni podaci koriste se za prikupljanje povijesnih podataka i za definiranje zadataka punjenja svakog EV-a, koji su dio optimizacijskog problema. Format agregiranog prikaza populacije električnih vozila koristi se za određivanje prosječne populacije u analizi dan unaprijed i za predviđanje budućih dolazaka električnih vozila.

Predloženi cjeloviti koncept upravljanja rasporedom punjenja skupom punjača postupno se definira kroz četiri poglavlja u ovoj doktorskoj disertaciji. Njima prethodi prvo, uvodno poglavlje u kojem se izlaže motivacija i kratki pregled trenutnog stanja područja istraživanja.

U Poglavlju 2. *Dan-unaprijed analiza fleksibilnosti* (*Day-ahead flexibility analysis*) uvode se funkcija cilja i ograničenja za optimizacijski problem pružanja usluge tercijarne regulacije frekvencije, te se ovaj optimizacijski problem definira u determinističkom i stohastičkom okruženju. Temelj optimizacijskog problema je jednostavan model agregatora koji se koristi i u Poglavlju 3. za modelsko prediktivno upravljanje u stvarnom vremenu. S dostupnim pojedinačnim podacima o dolascima i karakteristikama EV-a, svaki zadatak punjenja duž optimizacijskog horizonta je u potpunosti opisan i može se vizualizirati s envelopom punjenja. Granice enevelope sastoje se od trajektorija punjenja u načinu što je prije moguće i u načinu što je kasnije moguće. Svaki punjač s priključenim EV-om modeliran je s pripadajućim stanjem energije kao varijablom stanja te energijama pun-

jenja i pražnjenja kao upravljačkim varijablama. Sve tri varijable su naravno ograničene fizičkim ograničenjima koja proizlaze iz pojedinačnih podataka o EV-ima.

Funkcija troška, koju se minimizira u optimizacijskom problemu, sastoji se od nekoliko dijelova koji se odnose na različite dimenzije OP. Glavna varijabla funkcije troška je ukupna razmjena energije s mrežom koja je jednaka zbroju svih energija punjenja umanjenom za zbroj svih energija pražnjenja. Jedan dan unaprijed agregator sudjeluje na tržištu električne energije gdje kupuje energiju prema planiranom profilu potrošnje za sljedeći dan. Sljedeći dan agregator koristi kupljenu energiju i na kraju dana biva kažnjen za odstupanja od planiranog profila potrošnje. Agregator također daje ponude operatoru prijenosnog sustava na tržištu kapaciteta za regulaciju frekvencije za dan unaprijed. Ako je ponuda prihvaćena, agregator biva financijski nagrađen i mora biti u mogućnosti ispuniti ugovoreni kapacitet sljedeći dan u slučaju da bude aktiviran. U slučaju aktivacije, agregator je dodatno nagrađen za isporučenu regulacijsku energiju. Regulacijska snaga (kapacitet) ugovara se za svaki sat zasebno. Minimalna vremenska razlika između dvije uzastopne aktivacije je 8 h. Optimizacijski problem sadrži zaseban profil - zasebne varijable upravljanja i stanja, za svaki mogući slučaj aktivacije. Budući da su vrijeme i iznos aktivacije poznati agregatoru samo 15 minuta unaprijed, svi "alternativni" profili ili scenariji za različite slučajeve aktivacija moraju biti jednaki scenariju bez aktivacije do tog diskretnog vremenskog intervala. Taj tzv. „nominalni" profil potrošnje bit će deklariran mreži kao planirani profil za sljedeći dan. Nominalni profil tada je referenca za mjerenje smanjenja potrošnje u slučaju aktivacije. Optimizacijski problem spada u klasu minimizacije najgoreg troška što znači da konačnoj funkciji troška doprinosi samo onaj scenarij s najvišim operacijskim troškom. Osim OP, funkcija troška pokriva i penalizaciju degradacije baterije. Samo se pražnjenje kažnjava, i to troškom cijelog ciklusa punjenja, što uključuje i degradaciju baterije uzrokovanu dodatnim punjenjem.

Tržište kapaciteta regulacije frekvencije funkcionira po principu dražbe stoga je neizvjesno hoće li ponuđeni kapacitet biti ugovoren. Optimizacijski problem minimizira konačni trošak koji uključuje nagradu za ugovoreni kapacitet fleksibilnosti što može rezultirati time da nominalni scenarij bez aktivacije ne puni električna vozila u potpunosti u intervalima niže cijene električne energije, a sve kako bi se prilagodio i omogućio veću fleksibilnost agregatora. Budući da financijska nagrada za prilagodbu nije zajamčena, izlazak nominalnog scenarija iz vlastite financijski optimalne točke mogući je financijski gubitak za agregatora. Kako bi se taj potencijalni gubitak stavio pod kontrolu, prvi korak analize fleksibilnosti jest izračun optimalnog troška nominalnog scenarija bez razmatranog ugovoranja fleksibilnosti. Drugi korak je određivanje optimalnog rasporeda punjenja uz financijski optimalno ugovaranje fleksibilnosti pod uvjetom da ukupni trošak scenarija bez aktivacije ne smije biti veći od nominalnog scenarija iz prvog koraka, uvećanog za određeni

iznos koji je agregator spreman riskirati u slučaju da ponuda ne bude prihvaćena.

Za slučaj stohastičkog okruženja izvedena su šansna ograničenja (engl. chance constraints) iz ograničenja za klasični agregirani prikaz skupine vozila pomoću modela agregirane baterije. Uvedena je efektna mjera za nesigurnosti procesa punjenja vozila u agregiranom modelu s jednim spremnikom putem razlika envelopa najranijeg i najkasnijeg punjenja vozila te se takva ograničenja uvode u preostali problem planiranja rada sustava većeg broja punionica.

Poglavlje 3. *Stohastičko modelsko prediktivno upravljanje punjenja električnih vozila* (*Stochastic model predictive control of EV charging*) pokazuje način implementacije prediktivnog upravljanja odnosno principa pomičnog horizonta uz osiguranje da sustav punionica ostvaruje fleksibilnost na poziv iz elektroenergetskog sustava na optimalan način. Pritom se opet prikazuje način rada i u determinističkom problemu prediktivnog upravljanja, kako bi se mogla napraviti odgovarajuća usporedba pristupa. Optimizacijski problem modelskog prediktivnog upravljanja temeljen je na problemu definiranom u sklopu analize fleksibilnosti dan unaprijed, uz manje izmjene. Funkcija troška više ne sadrži dijelove i odgovarajuća ograničenja vezana uz dan-unaprijed cijenu električne energije te uz nagradu za ugovoreni kapacitet regulacije frekvencije. Nadalje, kao referentni profil potrošnje i referenca za određivanje isporučene regulacijske energije koristi se već poznati profil koji je mreži deklariran dan prije.

Budući da optimizacijski problem uključuje i prognozirane dolaske EV-a, dan je algoritam koji raspoređuje dobivene optimalne energije punjena i pražnjenja na EV-a koja su došla u posljednjem diskretnom vremenskom intervalu za vrijeme kojeg se optimizacijski problem rješavao. Za kumulativnu distribuciju vjerojatnosti nužnu za šansna ograničenja koristi se kumulativna distribucija greške prediktivnog modela. Šansna ograničenja primjenjuju se samo na prognozirana EV-a budući da su podaci o već priključenim EV-ima deterministički.

Poglavlje 4. *Agregirana reprezentacija populacije električnih vozila* (*Aggregated representation of electric vehicles population*) uvodi ključan element za uspješnu implementaciju planiranog sustava, a to je ovom disertacijom uvedeni postupak putem kojeg se način zauzimanja i korištenja punjača na blisko ekvivalentan način transformira i prikazuje u agregiranom obliku kao pet vremenski diskretnih signala. Uvedena je i inverzna transformacija kojom se iz agregiranog prikaza pomoću 5 navedenih diskretnih signala dobije natrag originalna populacija vozila ili populacija sa svojstvima bliska originalnoj, posebice u smislu pružanja usluge OP. Prednosti metode agregirane reprezentacije u odnosu na ostale načine prikaza skupine EV-a su sljedeće:

- obuhvaća sposobnost populacije električnih vozila da sudjeluje u OP;
- može opisati bilo koju populaciju EV i univerzalna je;

- svako električno vozilo u populaciji može imati različitu nominalnu snagu punjenja, relativni kapacitet i vrijeme priključenosti na punjač.

Agregirana reprezentacija sastoji se od pet vremenski diskretnih vektora. Prva dva vektora daju informacije o promjenama svih maksimalnih snaga punjenja povezanih s dolaskom i odlaskom električnih vozila u određenom diskretnom vremenskom intervalu. Treći vektor sadrži informaciju o hipotetskom smanjenju snage punjenja zbog dostizanja kapaciteta baterije u slučaju što ranijeg (*as soon as possible*, eng.) načina punjenja i stoga implicitno sadrži informaciju o kapacitetu električnih vozila koja su dio populacije. Na sličan način, u slučaju što kasnijeg načina punjenja (*as late as possible*, eng.), punjenje bi se uključilo u točno određenom trenutku kako bi baterija bila napunjena točno prije odlaska vozila. Upravo ta uvećanja snaga punjenja zabilježena su u četvrtom vektoru. Posljednji vektor predstavlja kumulativnu snagu punjenja populacije EV-a u načinu kontinuiranog punjenja gdje se EV puni konstantnom snagom od prvog diskretnog vremenskog intervala nakon njegova dolaska pa sve do posljednjeg prije odlaska vozila. Za dokaz dobrog čuvanja informacije iz originalne populacije provedena je iscrpna studija slučaja nad dostupnim podatcima s dvaju parkirališta električnih vozila s punionicama u SAD-u. Pokazano je da uvedena metoda predstavljanja populacije električnih vozila vremenskim signalima vrlo vjerno čuva ponašanje modela s obzirom na fleksibilnost.

Konačno, Poglavlje 5. *Predviđanje agregirane reprezentacije električnih vozila korištenjem XGBoost i LightGBM* (*Prediction of aggregated EV representation using XGBoost and LightGBM*) uvodi načine podešavanja i strukture generičkih modela pomoću kojih je moguće predviđati uvedene vremenski diskretne signale za reprezentaciju populacije električnih vozila. Prikazano je pouzdano predviđanje do 2 sata unaprijed što se pokazalo već dovoljnim za implementaciju prediktivnog upravljanja skupom punjača električnih vozila na parkiralištu po principu pomičnog horizonta.

Predviđanja budućih dolazaka EV-a nužna su za primjenu MPC-a. Većina istraživanja usmjerena je na predviđanje agregiranog profila opterećenja. Za koordinirano planiranje punjena EV-a potrebno je imati zahtjeve za punjenje, a spomenuta predviđanja opterećenja korisna su samo za mrežnog operatera za planiranje uravnoteženja sustava i nisu prikladni za uvedeni MPC. Čest pristup koji jest prikladan za planiranje punjenja EV-a je predviđanje budućih količina određenih tipova EV-a koji se razlikuju prema stanju napunjenosti pri dolasku, kao i prema vremenu dolaska i odlaska. Loša strana tog pristupa je ograničenje na konačan broj tipova. Kako bi se izbjeglo tu prepreku, u ovome se poglavlju predviđa agregirana reprezentacija budućih električnih vozila.

Modeli strojnog učenja, poput Extreme Gradient Boosting (XGBoost) i Light Gradient Boosting Machine (LightGBM), trenutno su među najpopularnijim i najperspektivnijim alatima u području strojnog učenja. Ovi nadzirani algoritmi široko se primjenjuju u in-

dustriji i istraživanju. Oba algoritma temelje se na konceptu gradijentnog pojačanja, gdje je ključna ideja učenje niza slabih modela, poput logičkih stabala, te njihovo postupno poboljšavanje kako bi se formirao snažan i robustan model. Dobiveni rezultati uspoređeni su s dvije jednostavne metode predviđanja. Prva je prosjek radnih dana, a druga je konstantnost koja pretpostavlja da se predviđana vrijednost neće mijenjati. Kao metrika za učenje modela korišten je korijen srednje kvadratne pogreške, dok su za analizu također izračunate srednja prosječna pogreška i simetrična srednja apsolutna postotna pogreška. Općenito, oba modela strojnog učenja nadmašuju spomenute jednostavne metode. Iznimka je u usporedbi pomoću simetrične srednje apsolutne postotne pogreške, gdje je teško interpretirati metriku zbog velikog broja nul elemenata u vektorima koji se predviđaju. U usporedbi između XGBoost i LightGbm, LightGBM je nešto bolji.

Svaki dio predloženog koncepta upravljanja rasporedom punjenja je zasebno testiran na dostupnim podacima s Kalifornijskog tehnološkog instituta, SAD. Podaci sadrže informacija o punjenju električnih vozila na 50 punjača instaliranih na parkiralištu fakultetske zgrade te su i na taj način dimenzionirane studije slučaja u ovome radu. Unatoč tome, sve metode i analize primjenjive su i na veće sustave, sve do granica računalnih kapaciteta računala na kojima se rješavaju optimizacijski modeli.

Ključne riječi: električna vozila, agregator EV-a, odziv potrošnje, tercijarna regulacija frekvencije, stohastičko modelsko prediktivno upravljanje, linearna optimizacija, šansna ograničenja, agregirana reprezentacija EV-a, Extreme Gradient Boosting, Light Gradient Boosting Machine

Contents

Chapter 1

Introduction

Growing number of electrical vehicles (EVs) without coordinated charging scheduling is going to threat power grids through load and operation cost spikes [1], [2]. Coordinated EV charging does not only solve the mentioned problem [3], but it brings added value to the power grid via ancillary services through demand response (DR) [4]. Data analysis [5] shows that average idle time of an EV (EV connected and not being charged) connected to a public charging point is 4 h, and even more when connected to a private one. These facts bring an opportunity for offering demand response through ancillary services such as tertiary frequency regulation, without any disruption for the EV owner. Some information about EV owner's preferences is necessary to avoid his dissatisfaction. An aggregator that operates a parking lot equipped with EV charging points can use a data set that is valuable in prediction of EVs behaviour and energy demand which is crucial for effective DR [6]. Flexibility of EVs and potential contribution to any aspect of demand response is hard to quantify. Authors in [7] quantify EVs flexibility in terms of load shifting. Flexibility is expressed as a power that can be reduced at a certain time for a certain time interval. The same authors propose a quantifying measure in [8] but only for load flattening and load balancing. To fully implement DR through charging scheduling, both the analysis of DR potential [9] and real-time scheduling method are needed.

In this thesis the assumption is that the aggregator has information on relative battery capacity (how much energy till full battery) that is also the requested energy to deliver to the EV, and then further on maximal charging power and EV departure time of every connected parked EV. These data could be gathered via EV owner's input through parking machine, mobile application directly or through future vehicle-to-grid communication infrastructure. Considering such a setup, with the known on-arrival commitment [10] of both present and future EVs, the aggregator has the data which gives the full description of the EV charging sessions.

Machine learning models are commonly used for prediction of EVs load in the aspect

of uncoordinated charging [11], [12], but such information cannot be used for charging scheduling, only for the production side management of the power grid. Access to on-arrival data, and the prediction of it, allows the aggregator to optimally schedule EV charging and to participate in demand response including ancillary service to the grid. Charging scheduling is insofar limited to present EVs' data. Prediction of the EVs data that are yet to come increases the aggregator's scheduling capacity. The general idea in this thesis is to use machine learning for the prediction of the future availability of EVs and then to apply model predictive control to determine control signals i.e., charging powers for individual EVs.

The state-of-the-art misses a method to describe a population of heterogeneous EVs connected to charging stations that is suitable both for population prediction based on machine learning and for charging scheduling with demand response ability assessment. As a solution to the aforementioned challenges, this thesis proposes a complete concept of charging scheduling of EVs that are operated by the aggregator. Its main usage steps are shown in Fig. 1.1.

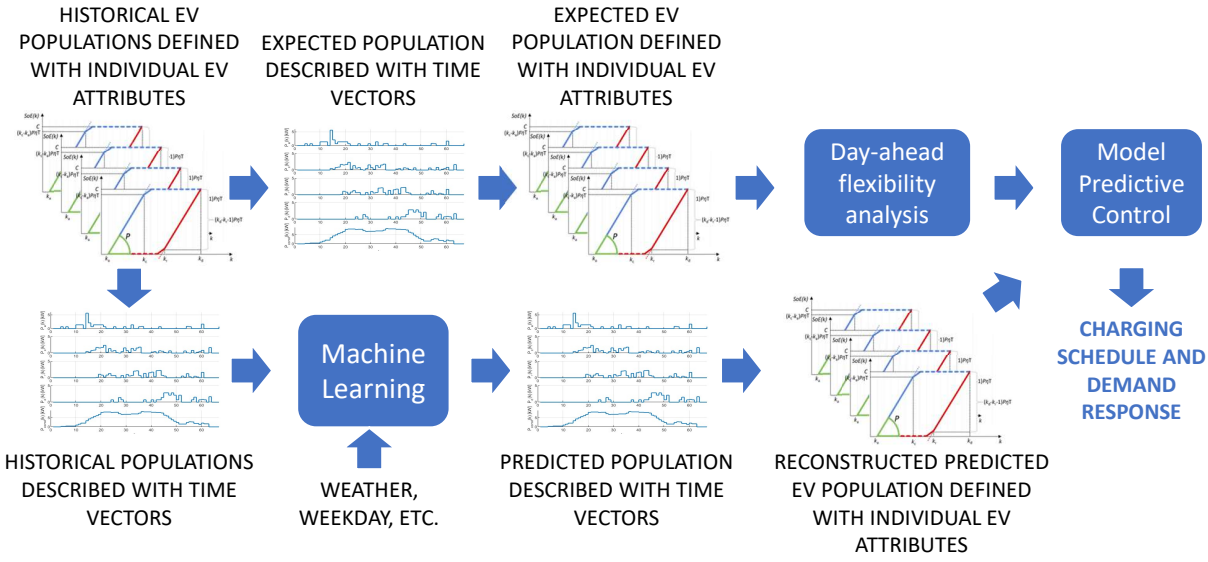

Figure 1.1: The proposed concept of charging scheduling of EVs that are operated by the aggregator [13].

The key element in these steps is the newly introduced aggregated representation of EV populations, which consists of two algorithms. The first transforms individual EV data into an aggregated view, and the second does the opposite, transforming the aggregated view back into individual EV data. The individual data is used to collect historical data and to define the charging tasks of each EV, which are part of the optimisation problem. The format of the aggregate representation of the population of electric vehicles is used to determine the average population in a day-ahead analysis and to predict future arrivals of electric vehicles.

Since parameters of future EVs are stochastic, it is reasonable to apply stochastic programming. Certainly, stochastic programming has conservatism and requires stronger computing resources thus it is a trade-off between these negative impacts and more reliable solutions. Most of the works dealing with it are based on stochastic programming described in [14] and some applied Sample Average Approximation Method [15] to reduce the number of possible scenarios. Choice of the appropriate approach is a trade-off between optimality and computing time. In this thesis, the approach with chance constraints is applied. Chance constraints were derived from the constraints for the classic aggregated battery model of a group of vehicles. An effective measure for the uncertainty of the vehicle charging process in the aggregated model with the aggregated state of energy is introduced by means of the difference of the upper and the lower bounds of the aggregated envelope, and such restrictions are introduced into the remaining problem of planning the operation of the system of a large number of filling stations

1.1 Contributions

The proposed research can be divided into four main parts that constitute the original scientific contribution. They are named and explained in the sequel.

(i) A method for aggregated representation of electric vehicles that generates discrete-time signals of powers related to vehicles charging envelopes which are suitable for demand response provision

An EV charging scheduling problem is defined with battery capacity, energy request, power of a battery converter, arrival time and departure time. To apply machine learning models for prediction, the data needs to be transformed in a time-series format. It is reasonable to focus on aggregated prediction of EVs since the aggregator is interested in total energy exchange with the power grid. At the same time individual constraints on EVs' batteries must not be neglected. The proposed method aggregatedly represents a population of EVs using a group of time-series data. Such representation can be predicted using machine learning model and transformed back to individual description to be used for charging schedule optimisation. Such approach captures flexibility of the EV population and gives credible information for demand response planning.

(ii) Artificial neural networks for stochastic prediction of the discrete-time signals of aggregated powers related to vehicles charging envelopes

ANNs and other machine learning models are a logical choice for predicting the mentioned set of time series data. Current trending models include light gradient boosting machine

(LightGBM) and extreme gradient boosting machine (XGBoost). Besides historical time series data realisation, presumed inputs to the model are time of day, day of week, day of year and weather. All these data should affect EVs owners' behaviour and directly influence the arrival pattern. One piece of the future time series are contributions of the already present EVs based of their on-arrival data. These contributions are also model inputs of interest. The machine learning models are trained and tested using a presently available real-world dataset [16].

(iii) A stochastic optimisation method for determining optimal day-ahead load and flexibility power profiles of a set of electric vehicles charging stations

Participating in demand response requires sending planned energy exchange profile to the power or distribution grid operator one day ahead. The sent profile is a reference next day for determining the aggregator's realisation of contracted amount of explicit demand response. Depending on the demand response scheme, the aggregator contracts flexibility power reserve with the grid one day ahead or on a weekly basis. The analysis is based on the average historical EV population for a certain weekday. Stochastic nature of the realisation of daily EV population is incorporated to optimisation problem using chance constraints. Such optimisation problem both maximises the expected aggregator's profit and guarantees fulfilling demand response according to the contract between the aggregator and the grid.

(iv) A stochastic model predictive control algorithm for real-time charging management of individual electric vehicles

The aggregator's real-time EV charging management is taking care about fulfilling all EVs' energy requests and the agreed obligations of the aggregate to the grid. The charging management is based on stochastic model predictive control (SMPC) in receding horizon manner. Since the optimisation problem also includes predicted arrivals of EVs, an algorithm is given that distributes the obtained optimal charging and discharging energies to the EVs that arrived in the last discrete time interval during which the optimisation problem was being solved.

1.2 Outline

The rest of the thesis is organised into five chapters. The day-ahead analysis of the EV population's flexibility capacity in Chapter 2 exploits the aggregated representation to obtain expected EV population used for the stochastic optimisation. The analysis provides the optimal flexibility capacity and the day-ahead energy consumption profile for the EV

aggregator which is required for the stochastic MPC algorithm given in Chapter 3 to enable real-time operation of the aggregator. The proposed aggregated representation of EV population is introduced in Chapter 4, including both algorithms for the construction of the aggregated representation and the reconstruction of the individual EV data. The proposed method is empirically proved to capture population's flexibility to offer demand response. Chapter 5 covers prediction of aggregated representation using machine learning models, necessary for model predictive control (MPC). Finally, general conclusions and future research opportunities are given in Chapter 6.

Chapter 2

Day-ahead flexibility analysis

There are two key challenges for the participation of the EV aggregator in frequency regulation - to ensure feasibility of contracted flexibility and to optimise long-term profit.

In this chapter, the proposed day-ahead analysis is introduced, as one part of the complete framework shown in Fig. 2.1. Feasibility is ensured using chance constraints that give measure of probability that some constraint will not be satisfied. Maximal long-term profit is obtained using statistical characteristics of the historical data which is described in Section 2.3. Furthermore, it must be assured that every scheduling scenario - without contracted flexibility and with contracted flexibility either with or without flexibility activation - is economically beneficial. The whole analysis algorithm is defined in the Section 2.4. The analysis of the results and discussion are given Section 2.5.

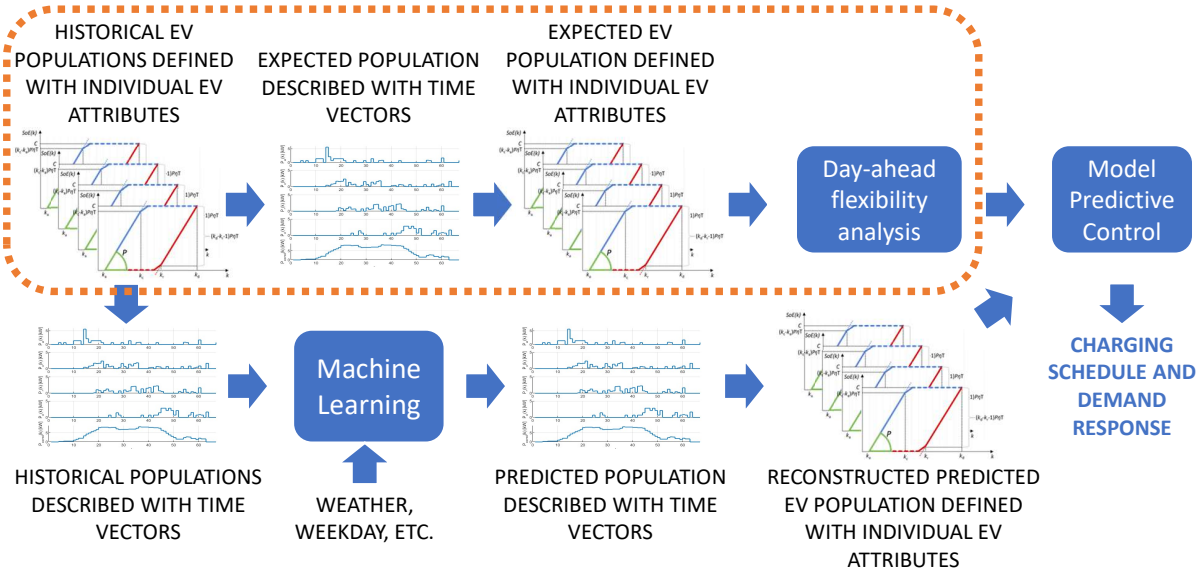

Figure 2.1: The proposed concept of EV charging scheduling exploiting historical data and aggregated representation.

The day-ahead flexibility analysis is carried out by solving linear optimisation problem which results in the optimal frequency regulation capacity to contract per every hour in

a day and the optimal overall energy consumption profile to declare to the power grid operator. Expected daily EV population is be obtained by summing all EV populations in the data sample from the historical data and then dividing by the number of days in the sample. This approach results in a big number of EVs in the average population which significantly increases the size of the optimisation problem. Solution to this problem is in the aggregated representation from Chapter 4 that enables us to reconstruct average individual population containing the acceptable number of EVs.

2.1 Aggregator and demand response model

The optimisation problem is an extension of the previous work introduced in [17] where a microgrid is replaced with n CPs, where n is always big enough to serve the whole population. Optimisation horizon is one day, from midnight to midnight, and starts and ends with the empty parking lot. The problem is solved one day-ahead to obtain optimal frequency regulation reserve power to contract with the transmission system operator. The purpose of the optimisation problem is to determine the frequency regulation power to contract with the power grid operator.

2.1.1 Charging point model

The 24-hours ahead scheduling problem engages n CPs, where n is equal to the maximum concurrent number of EVs in the population. In accordance with the elaboration in Section 3.2, number n could be even higher than the physically available number of CPs on the parking lot. Individual EV data necessary for the CP model consists of a set of parameters shown in Table 2.1, similar to [10].

Table 2.1: Set of parameters describing an individual EV (EV charging session)

P_{nom}	Maximum charging power of a charger or a battery
C	Relative energy capacity of the battery defined as the difference of the battery's nominal capacity and the state of energy at the arrival
k_{a}	The first discrete-time instant when EV charging is possible - the one after the arrival of the EV
k_{d}	Discrete-time instant of departure

A CP is modeled as a system with one state SoE_{cp} that is equal to zero when CP is not occupied. Otherwise, it is equal to the relative SoE of a connected EV, which is described as:

$$
\begin{gathered}
SoE_{cp}(k+1) = SoE_{cp}(k) + \eta_{\text{ch}} u_{\text{ch},cp}(k) - u_{\text{dch},cp}(k)/\eta_{\text{dch}}, \\
\forall k | k+1 \in \mathcal{O}_{cp}, \\
SoE_{cp}(k) = 0, \forall k | \begin{cases} k \in \mathcal{O}_{cp}, k-1 \in \mathcal{I}_{cp} \\ \text{or} \\ k \in \mathcal{I}_{cp} \end{cases},
\end{gathered} \tag{2.1}
$$

where k is discretisation 15-min interval, the index cp denotes a CP, $u_{\text{ch},cp}$ and $u_{\text{dch},cp}$ are charging and discharging energies of the CP, respectively, $\eta_{\text{ch}} = 0.9$ and $\eta_{\text{dch}} = 0.9$ are charging and discharging efficiency, respectively, $\mathcal{O}_{cp}$ is the set of time intervals in which the CP indexed with cp is occupied with an EV connected to the CP and $\mathcal{I}_{cp}$ is the set of time intervals when the CP is not occupied. It can be also seen that relative SoE is automatically initialised to zero at the arrival when the EV is connected to a CP. The value of the efficiency coefficients η_{ch} and η_{dch} are equal for all EVs since the predicted vehicle in the population is not made concrete (or personalised) and only represents a forthcoming generic charging task for the aggregator of the charging stations.

In the absence of an EV $u_{\text{ch},cp}(k)$ and $u_{\text{dch},cp}(k)$ must be zero. During an EV presence, the EV's battery charger defines power constraints:

$$
\begin{cases}
u_{\text{ch},cp}(k) + u_{\text{dch},cp}(k) \leq P_{\text{nom},i} T, \\
0 \leq u_{\text{ch},cp}(k) \leq P_{\text{nom},i} T, \\
0 \leq u_{\text{dch},cp}(k) \leq \begin{cases} 0, & \text{vehicle-to-grid disabled} \\ P_{\text{nom},i} T, & \text{vehicle-to-grid enabled} \end{cases},
\end{cases} \tag{2.2}
$$

where i denotes the corresponding EV connected to the charging point cp at the k^{th} discrete-time interval and T is discretisation time. EV relative battery capacity C_i constrains the CP state as follows:

$$
0 \leq SoE_{cp}(k) \leq C_i, \; k_{\text{a},i} \leq k < k_{\text{d},i}, \tag{2.3}
$$

$$
SoE_{cp}(k_{\text{d},i} - 1) + \eta_{\text{ch}} u_{\text{ch},cp}(k_{\text{d},i} - 1) - u_{\text{ch},cp}(k_{\text{d},i} - 1)/\eta_{\text{dch}} = \begin{cases} C_i, & k_{\text{d},i} \leq N, \\ C_i \frac{N - k_{\text{a},i}}{k_{\text{d},i} - k_{\text{a},i}} & k_{\text{d},i} > N. \end{cases} \tag{2.4}
$$

Constraint (2.4) ensures that EV_i leaves the parking lot with the battery charged to the

required level if the EV departs on the optimisation horizon. In the other case, when the EV departs outside of the horizon, the charging request is scaled proportionally to the ratio of the EV's staying time part on the horizon and the total staying time. Such approach 'fairly' allocates the charging task between the current optimisation horizon and the rest of the EV's staying time.

2.1.2 Explicit demand response scheme

Commercial rules for flexibility provision by the Croatian Transmission System Operator (TSO) are used as a setup for our case study. Unlike in [17], the aggregator contracts with the TSO frequency regulation reserve power $P_{\text{res}}(f)$ separately per every 15 min interval $f \in \mathbb{F}$ in a day, one-day-ahead. Set $\mathbb{F}$ is the set of all discrete-time instants when the activation can occur. Since the parking lots in the datasets we use for verification belong to faculty buildings, the set $\mathbb{F}$ contains only discrete-time intervals in period between 8:00 and 13:15 h to reduce the computational requirements due to lack of EVs outside of that period. According to the contract, the TSO can request consumption reduction P_{act} during a time interval that starts at discrete-time interval f which is not longer than 1 h. Request P_{act} is constant for the whole time interval and must be lower than $P_{\text{res}}(f)$. Minimum time T_{r} between starts of two consecutive activations is defined by the TSO. The aggregator is notified about the activation 15 min ahead of it.

2.1.3 Cost variables

In this subsection components of the cost function for energy exchange between the aggregator and the grid including DR functionality are introduced. These components include day-ahead energy cost, intra-day balancing penalties, peak power penalisation, frequency regulation reserve power revenue, activation energy revenue and battery degradation cost. The charging behaviour is indifferent to charging fee since the final amount of the energy given to the EVs is constant due to constraint (2.4) and thus the charging fee is not taken into account. The charging fee and payment streams for EV charging depend on the aggregator's business model and are not further discussed here.

The energy exchange with the grid in time interval $[kT, (k+1)T)$ is defined with:

$$E_{\text{g}}(k) = \sum_{cp=1}^{n} \left(u_{\text{ch},cp}(k) - u_{\text{dch},cp}(k) \right). \tag{2.5}$$

Day-ahead energy cost

The exchanged electrical energy cost J_{da} is calculated in the following way:

$$J_{\mathrm{da}}(\boldsymbol{E}_{\mathrm{g}}) = \sum_{k=1}^{N} c_{\mathrm{da}}(k) E_{\mathrm{g}}(k), \tag{2.6}$$

where $\boldsymbol{c}_{\mathrm{da}} \in \mathbb{R}^N$ is a vector of day-ahead prices for every 15-min discretisation interval, obtained from the market.

Intra-day balancing penalties

At the end of a day, deviation of the exhibited energy exchange profile $\boldsymbol{E}_{\mathrm{g}}$ from the day-ahead predicted/declared reference energy profile $\boldsymbol{E}_{\mathrm{g,ref}}$ is penalised with the cost function:

$$J_{\mathrm{id}}(\boldsymbol{E}_{\mathrm{g}}, \boldsymbol{E}_{\mathrm{g,ref}}) = \sum_{k=1} 1.2\, c_{\mathrm{da}}(k)\, |E_{\mathrm{g}}(k) - E_{\mathrm{g,ref}}(k)|\,, \tag{2.7}$$

$$\forall k \text{ s.t. } \begin{cases} 1 \leq k \leq N \\ k \notin \{k_{\mathrm{act}}, ..., k_{\mathrm{act}+3}\} \end{cases} \tag{2.8}$$

where $|\cdot|$ denotes the absolute value. It can be seen that in the interval of activation deviation is not penalised.

Peak power penalisation

The aggregator contracts peak power $P_{\mathrm{pp,c}}$ to the grid on a monthly basis. Peak power cost considered in this paper is derived based on peak power billing in Croatia [18],[19] (Fig. 2.2) and is defined with:

$$J_{\mathrm{pp}}(\boldsymbol{E}_{\mathrm{g}}) = c_{\mathrm{pp}} \varepsilon_{\mathrm{pp}}, \tag{2.9}$$

$$\text{s.t.} \begin{cases} \varepsilon_{\mathrm{pp}} \geq \varepsilon_{\mathrm{pp,past}}, \\ \varepsilon_{\mathrm{pp}} \geq 0.85 P_{\mathrm{pp,c}}, \\ \varepsilon_{\mathrm{pp}} \geq E_{\mathrm{g}}(k)/T,\ \forall k \in \{1, 2, ..., N\}, \\ \varepsilon_{\mathrm{pp}} \geq 3E_{\mathrm{g}}(k)/T - 2.1 P_{\mathrm{pp,c}},\ \forall k \in \{1, 2, ..., N\}, \end{cases} \tag{2.10}$$

where $\varepsilon_{\mathrm{pp}}$ is an auxiliary variable, c_{pp} is the price of peak power obtained from the grid and $\varepsilon_{\mathrm{pp,past}}$ is the maximum value of $\varepsilon_{\mathrm{pp}}$ since the beginning of the month until the optimisation is started.

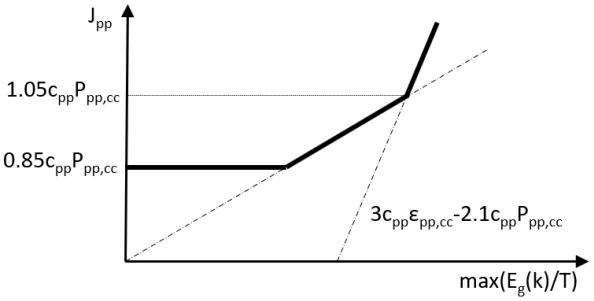

Figure 2.2: Peak power cost tariff.

Frequency regulation reserve power cost

The aggregator contracts unique reserve power $P_{\text{res}}(f)$ for every 15-minute interval the next day and it is rewarded with:

$$J_{\text{res}}(\boldsymbol{P}_{\text{res}}) = \sum_{f} c_{\text{res}} \text{sgn}(P_{\text{res}}(f)) P_{\text{res}}(f), \forall f \in \mathbb{F}, \tag{2.11}$$

where c_{res} is the reservation power price and $\text{sgn}(P_{\text{res}})$ is obtained from the TSO, where negative and positive values denote reduction and increase of power, respectively.

Frequency regulation energy cost

When the grid activates a part of or the whole agreed flexibility reserve, the aggregator is rewarded for the exhibited difference in electrical energy consumption compared to the declared consumption:

$$J_{\text{act}}(\boldsymbol{E}_{\text{g}}, \boldsymbol{E}_{\text{g,ref}}, P_{\text{act}}, f) = \sum_{k} c_{\text{act}}(k) \varepsilon_{\text{act}}(k), \quad f \leq k < f + 4, \tag{2.12}$$

$$\text{s.t.} \begin{cases} \varepsilon_{\text{act}}(k) \leq \text{sgn}(P_{\text{act}})(E_{\text{g}}(k) - \gamma(f) E_{\text{g,ref}}(k)), \\ \varepsilon_{\text{act}}(k) \leq \text{sgn}(P_{\text{act}}) P_{\text{act}} T, \\ \varepsilon_{\text{act}}(k) \geq \text{sgn}(P_{\text{act}})(1 - \alpha) P_{\text{act}} T, \end{cases} \tag{2.13}$$

where P_{act} is a regulation power request of the grid that must be of the same sign and in absolute value lower than $P_{\text{res}}(f)$, ε_{act} is an auxiliary variable, c_{act} is the price of regulation energy and $\alpha = 0.25$ is a tolerance factor. A correction factor γ compensates the aggregator's deviation from the reference profile $\boldsymbol{E}_{\text{g,ref}}$ prior to the moment of activation and corrects the reference. Coefficient γ is calculated as follows:

$$\gamma(f) = \frac{\sum_{j=-4}^{-1} E_{\text{g}}(f + j)}{\sum_{j=-4}^{-1} E_{\text{g,ref}}(f + j)}. \tag{2.14}$$

The definition in (2.14) introduces a nonlinearity in the optimisation problem in which $\boldsymbol{E}_{\mathrm{g,ref}}$ is also optimised and linear approximations are explained later in section 2.2.

EV battery degradation

Battery capacity is degraded by every charging and discharging action. Since the EV owner expects the battery is charged to the target state, battery charging is not penalised. In the case the EV owner agrees with discharging of the battery it is penalised with double degradation price since the battery must be charged again after the discharging:

$$J_{\mathrm{bd}}(\boldsymbol{u}_{\mathrm{dch}}) = 2c_{\mathrm{bd}} \sum_{k=1}^{N} \sum_{cp=1}^{n} u_{\mathrm{dch},cp}(k), \tag{2.15}$$

where c_{bd} is the battery degradation cost [20]. Expression (2.15) is formally correct both for the cases when the EV is owned by a person that needs to be reimbursed for the vehicle-to-grid service and when the aggregator owns the EV and it should take (2.15) into account for its long-term profit.

2.1.4 Worst-case problem

The considered optimisation problem consists of one scenario S_f for the activation at every time instant $f \in \mathbb{F}$ and of a scenario S_{n} without activation. Further on, indices f and n used for different variables denote a scenario to which a particular variable belongs. The information about the activation at the moment f becomes available between the time instants $f-1$ and f which means that all optimisation variables of the scenario S_f must be equal to the ones of the scenario S_{n} until the activation occurs. Such an optimisation problem can be qualified as the worst-case multi-stage recourse problem according to [21].

Constraints that connect scenarios S_{n} and S_f assure that all decision variables are calculated using only information available at the corresponding moment:

$$\begin{cases} SoE_{cp,f}(k) = SoE_{cp,\mathrm{n}}(k) & \forall k | 1 \leq k \leq f, \\ u_{\mathrm{ch},cp,f}(k) = u_{\mathrm{ch},cp,\mathrm{n}}(k) & \forall k | 1 \leq k < f, \\ u_{\mathrm{dch},cp,f}(k) = u_{\mathrm{dch},cp,\mathrm{n}}(k) & \forall k | 1 \leq k < f, \end{cases} \tag{2.16}$$

$$\forall f \in \mathbb{F},$$

$$\forall cp \in \{1, 2, ..., n\}.$$

When an activation occurs, it is certain that the next activation can occur at $f + T_{\mathrm{r}}/T$

at earliest, because of the recuperation period respected by the grid operator that utilises the flexibility. After the recuperation period has passed, i.e. for $k \geq f + T_\mathrm{r}/T$, constraints are added as follows:

$$\begin{cases} SoE_{cp,f}(k) = SoE_{cp,\mathrm{n}}(k) & \forall k | f + T_\mathrm{r}/T \leq k \leq N, \\ u_{\mathrm{ch},cp,f}(k) = u_{\mathrm{ch},cp,\mathrm{n}}(k) & \forall k | f + T_\mathrm{r}/T \leq k \leq N, \\ u_{\mathrm{dch},cp,f}(k) = u_{\mathrm{dch},cp,\mathrm{n}}(k) & \forall k | f + T_\mathrm{r}/T \leq k \leq N, \end{cases} \tag{2.17}$$
$$\forall f \in \mathbb{F},$$
$$\forall cp \in \{1, 2, ..., n\}.$$

Constraints (2.17) ensure that the aggregator is ready for the next activations that may occur after the recuperation period. Scenario S_f can be seen as a branch in a scenario tree which is then connected back to the scenario S_n.

2.2 Deterministic optimisation problem

It is assumed that the aggregator every day declares nominal energy exchange profile $E_{\mathrm{g,n}}$ to the grid entity that utilises the flexibility so $E_{\mathrm{g,n}}$ is used as a reference profile to calculate J_id and J_act. That causes a nonlinearity in calculating γ in (2.14). The nonlinearity is bypassed by adding constraints:

$$\begin{cases} \mathrm{sgn}(P_\mathrm{res}(f))E_{\mathrm{g,n}}(k) \geq \mathrm{sgn}(P_\mathrm{res}(f))E_{\mathrm{g},f}(k) \\ f - 4 + T_\mathrm{r}/T \leq k < f + T_\mathrm{r}/T, \ \forall f \in \mathbb{F} \end{cases}, \tag{2.18}$$

that limits γ to be equal to 1 in the worst case and allows us to use $\gamma = 1$ instead of (2.14).

Total costs J_n of the scenario without activation and J_f of the scenarios with activation at interval f are defined as:

$$J_\mathrm{n} = J_\mathrm{da}(\boldsymbol{E}_{\mathrm{g,n}}) + J_\mathrm{pp}(\boldsymbol{E}_{\mathrm{g,n}}) + J_\mathrm{bd}(\boldsymbol{u}_{\mathrm{dch,n}}), \tag{2.19}$$

$$\begin{aligned} J_f = & J_\mathrm{da}(\boldsymbol{E}_{\mathrm{g,n}}) + J_\mathrm{pp}(\boldsymbol{E}_{\mathrm{g},f}) + J_\mathrm{bd}(\boldsymbol{u}_{\mathrm{dch},f}) \\ & + J_\mathrm{act}(\boldsymbol{E}_{\mathrm{g},f}, \boldsymbol{E}_{\mathrm{g,n}}, P_\mathrm{res}(f), f) + J_\mathrm{id}(\boldsymbol{E}_{\mathrm{g},f}, \boldsymbol{E}_{\mathrm{g,n}}, f). \end{aligned} \tag{2.20}$$

It can be seen from (2.20) that every scenario assumes the grid will activate the whole contracted reserve power P_res.

The optimisation variables of the offline problem are $\boldsymbol{u}_{\text{ch}}$ and $\boldsymbol{u}_{\text{dch}}$ of all scenarios and the vector of contracted 15 min regulation power reserve $\boldsymbol{P}_{\text{res}}$ while the cost being minimised is:

$$J = \min_{\boldsymbol{u}_{\text{ch}}, \boldsymbol{u}_{\text{dch}}, \boldsymbol{P}_{\text{res}}} J_{\text{res}}(\boldsymbol{P}_{\text{res}}) + J_{\text{worst}},$$

$$\text{s.t.} \begin{cases} J_{\text{worst}} \geq J_{\text{n}} + \beta \sum_{\forall f} J_f, \\ J_{\text{worst}} \geq J_f + \beta J_{\text{n}} + \beta \sum_{\forall j \neq f} J_j \ , \ \forall f, \\ (2.1) - (2.20) \end{cases} \tag{2.21}$$

where β is empirically chosen equal to 0.001 and is used to prevent certain scenarios not being optimised, which would be a consequence of that only the worst scenario contributes to J_{worst} (case where $\beta = 0$).

2.3 Chance-constraints

Uncertainty of EV arrivals must be included in day-ahead analysis. Statistical transformation from the aggregated representation to individual EV data is a complicated task that remains for the future work. Because of that, the approach with aggregated chance-constrains is applied.

The method of chance-constraints in optimisation programming involves managing uncertain parameters in a problem with the assurance of a particular level of performance. Dealing with variables that are uncertain within a control system raises concerns about reliability and potential risks, creating complexities in predicting the most probable outcome. In stochastic optimisation, anticipated or nominal values are utilised for addressing these uncertainties. Although there is a degree of risk associated with these stochastic optimisation choices, they are generally considered conventional as they have been previously incorporated – a recognised "trade-off." However, in practical scenarios, these trade-offs are not always clearly defined, such as in the case of extreme weather occurrences. In such instances of uncertainty, it remains crucial to prepare for these events and formulate decisions around them. A prevalent approach in such cases is to accommodate unexpected events that might breach specific constraints, as long as the overall constraint satisfaction is upheld within a specified probability threshold. This implies ensuring particular levels of feasibility, which are termed as chance-constraints.

In the case of the EV charging scheduling, all individual EV data are uncertain parameters influencing EVs' state of energy and charging and discharging power. Thus, the

aggregated chance-constraints are superimposed to the individual constraints (2.2) - (2.4) and they are derived from the aggregated constraints (4.32),(4.35) and (4.36):

$$\mathbf{prob}(P_{\text{agg,ch}}(k) + P_{\text{agg,dch}}(k) <= P_{\max}(k)) > 1 - \alpha, \tag{2.22}$$

$$\mathbf{prob}(SoE_{\text{agg}}(k) \leq C_{\text{agg}}(k)) > 1 - \alpha, \tag{2.23}$$

$$\mathbf{prob}(SoE_{\text{agg}}(k) \geq R_{\text{agg}}(k)) > 1 - \alpha, \tag{2.24}$$

where $\boldsymbol{R}_{\text{agg}} \in \mathbb{R}^N$ and $\boldsymbol{C}_{\text{agg}} \in \mathbb{R}^N$ are lower and upper bound of the aggregated charging envelope of the EV population, respectively and vector $\boldsymbol{P}_{\max} \in \mathbb{R}^N$ denotes total nominal charging power connected to the charging points.Their statistical analysis is given in the next section. Parameter α is a user-defined probability that constraint will be violated. Vectors $\boldsymbol{P}_{\text{agg,ch}} \in \mathbb{R}^N$, $\boldsymbol{P}_{\text{agg,dch}} \in \mathbb{R}^N$ are total charging and discharging power, respectively, defined as:

$$P_{\text{agg,ch}}(k) = \sum_{cp}^{n} u_{\text{ch},cp}(k), \tag{2.25}$$

$$P_{\text{agg,dch}}(k) = \sum_{cp}^{n} u_{\text{dch},cp}(k), \tag{2.26}$$

where n is the number of charging points. Vector $\boldsymbol{SoE}_{\text{agg}} \in \mathbb{R}^N$ represents aggregated state of energy:

$$SoE_{\text{agg}}(k) = (\sum_{cp} SoE_{cp}(k),\ \forall cp \mid k \notin \mathcal{I}_{cp}) + (\sum_{i} C_i,\ |k_{\text{d},i} < k). \tag{2.27}$$

In this way the aggregator can have control over the risk that follows from uncertainty of EVs presence. With known cumulative density function (CDF) Φ for every element of the random vectors for every weekday, chance constraints can be rewritten to a linear constraints:

$$P_{\text{agg,ch}}(k) + P_{\text{agg,dch}}(k) \leq \Phi^{-1}_{\text{P},d,k}(1 - \alpha), \tag{2.28}$$

$$SoE_{\text{agg}}(k) \leq \Phi^{-1}_{\text{C},d,k}(1 - \alpha), \tag{2.29}$$

$$SoE_{\text{agg}}(k) \geq \Phi^{-1}_{\text{R},d,k}(\alpha), \tag{2.30}$$

where Φ^{-1} is inverse of CDF, indices P, C and R denote vectors while indices d and k day of week and discrete time interval, respectively.

2.3.1 Statistical analysis of daily aggregated EV data

For statistical analysis is used historical aggregated representation of every day. Due to obvious weekly pattern, seen in Fig. 5.4, analysis is done separately per every weekday. For Friday two separated analyses were conducted since in JPL every second Friday is free for the most of employees. By observing the histograms of the 8^{th} and 50^{th} elements random variable $\boldsymbol{P}_{\max}$, corresponding to 15-min discrete time intervals at 7:00 and 12:30, shown in Fig. 5.3, it can be seen that random variables cannot be easily described with some common probability distribution. Furthermore it can be seen that unique probability density function (PDF) should be determined for every discrete-time interval in a day separately. For the estimation of probability density function (PDF) of every element in $\boldsymbol{P}_{\max}$ a kernel density estimator (KDE) [22] is used:

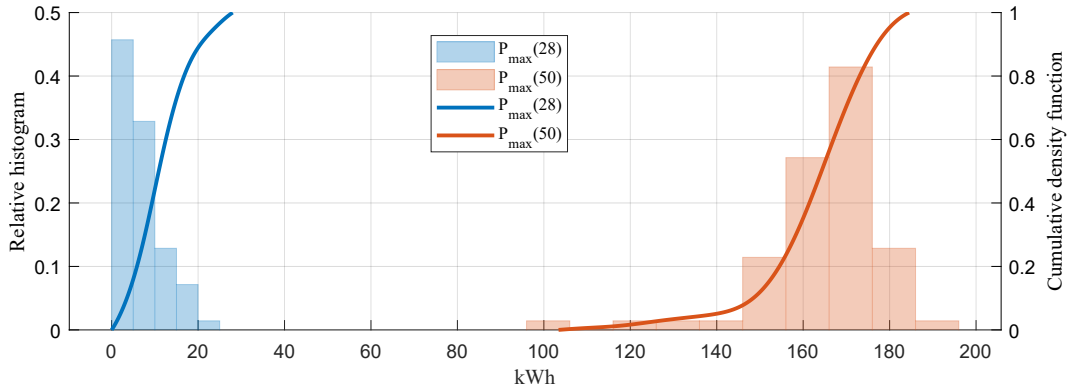

Figure 2.3: Histograms and cumulative density functions of all working Mondays' $P_{\max}(28)$ and $P_{\max}(50)$ that corresponds to 7:15 and 12:45 respectively.

$$\hat{f}_h(x) = \frac{1}{mh} \sum_{i=1}^{m} K_h \left(\frac{x - x_i}{h} \right), \tag{2.31}$$

where $\hat{f}_h(x)$ is the estimate of PDF $f(x)$ at x considering m observations $x_i \in X$, and $K_h(\cdot)$ is some kernel function for which h denotes the kernel smoothing parameter. A common choice for $K_h(\cdot)$ is the Gaussian kernel defined as follows:

$$K(x) = \frac{1}{\sqrt{2\pi}\sigma} e^{-\frac{x^2}{2\sigma^2}}, \tag{2.32}$$

where σ is standard deviation. As for smoothing parameter h, the Gaussian reference bandwidth is chosen according to Scott's rule [23]:

$$h = \left(\frac{1}{n} \right)^{(d+4)}, \tag{2.33}$$

where d is number of dimensions which is equal to 1 since the KDE is determined for every element of $\boldsymbol{P}_{\max}$, $\boldsymbol{C}_{\text{agg}}$ and $\boldsymbol{R}_{\text{agg}}$ separately.

Since $C_{\text{agg}}(k)$ and $R_{\text{agg}}(k)$ are highly correlated, as seen in Fig. 2.4., separate analysis would lead to contradicted and unfeasible constraints (2.23) and (2.24) which can be seen in Fig. 2.5 where histograms overlaps.

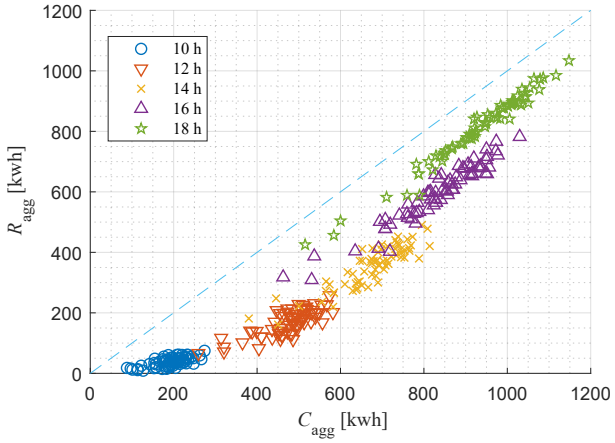

Figure 2.4: Correlation between vectors $\boldsymbol{C}_{\text{agg}}$ and $\boldsymbol{R}_{\text{agg}}$.

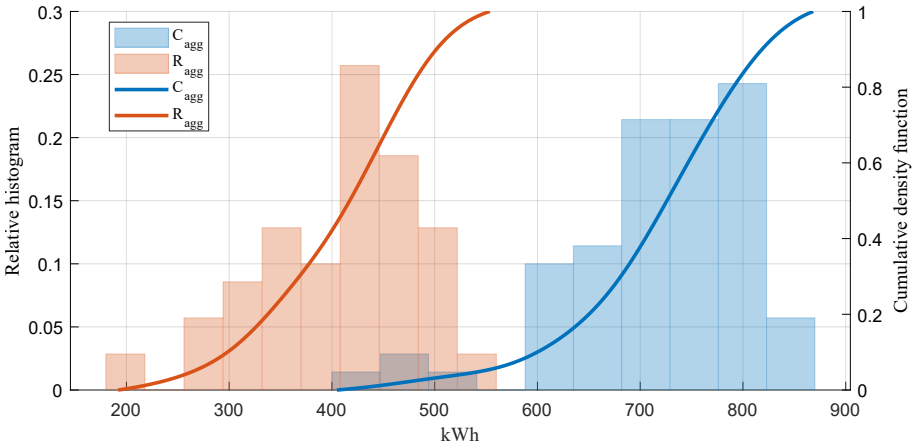

Figure 2.5: Histograms and cumulative density functions of all working Mondays' $C_{\text{agg}}(56)$ and $R_{\text{agg}}(56)$ that corresponds to 13:45.

The foundation of flexibility capacity is the area of the aggregated envelope between time vectors $\boldsymbol{C}_{\text{agg}}$ and $\boldsymbol{R}_{\text{agg}}$ as visualised in Fig. 2.6. More precisely, its distribution through the horizon. Thus vector $\boldsymbol{\Delta}_{\text{agg}} \in \mathbb{R}^N$ is defined as:

$$\Delta_{\text{agg}}(k) = C_{\text{agg}}(k) - R_{\text{agg}}(k). \tag{2.34}$$

It is vector $\boldsymbol{\Delta}_{\text{agg}}$ that implicitly quantifies EV populations' capability to participate in frequency regulation. Average EV population used in the analyses contains information for the expectation of the aggregator's nominal overall consumption profile while $\boldsymbol{\Delta}_{\text{agg}}$ limits

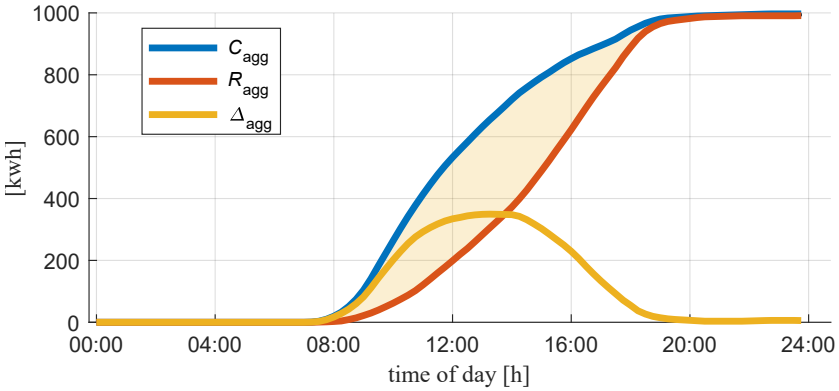

Figure 2.6: Example of vectors $\boldsymbol{C}_{\text{agg}}$ and $\boldsymbol{R}_{\text{agg}}$ with denoted $\boldsymbol{\Delta}_{\text{agg}}$.

deviations from it, i.e. moving EVs charging outside the activation intervals. Chance constraints (2.29) and (2.30) are adapted to:

$$SoE_{\text{agg}}(k) \leq \frac{\overline{C}_{\text{agg},d,k} + \overline{R}_{\text{agg},d,k}}{2} - \Phi^{-1}_{\Delta,d,k}(1-\alpha), \tag{2.35}$$

$$SoE_{\text{agg}}(k) \geq \frac{\overline{C}_{\text{agg},d,k} + \overline{R}_{\text{agg},d,k}}{2} + \Phi^{-1}_{\Delta,d,k}(1-\alpha), \tag{2.36}$$

where $\overline{C}_{\text{agg},d,k}$ and $\overline{R}_{\text{agg},d,k}$ are the mean value of the k^{th} elements of vectors $\boldsymbol{C}_{\text{agg}}$ and $\boldsymbol{R}_{\text{agg}}$, respectively, for weekday d. Function $\Phi^{-1}_{\Delta,d,k}(\cdot)$ is analogue CDF of element of vector $\boldsymbol{\Delta}$.

With the applied statistic analysis, final aggregated charging envelopes are shown in Fig. 2.7 while maximal total charging power is shown in Fig 2.8.

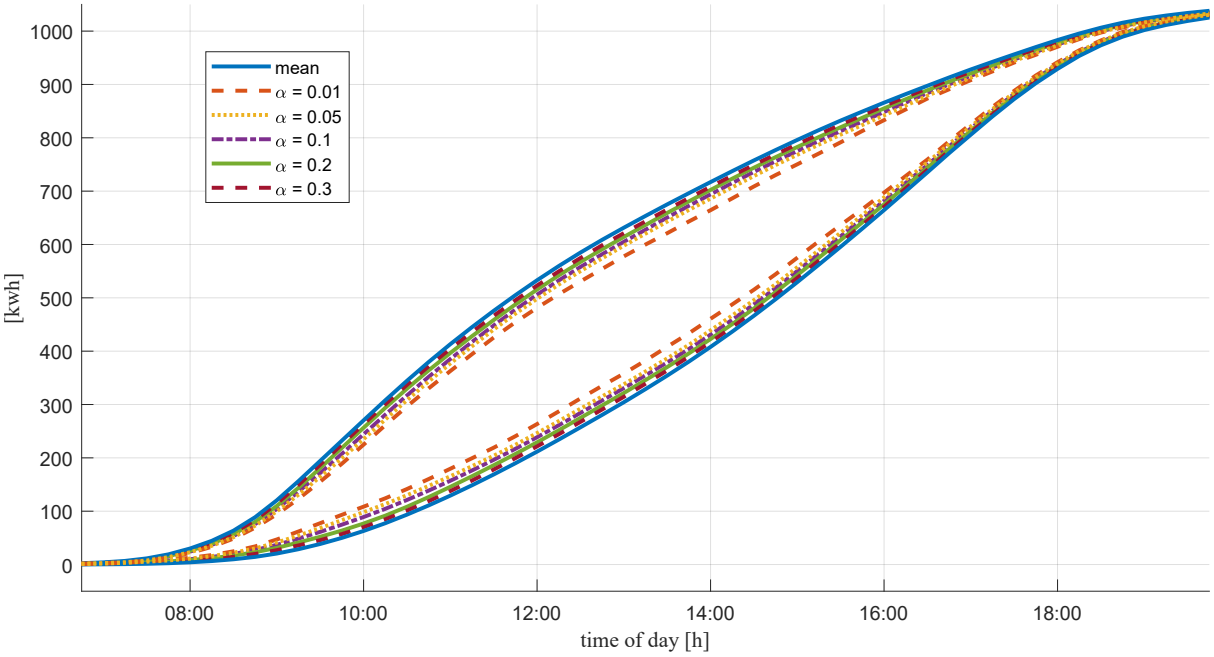

Figure 2.7: Aggregated charging envelope for different values of α

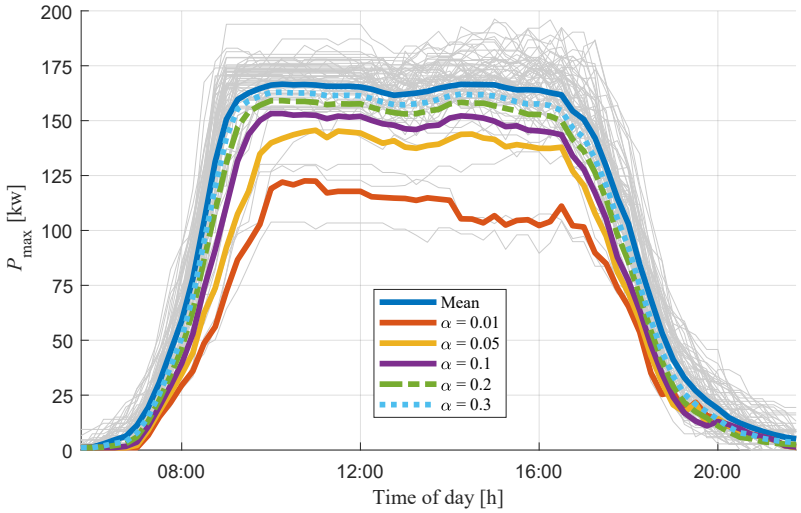

Figure 2.8: Maximal total charging power for different values of α.

2.4 Stochastic day-ahead analysis algorithm

The optimisation problem (2.21) used in Chapter 4 for the comparison of flexibility capacity of populations is now modified to enable cost-benefit analysis. The frequency regulation capacity market operates as an auction so it is uncertain if the offered capacity is going to be contracted. The optimisation problem (2.21) minimises the final cost that includes reward for contracted flexibility capacity $J_{\text{res}}(\boldsymbol{P}_{\text{res}})$ which can bring out that the nominal scenario without any activation does not entirely charge the EVs in the low electrical energy price intervals in order to adapt in service of flexibility. Since the reward for adapting is not guaranteed, that is a possible financial loss for the aggregator. In order to put that loss under control, the first step of the flexibility analysis is to calculate optimal cost of the nominal scenario without contracted flexibility. The second step is to determine the optimal charging schedules for contracting flexibility under condition that total cost of the scenario without flexibility activation must not be be higher than the nominal scenario from the first step.

2.4.1 Stochastic optimisation problem without flexibility

The aggregated chance-constraints (2.28) in superposition with the individual constraints (2.2) - (2.4) can cause infeasible solution in the optimisation problem. To determine the optimal EV charging schedule that minimally breaks aggregated chance-constraints, the part of the linear optimisation problem from Chapter 4 that refers to scenario 'n' without

flexibility activation is upgraded with soft-constraint variant of (2.28):

$$\begin{aligned} &J_{\text{soft}} = c_{\text{soft}} * \textstyle\sum_{k=1}^{N} \varepsilon_{\text{P}}(k) \\ \text{s.t.} \quad &\begin{cases} P_{\text{agg,ch}}(k) + P_{\text{agg,dch}}(k) - \varepsilon_{\text{P}}(k) \leq \Phi^{-1}_{\text{P},d,k}(1-\alpha), \\ \varepsilon_{\text{P}}(k) \geq 0, \end{cases} \end{aligned} \tag{2.37}$$

where J_{soft} denotes penal for breaching of soft-constraints, $\varepsilon_{\text{P}}(k)$ is auxiliary variable and c_{soft} is big enough penalty price to enforce maximal constraints satisfaction. Chance constraints (2.35) and (2.36) do not need to be implemented as soft constraint because they make aggregated charging envelope around $\frac{\overline{C}_{\text{agg},d,k}+\overline{R}_{\text{agg},d,k}}{2}$ which is by the definition charging trajectory for charging all EVs continuously through their whole staying time. Because of that, there is always at least one feasible charging trajectory, even when probability parameter α is equal to zero.

The complete optimisation problem for the scenario without contracted flexibility is defined as:

$$\begin{aligned} J_{\text{wcf}} &= (\min_{\boldsymbol{u}_{\text{h}},\, \boldsymbol{u}_{\text{dch}}} J_{\text{n}} + J_{\text{soft}}), \\ \text{s.t. } &(2.1)-(2.6), (2.9), (2.10), (2.15), (2.19)(2.35)-(2.37), \end{aligned} \tag{2.38}$$

where J_{wcf} is the total optimisation cost of the aggregator without contracted flexibility (wcf) that includes J_{soft}. For the economical analysis optimal daily operational cost of aggregator is calculated as $J^{*}_{\text{wcf}} = J_{\text{wcf}} - J_{\text{soft}}$ and as such is used for the optimisation problem with flexibility in the next subsection.

2.4.2 Stochastic optimisation problem with flexibility

After obtaining the EV charging schedule that minimally breaks aggregated chance-constraints, soft chance-constraint (2.37) can be replaced with:

$$P_{\text{agg,ch}}(k) + P_{\text{agg,dch}}(k) \leq P_{\text{max,wcf}}(k), \tag{2.39}$$

where $\boldsymbol{P}_{\text{max,wcf}}$ is found using:

$$P_{\text{max,wcf}}(k) = \mathbf{max}\left(\Phi^{-1}_{\text{P},d,k}(1-\alpha), |\boldsymbol{u}_{\text{ch,wcf}}(k) + \boldsymbol{u}_{\text{dch,wcf}}(k)|\right). \tag{2.40}$$

Vectors $\boldsymbol{u}_{\text{ch,wcf}}$ and $\boldsymbol{u}_{\text{dch,wcf}}$ are the optimal arguments for optimisation problem without contracted flexibility (2.38), $\mathbf{max}(\cdot)$ is max operator and $|\cdot|$ is first norm of vector. The conducted correction for probability parameter $\alpha = 0.05$ for Monday is shown in Fig. 2.9.

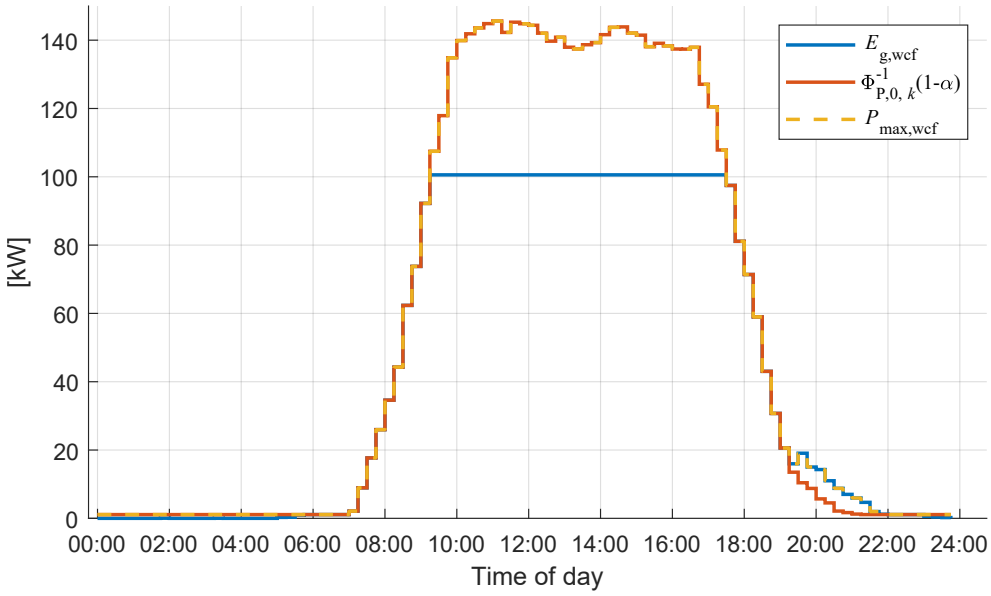

Figure 2.9: Vector $\boldsymbol{P}_{\text{max,wcf}}$ for Monday and $\alpha = 0.05$ after correction using (2.40).

With determined J^*_{wcf} from the optimisation problem (2.38) the aggregator can choose the value at risk V_{ar} that can be lost if the offer for frequency regulation capacity is not accepted from the power grid operator. Using the obtained J^*_{wcf} the former optimisation problem (2.21) is modified as follows:

$$J = \min_{\boldsymbol{u}_{\text{ch}}, \boldsymbol{u}_{\text{dch}}, \boldsymbol{P}_{\text{res}}} J_{\text{res}}(\boldsymbol{P}_{\text{res}}) + J_{\text{worst}},$$

$$\text{s.t.} \begin{cases} J_{\text{worst}} \geq J_{\text{n}} + \beta \sum_{\forall f} J_f, \\ J_{\text{worst}} \geq J_f + \beta J_{\text{n}} + \beta \sum_{\forall j \neq f} J_j \ , \ \forall f, \\ J_{\text{n}} \leq J^*_{\text{wcf}} + V_{\text{ar}} \\ (2.1) - (2.20), (2.35), (2.36), (2.39) \end{cases} \tag{2.41}$$

2.4.3 Final day-ahead algorithm

To conclude and as an abstract of the whole procedure, all steps are summarised in the Algorithm 1.

Algorithm 1 Day-ahead flexibility analysis

Require: Historical daily EV populations, α,V_{ar} c_{da}, c_{act}, c_{res}
Ensure: $\boldsymbol{P}_{\text{res}}$, $\boldsymbol{u}_{\text{ch}}$, $\boldsymbol{u}_{\text{dch}}$
From historical daily EV populations generate mean aggregated representation using Algorithm 6
Find CDF for vectors $\boldsymbol{P}_{\text{agg,max}}$, $\boldsymbol{C}_{\text{agg}}$ and $\boldsymbol{R}_{\text{agg}}$ (2.31)-(2.36)
Solve (2.38) to find J^*_{wcf}
Find $\boldsymbol{P}_{\text{max,wcf}}$ using (2.40)
Solve (2.41)

2.5 Results and discussion

In this section an extensive analysis of the results is given for the weekday Monday and with probability parameter $\alpha = 0.05$. Value at risk V_{ar} is arbitrarily chosen to enable the EV population to show a significant part of its flexibility capacity. The rest of the prices and parameters is the same as in Section 4.3.

Difference in total present nominal charging power $\boldsymbol{P}_{\text{max}}$ and total charged energy $\boldsymbol{R}_{\text{agg}}$ varies between same weekday. Thus analysis of the optimal contracted peak power ought to be separated. For the flexibility analysis the critical parameters are those that limit frequency regulation capacity - $\boldsymbol{P}_{\text{max}}$ and $\boldsymbol{\Delta}_{\text{agg}}$, while for the peak power analysis the distribution and the upper values of $\boldsymbol{P}_{\text{max}}$ and $\boldsymbol{R}_{\text{agg}}$ should be examined, which is left for the future work. In spite of that, both results with and without peak-power optimisation are given in this section to give valuable insight in critical costs and revenues.

Values of the electrical prices used in the optimisation problem (2.21) are as follows: $c_{\text{pp}} = 0.116$ €/kW, $c_{\text{res}} = -0.0162$ €/kW, $c_{\text{act}} = 0.065$ €/kWh, $c_{\text{batt}} = 0.226$ €/kWh [20]. Vector of day-ahead prices $\boldsymbol{c}_{\text{da}}$ is shown in Fig. 2.10. Discretisation time is $T = 15$ min and recuperation period is $T_{\text{r}} = 24$ h.

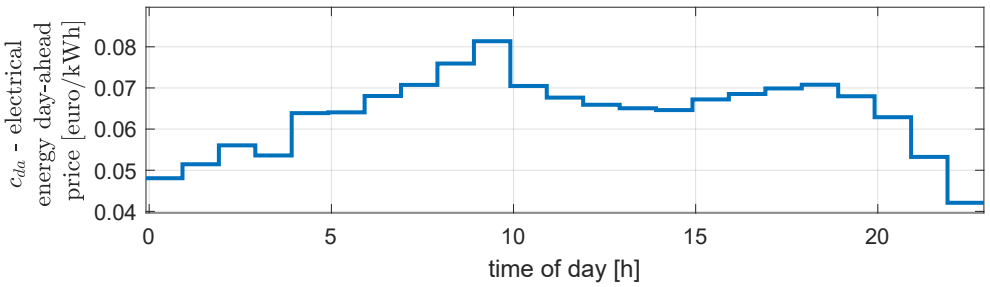

Figure 2.10: Day-ahead electrical energy price profile. [13]

2.5.1 Neglected peak power optimisation

In this subsection are presented optimisation results obtained using optimisation problems (2.38) and (2.41) with excluded J_{pp} and constraints (2.9) and (2.10) that define it. It is

visible in Fig. 2.11. that constraint $J_{\mathrm{n}} \leq J^{*}_{\mathrm{wcf}} + V_{\mathrm{ar}}$ is satisfied. Indeed, there was no no need to exploit the whole amount of $V_{\mathrm{ar}} = 5€$, the daily operation cost of scenario without flexibility activation (with excluded reservation reward J_{res}) is only 1.16 € higher than the cost without contracted flexibility J^{*}_{wcf}.

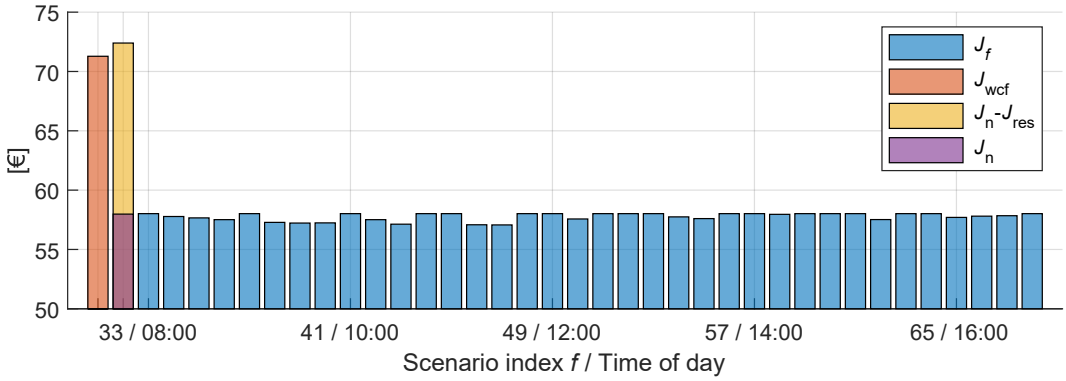

Figure 2.11: Results of day-ahead flexibility analysis for Monday and $\alpha = 0.05$

Figure 2.12. clearly shows the cause why the scenario without flexibility activation $\boldsymbol{E}_{\mathrm{g,n}}$ is removed from the optimal point and charges the EVs in more expensive hours. More precisely, a part of charging between 12:00 and 16:00 was shifted outside the interval, where energy prices are higher, especially at 9:00. It is also visible how scenarios with activation $\boldsymbol{E}_{\mathrm{g,34}}$ and $\boldsymbol{E}_{\mathrm{g,57}}$, that correspond to 8:15 and 14:00, charge EVs, from two possible hours during recuperation period, in the one hour with the lower prices. During morning the scenario $\boldsymbol{E}_{\mathrm{g,n}}$ charges the EVs to be as higher from the activation scenarios as possible. Furthermore, it is interesting to see that chosen flexibility activation price

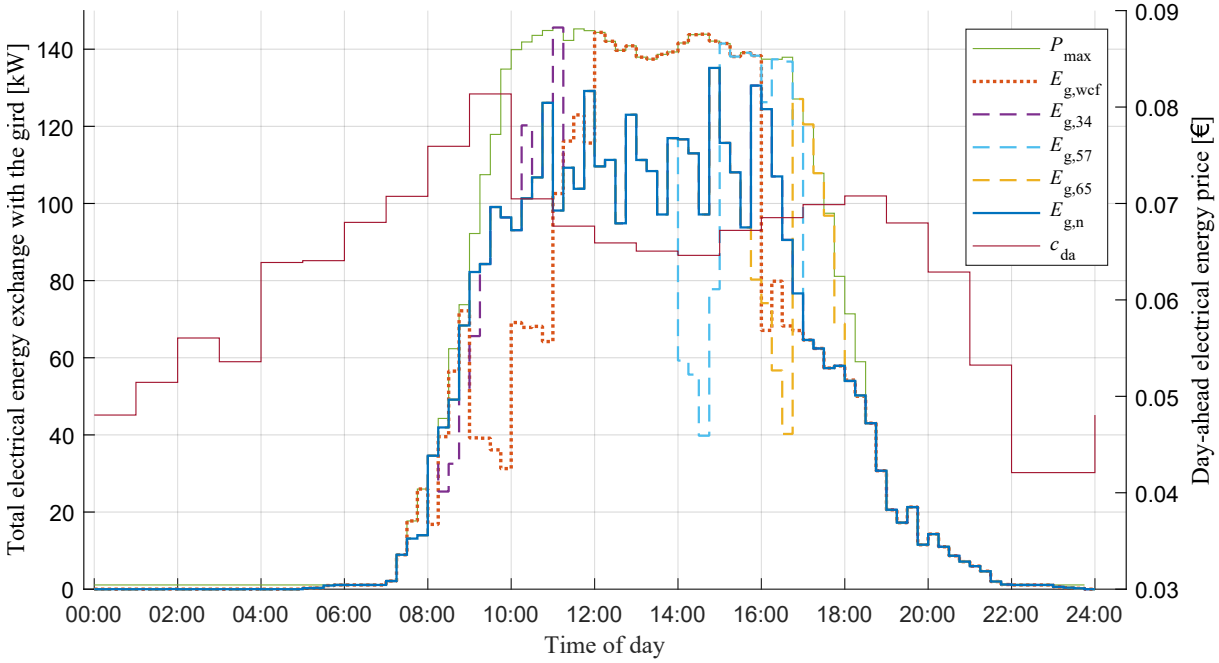

Figure 2.12: Comparison for scenario costs for Monday and $\alpha = 0.05$

(frequency regulation energy price) is just high enough to cover all extra costs that are a consequence of the activation. Only couple of activation scenarios obtained extra profit in comparison to the scenario without activation. The first extra cost of the activation is intra-day balancing penalties for the deviation from the nominal total electrical energy exchange with the grid during the recuperation period. As it can be seen in an example in Fig.2.12. where the scenario with activation at 14:00 compensates missed charging two hours later when the day-ahead energy price is higher. Not to mention the extra cost of battery degradation and the additional losses on battery power converters if EV batteries are discharged as shown With the converter efficiency $\eta = 0.9$, for the 1 kWh discharged another 1 kWh/0.9^2 = 1.23 kWh must be charged to meet starting state of the energy. The optimal regulation capacity depending on the probability variable α is given in Fig. 2.13. In the main part of a day, saturation is visible already above $\alpha = 0.1$. It is interesting how capacity at the edges of a day rises at he expense of the capacity at noon. The last significant contracted regulation capacity is at 16:00. The explanation can be seen in Fig. 2.12. To contract capacity at 17:00 it means that the last possible activation interval is 17:45-18:45 but already at 18:30 there is no manoeuvring space, especially to recuperate, because $\boldsymbol{P}_{\mathrm{max,wcf}}$ overlaps with both $\boldsymbol{E}_{\mathrm{g,wcf}}$ and $\boldsymbol{E}_{\mathrm{g,n}}$.

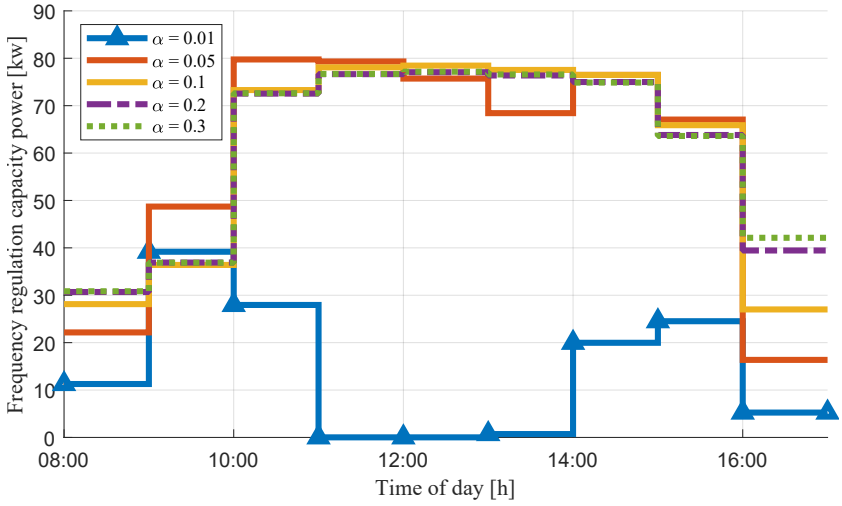

Figure 2.13: Optimal frequency regulation capacity for Monday.

Cost analysis of the obtained results is given in Table 2.2. Scenarios with contracted flexibility are compared with standard as-soon-as-possible (ASAP) charging and the charging profile that is result of the optimisation problem (2.38) without considered flexibility. Significant savings are mostly result of the contracted flexibility while most of the reward for the activation of flexibility is used to cover additional intra-day balancing penalties emerged from the EV charging after the activation. In Table 2.2 are also shown result for the best and the worst case of flexibility activation.

Table 2.2: Offline analysis results without peak power shaving.

	J_{da}	J_{id}	J_{res}	J_{act}	Total	Savings	Savings /%
ASAP charging	74.22	/	/	/	74.22	/	/
Without contracted flexibility	71.28	/	/	/	71.28	-2.94	-3.96
Without activation	72.70	/	-14.42	/	57.98	-16.24	-21.88
With activation - worst	72.30	1.94	-14.42	-1.81	58.02	-16.2	-21.83
With activation - best	72.30	5.65	-14.42	-6.48	57.07	-17.15	-23.11

2.5.2 Included peak power optimisation

Results obtained using optimisation problems (2.38) and (2.41), including peak power optimisation show even bigger savings in comparison with optimisation with neglected peak power.A consequence of the included peak power optimisation is clearly seen in Fig. 2.14. Energy consumption $\boldsymbol{E}_{\text{g,wcf}}$ is cut off in the middle of a day, reducing it's maximal value which corresponds to the lowest peak power cost of the scenario WCF in Table 2.3. Similarly, scenarios with activation give priority to peak power minimisation at the expense of the higher energy prices. The scenario with the highest peak power cost compensates it with reward for fulfilled activation.

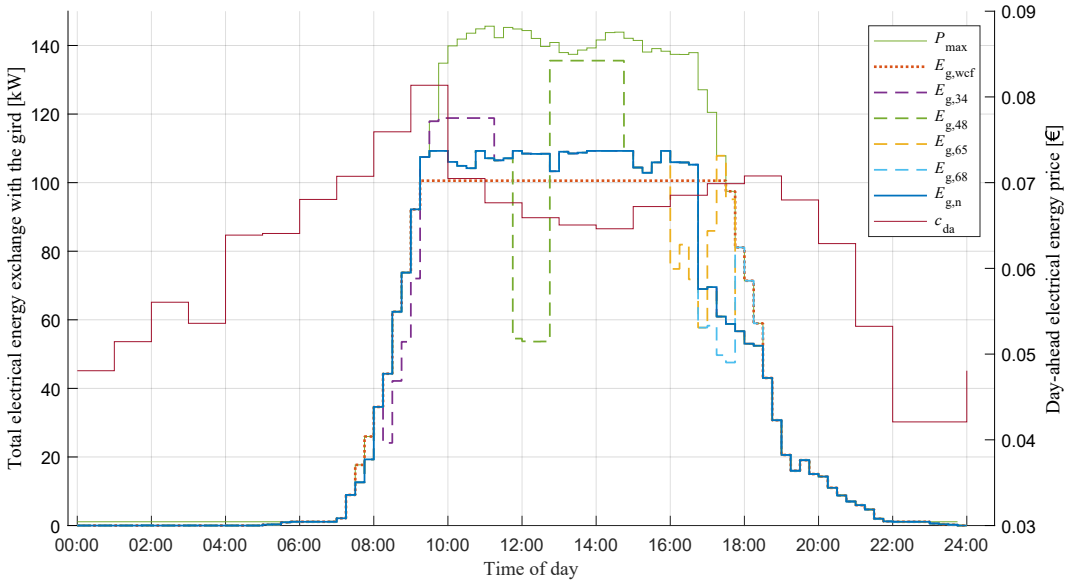

Figure 2.14: Results of day-ahead flexibility analysis for Monday and $\alpha = 0.05$

Similar as in analyses without included peak power optimisation, the operational cost of the scenario without activation is only 0.97 € higher than scenario without contracted flexibility. It can be seen in Fig. 2.15 that costs of most scenarios are the same as the highest one which is justified with worst case optimisation where scenarios adapt to reduce the cost of the critical scenario at the expense of increasing their cost.

Table 2.3: Offline analysis results.

Scenario	$J_{\text{da}} + J_{\text{bd}}$	J_{pp}	J_{id}	J_{act}	J_{res}	Total	Savings	Savings /%
ASAP charging	74.22	17.64	/	/	/	91.86	/	/
Without contracted flexibility	72.72	11.67	/	/	/	84.39	-7.47	-10.06
Without activation	72.70	12.67	/	/	-14.44	70.92	-20.94	-28.21
With activation - worst	74.86	12.67	1.23	-1.23	-14.44	73.10	-18.76	-25.28
With activation - best	72.73	12.67	2.46	-2.72	-14.44	70.70	-21.16	-28.51
Max peak power	72.60	15.73	5.17	-5.97	-14.44	73.10	-18.76	-25.28

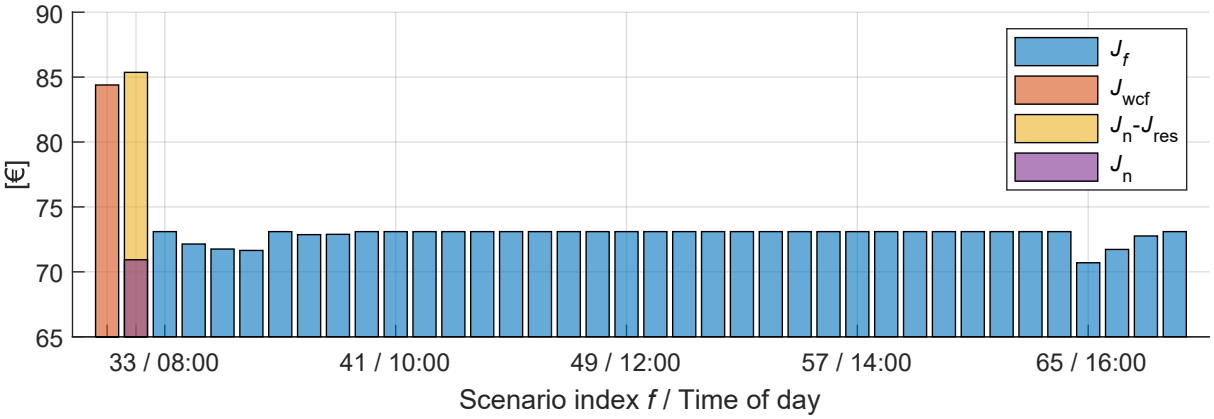

Figure 2.15: Comparison for scenario costs for Monday and $\alpha = 0.05$

2.6 Conclusion

This chapter proposed day-ahead analysis of the EV aggregator's demand response capacity based on stochastic worst-case optimisation. The analysis offers control over the possible financial loss if the flexibility is not contracted with the power grid operator on day-ahead frequency regulation market. By applying chance-constraints and statistical analysis of real-world historical data, the aggregator can influence the certainty of fulfilling contracted flexibility. Conducted analysis showed flexibility capacity of 80 kW for a parking lot equipped with 52 EV charging points.

Chapter 3

Stochastic model predictive control of EV charging

In this chapter the optimisation problem is modified to enable model predictive control (MPC) in a way that it is solved every 15 minutes, within one discretisation interval, and only control variables of the first interval are applied to the system - charging points of the aggregator. In this situation, the individual data of the present EVs is known while the future EVs are predicted and aggregated constraints are applied only on them. The MPC, marked orange, is the final part of the EV charging scheduling concept proposed in this thesis, shown in Fig. 3.1.

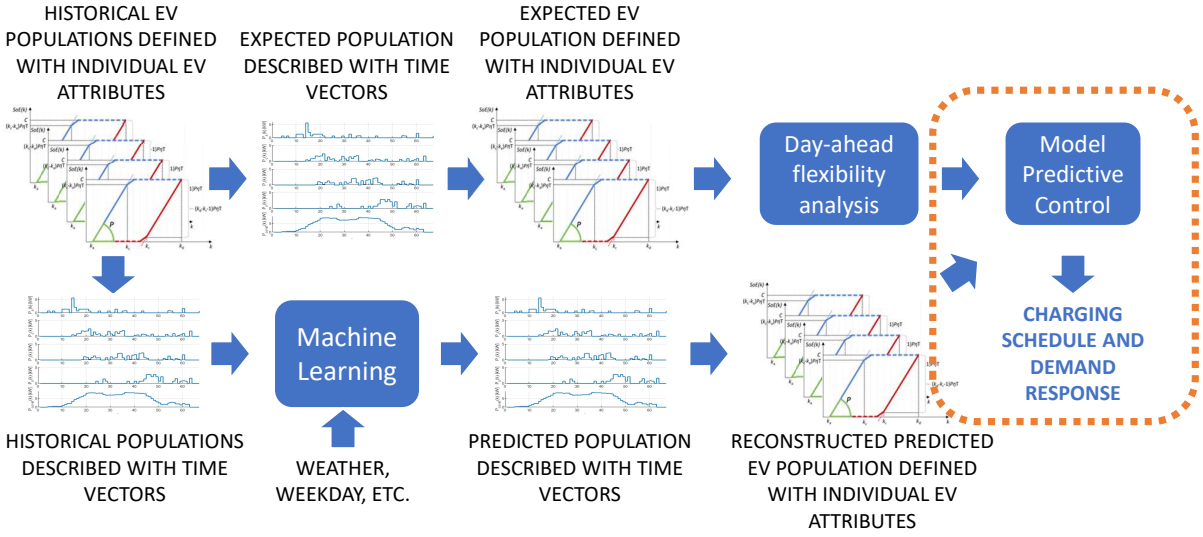

Figure 3.1: The proposed concept of EV charging scheduling exploiting historical data and aggregated representation.

The optimisation problem is slightly different than the problem (2.41) from the previous chapter and it is defined in section 3.1. The first discretisation interval includes charging of EVs that arrived in the previous interval. Since that EVs are not known prior

to the start of solving the optimisation problem, they are part of the future EV population. Because of that, there is a need for the algorithm to allocate the predicted optimal charging power to the new arrived EVs. The algorithm is given in Section 3.2 while the conducted simulations and discussion are given in Section 3.3. The conclusion is given in Section 3.4

3.1 Optimisation problem

After the declared daily energy consumption profile and the optimal regulation capacity are obtained using day-ahead analysis, they are offered and potentially contracted on the day-ahead energy and regulation capacity market. Costs of scenarios with and without activation are defined, respectively, as:

$$\begin{aligned} J_{\mathrm{n}} =& J_{\mathrm{pp}}(\boldsymbol{E}_{\mathrm{g,n}}) + J_{\mathrm{bd}}(u_{\mathrm{ch,n}}, u_{\mathrm{dch,n}}) \\ &+ J_{\mathrm{id}}(\boldsymbol{E}_{\mathrm{g,n}}, \boldsymbol{E}^*_{\mathrm{g}}) + J_{\mathrm{act}}(\boldsymbol{E}_{\mathrm{g,n}}, \boldsymbol{E}^*_{\mathrm{g}}, \mathrm{P}^*_{\mathrm{act}}, i_{\mathrm{last}}) \end{aligned}. \tag{3.1}$$

$$\begin{aligned} J_f =& J_{\mathrm{pp}}(\boldsymbol{E}_{\mathrm{g},f}) + J_{\mathrm{bd}}(u_{\mathrm{ch},f}, u_{\mathrm{dch},f}) \\ &+ J_{\mathrm{id}}(\boldsymbol{E}_{\mathrm{g},f}, \boldsymbol{E}^*_{\mathrm{g}}) + J_{\mathrm{act}}(\boldsymbol{E}_{\mathrm{g,f}}, \boldsymbol{E}^*_{\mathrm{g}}, \mathrm{P}_{\mathrm{res,d}}, f) \end{aligned} \tag{3.2}$$

It can be seen that J_{id} and J_{act} take declared $\boldsymbol{E}^*_{\mathrm{g}}$ as a reference for calculation of the deviation.

Correction coefficient γ used in J_{act} to adapt reference according to historical energy consumption is determined using scenario without activation and the declared energy consumption profile $\boldsymbol{E}^*_{\mathrm{g}}$:

$$\gamma(f) = \frac{\sum_{j=-4}^{-1} E_{\mathrm{g},n}(f+j)}{\sum_{j=-4}^{-1} E^*_{\mathrm{g}}(f+j)}. \tag{3.3}$$

Of course, for the first four discrete time intervals, historical data supplements intervals that precede start of optimisation horizon. In the case of consecutive activations, the scenario with the first activation will be realised and it will determine γ for the scenario with next activation. To ensure that γ will not be worse (lower) than the planned one obtained using the scenario without activation, additional constraint is added as follows:

$$\begin{cases} \mathrm{sgn}(P_{\mathrm{res}}(f))E_{\mathrm{g,n}}(k) \geq \mathrm{sgn}(P_{\mathrm{res}}(f))E_{\mathrm{g},f}(k), \\ k \leq N, \\ f - 4 + T_{\mathrm{r}}/T \leq k < f + T_{\mathrm{r}}/T, \ \forall f \in \mathbb{F} \end{cases}. \tag{3.4}$$

As it can be seen, the constraint ensures that γ for the next possible scenarios is at least

the same as one obtained using the scenario without activation. For the MPC, care must be taken for γ after the horizon so that feasibility and economical gain are not jeopardised. In the day-ahead analysis it was ensured $\gamma \geq 1$ which must be then guaranteed in the future as far as possible and the last variables influencing future γ must be constrained using soft constraint:

$$\begin{cases} J_\gamma = c_{\text{soft}} * \sum_{k=1}^{N} \varepsilon_\gamma(k), \\ \text{sgn}(P_{\text{res}}(f))E^*_{\text{g}}(k) \geq \text{sgn}(P_{\text{res}}(f))E_{\text{g},n}(k) - \varepsilon_\gamma(k), \\ N - 7 < k \leq N, \\ \varepsilon_\gamma(k) \geq 0. \end{cases} \tag{3.5}$$

3.1.1 Deterministic optimisation problem

The deterministic optimisation problem is omniscient about all the future EVs. Because of that, there is no need for the aggregated soft constraints as in the previous chapter. The final optimisation problem is defined as:

$$J = \min_{\boldsymbol{u}_{\text{ch}}, \boldsymbol{u}_{\text{dch}}} J_{\text{worst}} + J_\gamma,$$

$$\text{s.t.} \begin{cases} J_{\text{worst}} \geq J_{\text{n}} + \beta \sum_{\forall f} J_f, \\ J_{\text{worst}} \geq J_f + \beta J_{\text{n}} + \beta \sum_{\forall j \neq f} J_j \ , \ \forall f, \\ (2.1) - (2.10), (2.12) - (2.20), (3.1) - (3.5) \end{cases} \tag{3.6}$$

3.1.2 Stochastic optimisation problem

The unfulfilled requested flexibility activation includes penalties for the aggregator and if it occurs more often than allowed by the power grid operator, the aggregator will be disqualified from the regulation market. To guarantee the feasibility of all the possible scenarios with activation, more conservative approach is needed because of the uncertainty of the predicted EV population. Unlike the deterministic optimisation problem, the stochastic version distinguishes already present and predicted EVs. Because of that the aggregated chance-constraints (2.37) are applied only to predicted EVs.

$$J = \min_{\boldsymbol{u}_{\mathrm{ch}}, \boldsymbol{u}_{\mathrm{dch}}} J_{\mathrm{worst}} + J_{\gamma},$$

$$\text{s.t.} \begin{cases} J_{\mathrm{worst}} \geq J_{\mathrm{n}} + \beta \sum_{\forall f} J_f + J_{\mathrm{soft}}(u_{\mathrm{ch,n}}, u_{\mathrm{dch,n}}), \\ J_{\mathrm{worst}} \geq J_f + \beta J_{\mathrm{n}} + \beta \sum_{\forall j \neq f} J_j + J_{\mathrm{soft}}(u_{\mathrm{ch},f}, u_{\mathrm{dch},f}) \ , \ \forall f, \\ (2.1) - (2.10), (2.12) - (2.20), (2.37), (3.1) - (3.5) \end{cases} \tag{3.7}$$

3.2 Implementation of model predictive control

Model predictive control solves the optimisation problem where the first control variables $\boldsymbol{u}_{\mathrm{ch}}(1)$ and $\boldsymbol{u}_{\mathrm{dch}}(1)$ correspond to the next 15-minute interval. Thus, the charging of predicted EVs are optimised and included in planned total energy exchange $E_{\mathrm{g}}(1)$. For the realisation of the planned $E_{\mathrm{g}}(1)$ planned charging energies of the predicted EVs must be allocated to the newly arrived EVs. Algorithm 2 defines the mentioned charging energy allocation procedure.

The first priority is to ensure newly arrived EVs will be fully charged at departure. Afterwards the remaining energy, if there is any, is divided between the newly arrived EVs. In the case when charging energy for ensuring the newly arrived EVs will be fully charged exceeds the planned energy, charging of already present EVs is reduced. Of course, there is possibility that planned $E_{\mathrm{g}}(1)$ is not feasible, i.e. $\Delta P \neq 0$ at the end of Algorithm 2, due to significant error of the predicted EV population. Such situation did not occur during testing, despite the prediction error in simulation of stochastic MPC.

The important consequence of Algorithm 2 is the absence of the limitation on the predicted EVs in the first discrete-time interval and the rest of the optimisation horizon, regardless the number of free physical charging point operated by the EV aggregator.

3.2.1 Computational requirements

Linear optimisation problem (3.7) was set up in Python [24] using Numpy [25] and Scipy [26] modules and as a solver IBM Cplex [27] was used. Computations were run on a Windows10 personal computer with processor Intel Core i7-3770K CPU @ 3.50 GHz (4 cores) and 16 GB RAM. Computational time significantly varies. For a certain optimisation horizon computational time depends on the size of EV population since the number of charging point, i.e. state and control variables, is equal to the maximal number of present EVs. Both deterministic and stochastic MPC were tested with the same dataset where the maximal number of present EVs is 52. Size of the linear program changes through

Algorithm 2 Algorithm for applying the solution of (3.7) to the physical charging points.

P_p = sum of the optimal charging powers for the predicted EVs $u_{\mathrm{ch},p}(0)$ for the first interval
Charge the newly arrived EVs if needed to ensure feasibility of $SoE_i(k_{\mathrm{d},i}) = C_i$, sum those charging powers to P_f
Calculate $\Delta P = P_\mathrm{p} - P_\mathrm{f}$
if $\Delta P > 0$ **then**
Divide available charging power ΔP to the rest of the newly arrived EVs, by maximising $u_{\mathrm{ch},i}$ under constraints:

- $u_{\mathrm{ch},i} \leq P_{\mathrm{nom},i}$
- $u_{\mathrm{ch},i} T \leq C_i$
- $u_{\mathrm{ch},i} \leq \frac{C_i/T(P(k_{\mathrm{d},i}-k_{\mathrm{a},i}-1))}{\sum_j C_j/(P_j T(k_{\mathrm{d},j}-k_{\mathrm{a},j}-1)),\, \forall \text{ newly arrived } EV_j} \Delta P$

Update $\Delta P = P_p - P_f - \sum_i u_{\mathrm{ch},i}$
while $\Delta P > 0$ and there are more newly arrived EVs **do**
Maximise charging power of arrived EVs, if possible, with constraints:

- $u_{\mathrm{ch},i} \leq P_{\mathrm{nom},i}$
- $u_{\mathrm{ch},i} T \leq C_i$
- $u_{\mathrm{ch},i} \leq \Delta P$

Update $\Delta P = P_\mathrm{p} - P_\mathrm{f} - \sum_i u_{\mathrm{ch},i}$
end while
while $\Delta P > 0$ and there are more already present EVs **do**
Maximise charging power $u_{\mathrm{ch},j}$ to $u^+_{\mathrm{ch},j}$ of the already present EVs, with constraints:

- $u^+_{\mathrm{ch},j} \leq P_{\mathrm{nom},j}$
- $u^+_{\mathrm{ch},j} T \leq C_j$
- $u^+_{\mathrm{ch},j} - u_{\mathrm{ch},j} \leq \Delta P$

Update $\Delta P = P_\mathrm{p} - P_\mathrm{f} - \sum_i u_{\mathrm{ch},i} - \sum_j (u^+_{\mathrm{ch},j} - u_{\mathrm{ch},j})$
end while
else
while $\Delta P < 0$ and there are more already present EVs **do**
Reduce charging power $u_{\mathrm{ch},j}$ to $u^+_{\mathrm{ch},j}$ of the already present EVs, with constraints:

- $u^+_{\mathrm{ch},j} \geq 0$
- $SoE_j(k_{\mathrm{d},j}) = C_j$
- $u^+_{\mathrm{ch},j} - u_{\mathrm{ch},j} \geq \Delta P$

Update $\Delta P = P_\mathrm{p} - P_\mathrm{f} + \sum_j (u_{\mathrm{ch},j} - u^+_{\mathrm{ch},j})$
end while
end if

day since there are no scenarios with activation during night and during the recuperation period after the occurred activation. Only for horizon of 12 h computational time is close to limiting 15 minutes while the rest of the considered horizon lengths have adequate computational time. The optimisation problem with the shortest horizon of 2 h is solved under 15 seconds.

3.3 Simulation and results

Simulations are run for two Mondays, of which the first is ”under-EV-populated” and the other is ”over-EV-populated”. Under- and over-EV-populated denote that the total EV population energy request is lower and higher than the average, respectively. The first Monday is 24/09/2018 and the second is 21/10/2019. Characteristic of the two daily EV populations are given in Fig. 3.2. and 3.3. It is worth mentioning that during initial simulations without the constraint on final SoE for EV departing after the horizon in (2.4), MPC could not have enable feasible activations near the end of day.

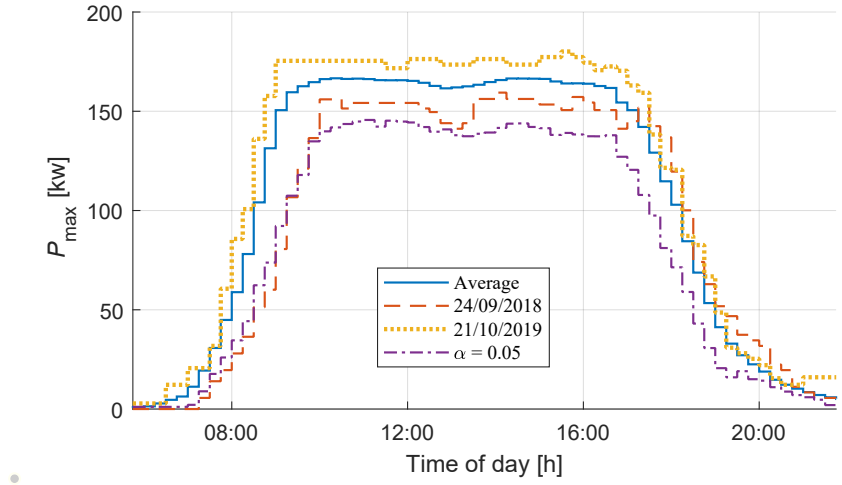

Figure 3.2: Total nominal charging power of present EVs for simulation days.

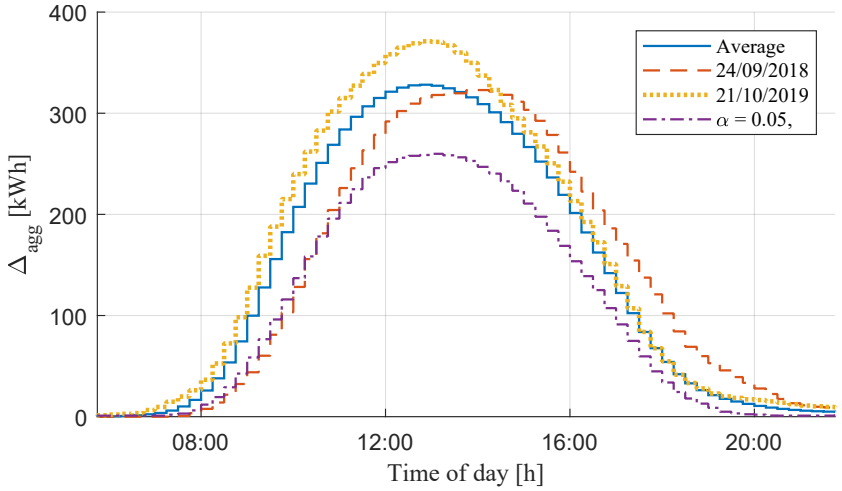

Figure 3.3: Values of Δ_{agg} for simulation days.

3.3.1 Deterministic MPC

In Fig. 3.4 it can be seen that the energy consumption in several activations is reduced more than requested. The reason is to reduce intra-day balancing penalties, since the

deviation from declared consumption profile E_g^* is not penalised during the activation. By over-reduction during the activation, EVs can be charged later when the deviation is penalised.

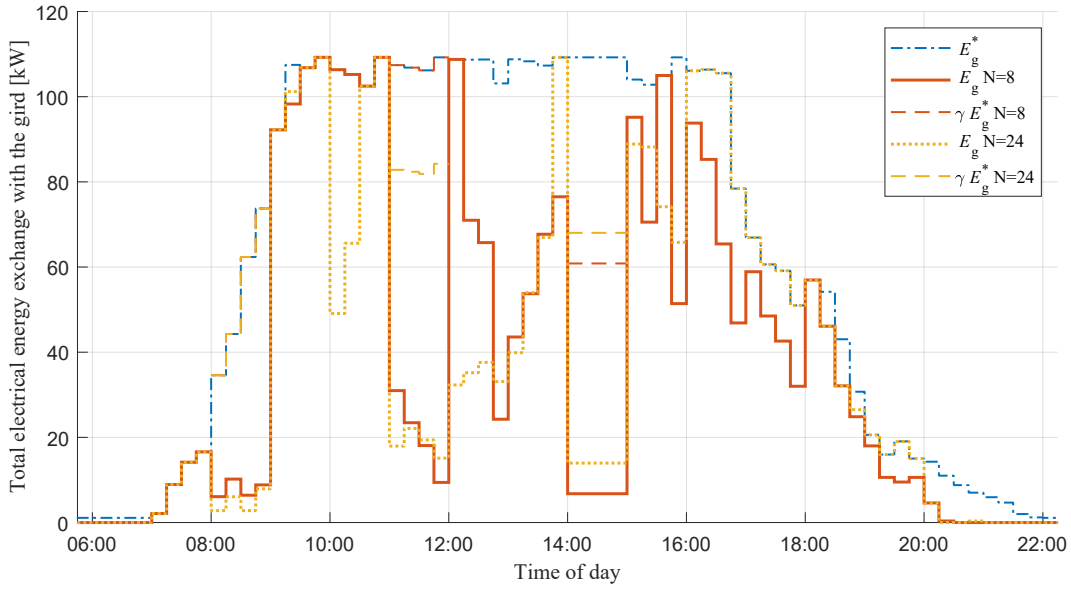

Figure 3.4: Comparison of deterministic MPC with horizons of 2 h and 6 h, with two activations occurred, for Monday with under-average population.

Benefits of longer optimisation horizon can be seen in Fig. 3.5. where longer horizon recognise the need for earlier charging in order to prevent surpassing the contracted peak power.

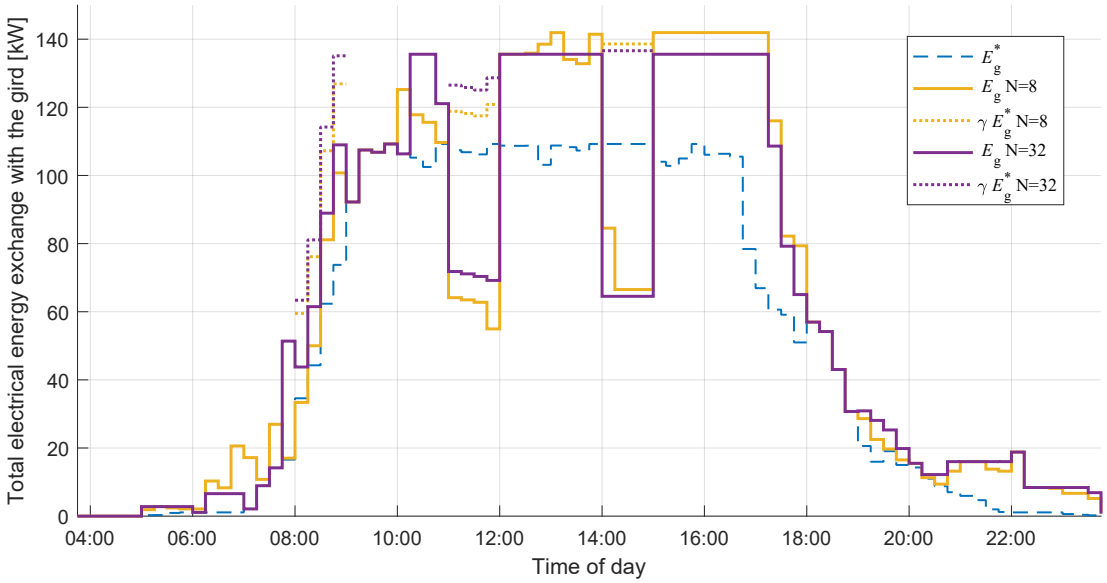

Figure 3.5: Comparison of deterministic MPC with horizons of 2 h and 8 h, with three activations occurred, for Monday with above-average population

MPC with horizon of 8 h (32 steps ahead) at 10:00 can see total charging request until 18:00 and thus starts charging with the contracted peak power already at 10:15. Both Fig.

3.4 and Fig. 3.5 show how correction coefficient γ influence flexibility reference according to the total energy exchange one hour prior to activation. It is shown in Table 3.1 how intra-day balancing penalties significantly reduces with the number of activations in under-average day, which is not the case for above average day. Due to additional charging during recuperation period after activation, intra-day penalties increases with the number of activation but the reward for fulfilled activation surpasses it and the aggregator makes a profit at the end.

Table 3.1: Cost analysis of deterministic MPC with the horizon of 6 h.

Monday with under-average population

Scenario	ΔJ_{pp}	J_{id}	J_{bd}	J_{res}	J_{act}	Total	Savings	Savings /%
ASAP charging	0.00	37.74	0.00	/	/	37.74	/	/
Without contracted flexibility	0.00	33.60	0.00	0.00	0.00	33.60	-4.14	-16.75
Without activation	0.00	33.76	0.00	-14.44	0.00	19.32	-18.42	-48.81
With activation: 47	0.00	26.67	0.04	-14.44	-7.63	4.64	-33.10	-87.71
With activations: 37, 53	0.00	19.55	0.00	-14.44	-13.70	-8.58	-46.32	-122.73
With activations: 33, 45, 58	0.00	15.32	4.94	-14.44	-15.77	-8.45	-46.19	-122.39

Monday with above-average population

Scenario	ΔJ_{pp}	J_{id}	J_{bd}	J_{res}	J_{act}	Total	Savings	Savings /%
ASAP charging	1.41	12.43	0.00	/	/	13.84	/	/
Without contracted flexibility	0.00	13.37	0.00	0.00	0.00	13.37	-0.47	-3.40
Without activation	0.00	13.57	0.00	-14.44	0.00	-0.87	-14.71	-106.29
With activation: 47	0.00	18.06	0.00	-14.44	-6.26	-2.65	-16.49	-119.15
With activations: 37, 53	0.40	19.40	0.00	-14.44	-11.60	-6.24	-20.08	-145.09
With activations: 33, 45, 58	0.03	20.78	0.00	-14.44	-16.67	-10.31	-24.15	-174.49

How realised total cost depends on the length of the optimisation horizon is shown in Table 3.2. The total cost for one realisation of activation does not drop continuously. The reason might be in the nature of the worst-case analysis. On the longer horizon, the optimisation problem minimises the worst scenario that is not certain to happen at all, causing adoption at the expense of the near future scenario.

Table 3.2: Deterministic MPC results for different horizons

Monday with under-average population					
/€	2 h	4 h	6 h	8 h	10
ASAP charging	37.74	37.74	37.74	37.74	37.74
Without contracted flexibility	33.58	33.64	33.60	33.58	33.58
Without activation	33.85	33.93	33.72	33.75	33.75
With activation: 47,	23.60	18.97	18.77	18.86	18.84
With activation: 37, 53	9.57	6.30	5.11	5.14	5.14
With activation 33, 45, 57	5.71	-1.61	-0.91	-0.83	-0.81
Monday with above-average population					
/€	2 h	4 h	6 h	8 h	10 h
ASAP charging	13.84	13.84	13.84	13.84	13.84
Without contracted flexibility	13.50	13.40	13.37	13.40	13.39
Without activation	14.07	13.73	13.57	13.86	13.89
With activation: 47,	13.81	12.27	11.79	10.54	10.74
With activation: 37, 53	8.25	7.79	8.20	8.38	8.26
With activation 33, 45, 57	3.68	1.99	4.13	2.11	-0.76

3.3.2 Stochastic MPC

For the validation of the stochastic MPC the prediction error is simulated by randomly changing parameters of the original futures EVs using following equations:

$$P_{\mathrm{nom},p} = P_{\mathrm{nom},i} * \mathcal{N}(1, 0.3^2), \tag{3.8}$$

$$C_{\mathrm{nom},p} = C_{\mathrm{nom},i} * \mathcal{N}(1, 0.3^2), \tag{3.9}$$

$$k_{\mathrm{a},p} = \max(0, k_{\mathrm{a},i} + \mathrm{round}(\mathcal{N}(0, 0.3^2))), \tag{3.10}$$

$$k_{\mathrm{d},p} = \max(3, k_{\mathrm{d},i} + \mathrm{round}(\mathcal{N}(0, 0.3^2))), \tag{3.11}$$

where index i and P denote the original future EV and predicted EV, respectively. $\mathcal{N}(\mu, \sigma)$ is a normally distributed random variable with mean μ and variance σ^2. The used value of variance $\sigma^2 = 0.3^2$ is chosen as the value that represents quite significant prediction error. After applying (3.8)-(3.11) some predicted EVs can be unfeasible so the full procedure of generating predicted EV population that ensures the EV feasibility is given in Algorithm 3. Seed for random number generator at the beginning of every iteration of Algorithm 3 is the same for every simulation with different horizon to ensure that all horizons are validated with same prediction on the shared part of the horizon.

Several iterations of stochastic MPC with longer horizon could not have fulfil activa-

Algorithm 3 Generating noised EVs prediction

Require: m real future EVs on the horizon, indexed with i
Ensure: m predicted future EVs, indexed with p

```
m = 0
while i ≤ m do
    Apply noise using (3.8)-(3.11)
    if (k_{d,p} − k_{a,p} − 1)P_{nom,p}T < C_{nom,p} then
        Δ_C = C_{nom,p} − (k_{d,p} − k_{a,p} − 1)P_{nom,p}T
        P_{nom,p} = P_{nom,p}(1 + Δ_C / (2(k_{d,p} − k_{a,p} − 1)P_{nom,p}T))
        C_{nom,p} = C_{nom,p} − Δ_C
    end if
    m = m + 1
    Add EV_p to the predicted population
end while
```

tions close to the end of the horizon, but the later iterations that have had updated information of the present EV population successfully planed all possible activations. That is reasonable because the share of the flawed predicted EVs in population population increases along the optimisation horizon.

Simulation results in Table 3.3 show expected descending trend of total operational cost with the number of activations. Total cost of the stochastic MPC for the above-average population is higher than the ASAP-charging baseline, but when the savings from flexibility reward and day-ahead energy market are taken into account, the aggregator makes profit at the end.

The performance of deterministic and stochastic MPC is compared in Fig. 3.6 and Fig. 3.7. Stochastic MPC has higher cost in most simulations. Simulations with lower cost of stochastic MPC can be justified with the worst case scenario minimisation. A charging schedule based on a flawed prediction may be more favourable for a non-critical activation scenario in a worst-case optimisation than the schedule obtained from perfect prediction

3.4 Conclusion

In this chapter the optimisation problems for deterministic and stochastic MPC are defined to enable the EV aggregator to participate in tertiary frequency regulation. Both MPCs are validated for different horizon lengths on two days, one with under-average and one with above-average EV populations. Simulations showed that the MPC can ensure feasibility of all flexibility activation and economical benefits for the EV aggregator.

Table 3.3: Stochastic MPC results for different horizons

Monday with under-average population

/€	2 h	4 h	6 h	8 h	10 h
ASAP charging	37.74	37.74	37.74	37.74	37.74
Without contracted flexibility	33.78	33.63	33.61	32.59	33.90
Without activation	33.90	34.50	34.90	33.21	35.19
With activation: 47,	25.25	22.82	23.70	19.46	24.67
With activation: 37, 53	9.69	7.90	5.67	4.21	5.77
With activation 33, 45, 57	5.55	-0.69	-0.50	-2.95	-0.30

Monday with above-average population

/€	2 h	4 h	6 h	8 h	10 h
ASAP charging	13.84	13.84	13.84	13.84	13.84
Without contracted flexibility	13.50	13.41	13.37	13.49	13.50
Without activation	14.06	13.54	14.30	15.49	15.59
With activation: 47,	12.16	12.72	12.97	13.87	14.32
With activation: 37, 53	8.04	9.55	9.18	9.52	9.26
With activation 33, 45, 57	2.82	1.11	2.93	4.05	3.18

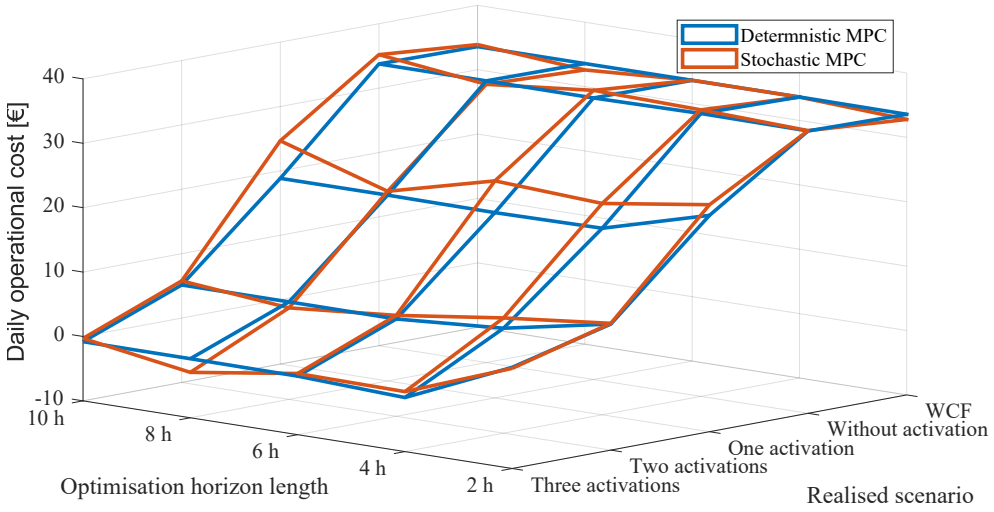

Figure 3.6: Deterministic and stochastic MPC results comparison for under-average population

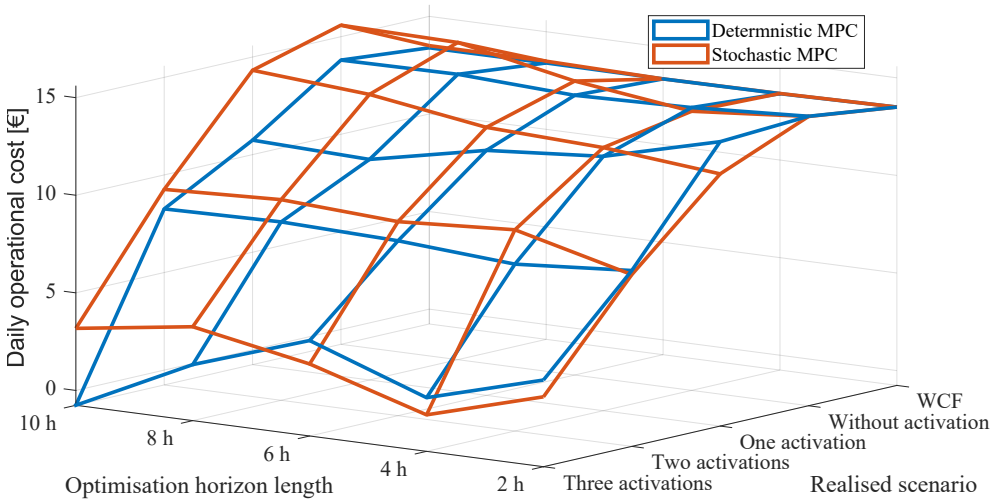

Figure 3.7: Deterministic and stochastic MPC results comparison for above-average population

Chapter 4

Aggregated representation of electric vehicles population

4.1 Introduction

4.1.1 Motivation and hypothesis

The state-of-the-art misses a method to describe a population of heterogeneous EVs connected to charging stations that is suitable both for population prediction based on machine learning and for charging scheduling with demand response ability assessment. The method to fill the mentioned gap is in this chapter. Its main usage steps are shown in Fig. 4.1.

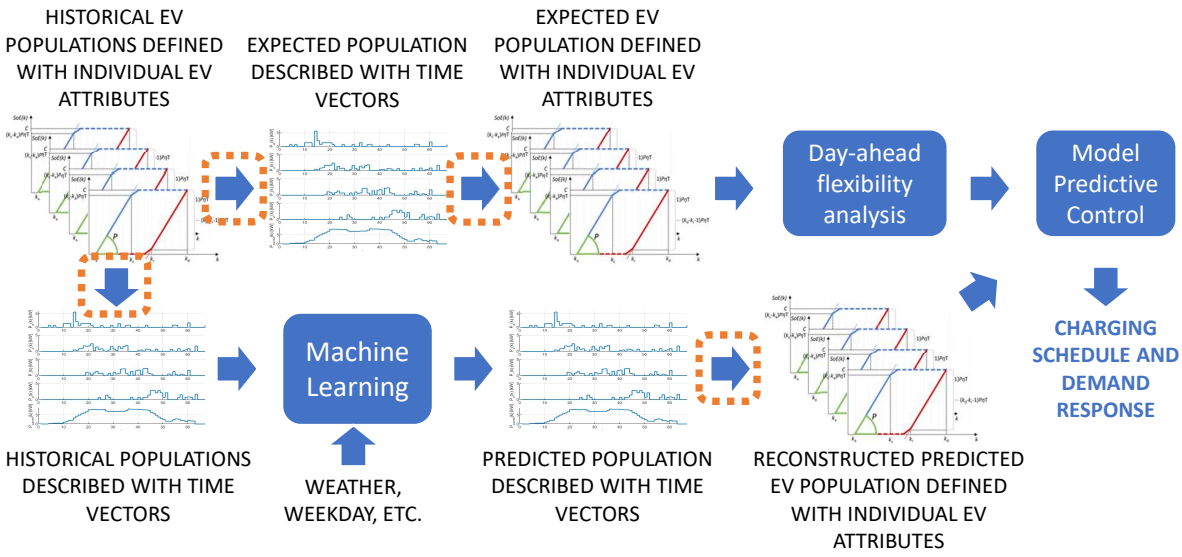

Figure 4.1: The proposed concept with the chapter focus marked with orange [13].

The proposed method transforms historical individual on-arrival commitment data

[10] to five discrete-time vectors related to envelopes of feasible charging powers and charging states for the EV population whereas these signals are suitable for quantification of demand response ability. The method has the following features:

- it captures population's flexibility to offer demand response;
- it can describe any EV population represented in discrete-time;
- it allows that every EV has a different nominal charging power, relative capacity and connection time.

From the first and the most important feature follows the main hypothesis of this chapter: the proposed aggregated representation of an EV population has small enough loss of information so it can be used for charging scheduling and DR of an EV aggregator.

The aggregated representation and the corresponding reconstructed individual EV data can be input to any optimisation problem or demand response scheme that is compatible with individual EV description in Table 4.1.

4.1.2 EV aggregator context

This thesis is focused on a parking lot equipped with charging points (CPs) that are controlled by an aggregator. The aggregator is an entity that achieves a profit by demand response in excess to selling electrical energy to the EVs. Charging schedule and power of all CPs is optimised by the aggregator to maximise its profit while respecting charging needs of the EVs. Its corresponding optimisation problems for day-ahead analysis and MPC control are given in the later chapters. On its arrival to the parking lot and connection to the CP, the EV owner provides the data about the planned departure time, its charging target and allowed power. With this data an EV becomes a charging task for the aggregator.

An EV population is made of all EVs connected to the aggregator's CPs during any time interval of interest. The number of the CPs is finite and is not important for the proposed method. The aggregator optimises the charging schedule for the whole population at once. The concept of the aggregator control that utilises the proposed representation method for the population of charging EVs is shown in Fig. 4.1.

4.1.3 Outline

The remainder of the chapter is organised as follows. Section 4.2 describes the proposed representation method. The charging optimisation problem used to exploit the introduced representation is briefly introduced in Section 4.3 and the validation of the main hypothesis is given in Section 4.4. The conclusion is given in Section 4.5.

Table 4.1: Set of parameters describing an individual EV (EV charging session)

P_{nom}	Maximum charging power of a charger or a battery
C	Relative energy capacity of the battery defined as the difference of the battery's nominal capacity and the state of energy at the arrival
k_{a}	The first discrete-time instant when EV charging is possible - the one after the arrival of the EV
k_{d}	Discrete-time instant of departure

4.2 Individual Vehicle Data and Aggregated Representation

Individual EV data consists of a set of parameters shown in Table 4.1, similar to [10]. From the optimisation perspective, an EV charging task consists of constraints on relative state of energy SoE_i, charging $u_{\text{ch},i}$ and discharging energies $u_{\text{dch},i}$, where index 'i' denotes different EVs. Relative SoE_i is always zero at the moment of the arrival and equal to relative capacity C_i at the moment of departure. These constraints can be visualised with Fig. 4.2, similar to approaches in [28, 29, 30]. Full blue line is the upper constraint on EV's state of energy based on as-soon-as-possible (ASAP) charging and derived from the EV's nominal maximum charging power $P_{\text{nom},i}$, relative capacity C_i and discretisation time T. Full red line is the lower constraint based on as-late-as-possible (ALAP) charging and taking care about the EV being fully charged at the departure time instant. In Fig. 4.2. it can be seen that full blue and red lines are not completely straight which is a consequence of time discretisation and that C is not a multiple of $P_{\text{nom}}\eta_{\text{ch}}T$, where η_{ch} denotes the charging efficiency of the battery and its corresponding power converter that is assumed to be the same for all EVs. This assumption is justified considering that the historical EV data comes only from the side of CPs as charging tasks, as described in subsection 4.4.1, and so no data from the vehicle is needed. Namely, effectively the relative capacity in the representation of the EV could be also regarded as C/η_{ch}, i.e. as already with included efficiency.

Dashed blue line is explicitly defined with C while dashed red line is a consequence of a decision that in any case the EV should not leave the parking lot with less energy than it has arrived with, no matter if the owner approved possible discharging of the battery or not. Both in Fig. 4.2. and further in this thesis, $k \in \{1, 2, ..., N\}$ denotes a discrete-time instant where $N \in \mathbb{N}$ is the length ofobserving horizon on which the EV population is analysed. The observing horizon matches optimisation or prediction horizon, depending on the application of the aggregated representation.

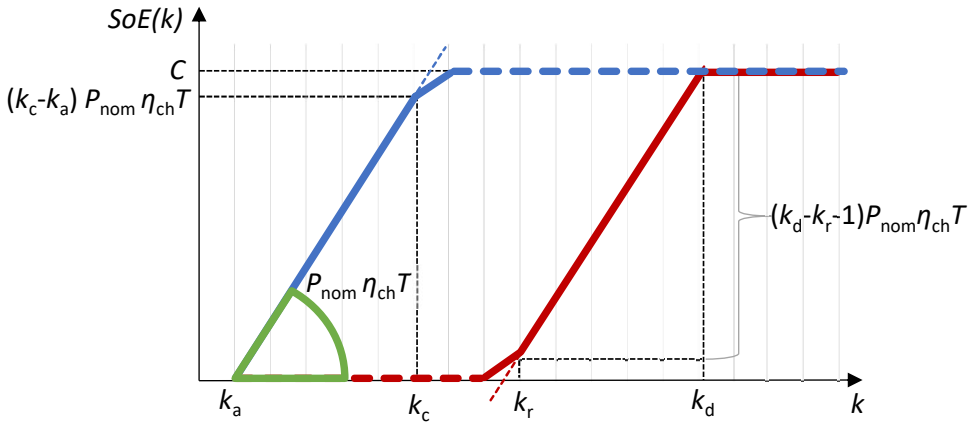

Figure 4.2: Visualisation of envelope of feasible charging powers and charging states for a vehicle connected to the charging point, where k_c and k_r are auxiliary characteristic discrete-time instants defined in subsection 4.2.1. [13]

The proposed method represents an EV population with five discrete-time signals related to envelopes of feasible charging powers and charging states whereas one such envelope is shown in Fig. 4.2. The method consists of two algorithms, marked with orange dashed line in Fig. 4.1. The first, Algorithm 4, constructs the five discrete-time signals from the individual data while the other, Algorithm 5, reconstructs the individual EV data of the population back from the discrete-time signals. Algorithm 4 is used to transform historical individual EV data to obtain data that can be input to a machine learning model. The output of the model is the predicted population described with aggregated representation and needs to be transformed to individual EV data using Algorithm 5 to be used for the optimisation problem construction.

The feasible solution in Algorithm 5 cannot be guaranteed. Algorithm 5 is thus upgraded to Algorithm 6 that can always return an EV population described with individual EV data. Algorithm 6 was used to experimentally validate the main hypothesis about near-equivalence of the optimisation results obtained with the original and the reconstructed EV population.

4.2.1 Aggregated representation

Input in Algorithm 4 is an EV population described with individual data and length N of the observing horizon of interest. The outputs of the algorithm are discrete-time signals $\boldsymbol{P}_{\mathrm{a}}$, $\boldsymbol{P}_{\mathrm{c}}$, $\boldsymbol{P}_{\mathrm{d}}$, $\boldsymbol{P}_{\mathrm{r}}$ and $\boldsymbol{P}_{\mathrm{const}}$ that together describe the original EV population.

Two characteristic discrete-time instants, $k_{\mathrm{c},i}$ and $k_{\mathrm{r},i}$, are determined for every EV in the population to calculate the EV's contribution to the time vectors of the population. Time instants $k_{\mathrm{c},i}$ and $k_{\mathrm{r},i}$ are shown in Fig. 4.2 and it can be seen that $k_{\mathrm{c},i}$ is the last time instant of ASAP charging while $k_{\mathrm{r},i}$ is the first time instant of charging with the

maximum power in ALAP case. The time instants are derived as follows:

$$k_{\mathrm{c},i} = k_{\mathrm{a},i} + \left\lfloor \frac{C_i}{P_{\mathrm{nom},i} T \eta_{\mathrm{ch}}} \right\rfloor, \tag{4.1}$$

$$k_{\mathrm{r},i} = k_{\mathrm{d},i} - \left\lfloor \frac{C_i}{P_{\mathrm{nom},i} T \eta_{\mathrm{ch}}} \right\rfloor, \tag{4.2}$$

where i denotes a specific EV.

The first time vector $\boldsymbol{P}_{\mathrm{c}} \in \mathbb{R}^N$ carries information about the charging power decrement in case of ASAP charging due to reaching battery capacity and thus implicitly contains information about the capacity of EVs that are part of the population. It is constructed using the characteristic time instant $k_{\mathrm{c},i}$ and can be defined as:

$$P_{\mathrm{c}}(k) = \sum_i P_{\mathrm{nom},i},\ \forall i | k_{\mathrm{c},i} = k. \tag{4.3}$$

Equation (4.3) is only valid under the assumption that $P_{\mathrm{nom},i}\eta_{\mathrm{ch}}T(k_{\mathrm{c},i} - k_{\mathrm{a},i}) = C_i$. The assumption can be avoided if it is defined that in ASAP charging mode the EV charging will be turned off gradually through two steps, as shown in Fig. 4.2. The initial maximal charging power $P_{\mathrm{nom},i}$ is first reduced at the time instant $k_{\mathrm{c},i}$ to $P_{\mathrm{rem},i}$ so that the EV will be fully charged right at the next time instant. Power $P_{\mathrm{rem},i}$ is determined with:

$$P_{\mathrm{rem},i} = \frac{\mathrm{mod}(C_i, P_{\mathrm{nom},i}\eta_{\mathrm{ch}}T)}{\eta_{\mathrm{ch}}T}, \tag{4.4}$$

where $\mathrm{mod}(\cdot,\cdot)$ is the remainder (modulo) operator. Then, at time instant $k_{\mathrm{c},i}+1$ charging is completely turned off. Using (4.4) vector $\boldsymbol{P}_{\mathrm{c}}$ is finally defined with:

$$\begin{aligned} P_{\mathrm{c}}(k) = \sum_i (P_{\mathrm{nom},i} - P_{\mathrm{rem},i}) + \sum_j P_{\mathrm{rem},j}, \\ \forall i \mid k_{\mathrm{c},i} = k,\ \ \forall j \mid k_{\mathrm{c},j} = k-1. \end{aligned} \tag{4.5}$$

It can be seen that the first and the second sum correspond to power decrements from the first and the second step, respectively, represented with full blue lines in Fig. 4.2.

Similarly, in the case of ALAP charging mode, EV charging is gradually turned on just on time so that EV is fully charged at $k_{\mathrm{d},i}$. Vector $\boldsymbol{P}_{\mathrm{r}} \in \mathbb{R}^N$ carries information about the mentioned charging power increments in ALAP charging mode, marked with full red lines in Fig. 4.2. and it is defined as:

$$\begin{aligned} P_{\mathrm{r}}(k) = \sum_i P_{\mathrm{rem},i} + \sum_j (P_{\mathrm{nom},j} - P_{\mathrm{rem},j}), \\ \forall i \mid k_{\mathrm{r},i} = k+1,\ \ \forall j \mid k_{\mathrm{r},j} = k. \end{aligned} \tag{4.6}$$

The subsequent two vectors are quite intuitive – $\boldsymbol{P}_{\mathrm{a}}(k) \in \mathbb{R}^N$ and $\boldsymbol{P}_{\mathrm{d}}(k) \in \mathbb{R}^N$ give information about power of all maximum charging powers related to EVs arriving and departing at time interval k, respectively:

$$P_{\mathrm{a}}(k) = \sum_i P_{\mathrm{nom},i} \ \forall i | k_{\mathrm{a},i} = k, \tag{4.7}$$

$$P_{\mathrm{d}}(k) = \sum_i P_{\mathrm{nom},i} \ \forall i | k_{\mathrm{d},i} = k. \tag{4.8}$$

The last vector $\boldsymbol{P}_{\mathrm{const}} \in \mathbb{R}^N$ is the cumulative EV population charging power in the *constant* charging mode where an EV is being charged with constant power from the first time instant after its arrival $k_{\mathrm{a},i}$ until the last time instant before departure $k_{\mathrm{d},i}$. Of course, constant charging power for every EV is determined so that the EV is fully charged at departure. Vector $\boldsymbol{P}_{\mathrm{const}}$ is defined as:

$$\begin{aligned} P_{\mathrm{const}}(k) = \sum_i \frac{C_i}{T(k_{\mathrm{d},i} - k_{\mathrm{a},i})\eta_{\mathrm{ch}}}, \\ \forall i \mid k_{\mathrm{a},i} \leq k < k_{\mathrm{d},i}. \end{aligned} \tag{4.9}$$

Finally, the construction procedure of $\boldsymbol{P}_{\mathrm{a}}, \boldsymbol{P}_{\mathrm{c}}, \boldsymbol{P}_{\mathrm{r}}, \boldsymbol{P}_{\mathrm{d}}$ and $\boldsymbol{P}_{\mathrm{const}}$ is described with Algorithm 4.

Algorithm 4 Construction of population describing vectors

Require: $\mathcal{EV}_1$ described with tuples $(P_{\mathrm{nom}}, C, k_{\mathrm{a}}, k_{\mathrm{d}})$
Ensure: $\mathcal{EV}_2$ described with $\boldsymbol{P}_{\mathrm{a}}, \boldsymbol{P}_{\mathrm{c}}, \boldsymbol{P}_{\mathrm{r}}, \boldsymbol{P}_{\mathrm{d}}, \boldsymbol{P}_{\mathrm{const}}$
  initialise $\boldsymbol{P}_{\mathrm{a}}, \boldsymbol{P}_{\mathrm{c}}, \boldsymbol{P}_{\mathrm{r}}, \boldsymbol{P}_{\mathrm{d}}, \boldsymbol{P}_{\mathrm{const}} = \boldsymbol{0} \in \mathbb{R}^N$
  for all $EV_i \in \mathcal{EV}_1$ **do**
    calculate k_{c} and k_{r} ▷ (4.1), (4.2)
    add contribution of EV_i to $\boldsymbol{P}_{\mathrm{a}}, \boldsymbol{P}_{\mathrm{c}}, \boldsymbol{P}_{\mathrm{r}}, \boldsymbol{P}_{\mathrm{d}}, \boldsymbol{P}_{\mathrm{const}}$ ▷ (4.4)-(4.9)
  end for

An example of a population represented with these vectors and time discretisation $T = 15$ min can be seen in Fig. 4.3. Every colour represents a contribution of one EV.

4.2.2 Reconstruction of individual EV data

In this subsection it is shown how individual EVs descriptions can be reconstructed from the aggregated representation introduced in the previous section.

Lemma 4.2.1 allows to describe any EV population with a population $\mathcal{EV}_2$ that contains only EVs with ratio $\frac{C}{P_{\mathrm{nom}} T \eta_{\mathrm{ch}}} \in \mathbb{N}$ which enables reversible transformation between individual data tuple $(P_{\mathrm{nom}}, C, k_{\mathrm{a}}, k_{\mathrm{d}})$ and the tuple $(P_{\mathrm{nom}}, k_{\mathrm{a}}, k_{\mathrm{c}}, k_{\mathrm{r}}, k_{\mathrm{d}})$. Discrete-time instants k_{c} and k_{r} are derived from individual data by using (4.1) and (4.2) while in opposite

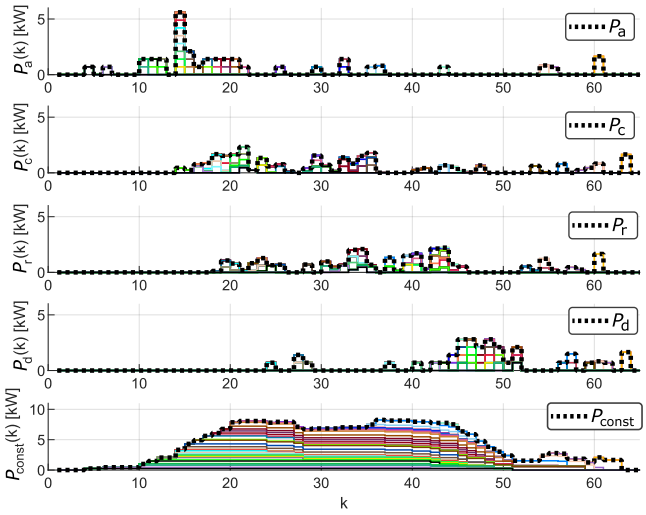

Figure 4.3: Example of a population containing all EVs from one day, represented using vectors $\boldsymbol{P}_\mathrm{a}, \boldsymbol{P}_\mathrm{c}, \boldsymbol{P}_\mathrm{r}$, $\boldsymbol{P}_\mathrm{d}$ and $\boldsymbol{P}_\mathrm{const}$. The last EV (orange) departed at $k = 64$ and the rest of the day is not shown for brevity. [13]

direction P_nom is calculated from:

$$C_i = P_{\mathrm{nom},i}(k_{\mathrm{c},i} - k_{\mathrm{a},i})T\eta_\mathrm{ch}. \tag{4.10}$$

Lemma 4.2.1. *Electric vehicle EV_1 with $\frac{C_1}{P_{nom,1}T\eta_\mathrm{ch}} \in \mathbb{R}$ can be rewritten as EV_2 and EV_3 defined with attributes obtained from equations:*

$$\left\lfloor \frac{C_1}{P_{nom,1}T\eta_\mathrm{ch}} \right\rfloor = \frac{C_2}{P_{nom,2}T\eta_\mathrm{ch}} = \frac{C_3}{P_{nom,3}T\eta_\mathrm{ch}} - 1\,, \tag{4.11}$$

$$P_{nom,2} = P_{nom,1} - P_{\mathrm{rem},1}, \tag{4.12}$$

$$P_{nom,3} = P_{\mathrm{rem},1}, \tag{4.13}$$

$$C_1 = C_2 + C_3, \tag{4.14}$$

where $\frac{C_2}{P_{nom,2}T\eta_\mathrm{ch}} \in \mathbb{N}$, $\frac{C_3}{P_{nom,3}T\eta_\mathrm{ch}} \in \mathbb{N}$, time instants k_a and k_d are the same for all three EVs.

Thus, the set $\mathcal{K}_N$ of all possible unique tuples $(k_{\mathrm{a},i}, k_{\mathrm{c},i}, k_{\mathrm{r},i}, k_{\mathrm{d},i})$ is defined:

$$\mathcal{K}_N = \left\{ (k_\mathrm{a}, k_\mathrm{c}, k_\mathrm{r}, k_\mathrm{d}) \,\middle|\, \begin{array}{c} 1 < k_\mathrm{d} \leq N, \\ 1 \leq k_\mathrm{a} < k_\mathrm{c} \leq k_\mathrm{d}, \\ 1 \leq k_\mathrm{a} \leq k_\mathrm{r} < k_\mathrm{d}, \\ k_\mathrm{d} - k_\mathrm{r} = k_\mathrm{c} - k_\mathrm{a} \end{array} \right\}. \tag{4.15}$$

Constraints on $k_\mathrm{a}, k_\mathrm{c}, k_\mathrm{r}$ and k_d in (4.15) assure that all EVs are feasible meaning that they depart after they arrive and respect the assumption that they will be fully charged.

It is possible that two or more EVs have the same parameters $(k_\mathrm{a}, k_\mathrm{c}, k_\mathrm{r}, k_\mathrm{d}) \in \mathcal{K}_N$. Lemma 4.2.2 allows to represent them with only one EV and population $\mathcal{EV}_2$ can consist of only one EV for every element in $\mathcal{K}_N$ with associated power $P_{\mathrm{sol},i} \geq 0$ in order to describe any original population. Dimension M_N of vector $\boldsymbol{P}_\mathrm{sol} \in \mathbb{R}^{M_\mathrm{N}}$ is equal to the cardinal number of the set $\mathcal{K}_N$.

Lemma 4.2.2. *All electric vehicles with the same arrival k_a, departure k_d and the same ratio $\frac{C_i}{P_{nom,i} T \eta_\mathrm{ch}} \in \mathbb{N}$ can be represented as one electric vehicle with $C = \sum_i C_i$ and $P = \sum_i P_{nom,i}$.*

For easier following, proofs of Lemma 4.2.1 and Lemma 4.2.2 are given at the end of this subsection.

For a population $\mathcal{EV}_2$ to have the same aggregated representation as the original population $\mathcal{EV}_1$, $\boldsymbol{P}_\mathrm{sol}$ must be a solution of the following underdetermined equation system:

$$\begin{cases} \sum_i P_{\mathrm{sol},i} = P_\mathrm{a}(k), \ \ \forall i \in \{1,2,...,M_\mathrm{N} \mid k_{\mathrm{a},i} = k\}, \\ \sum_i P_{\mathrm{sol},i} = P_\mathrm{c}(k), \ \ \forall i \in \{1,2,...,M_\mathrm{N} \mid k_{\mathrm{c},i} = k\}, \\ \sum_i P_{\mathrm{sol},i} = P_\mathrm{d}(k), \ \ \forall i \in \{1,2,...,M_\mathrm{N} \mid k_{\mathrm{d},i} = k\}, \\ \sum_i P_{\mathrm{sol},i} = P_\mathrm{r}(k), \ \ \forall i \in \{1,2,...,M_\mathrm{N} \mid k_{\mathrm{r},i} = k\}, \\ \sum_i P_{\mathrm{sol},i} \frac{k_{\mathrm{c},i} - k_{\mathrm{a},i}}{k_{\mathrm{d},i} - k_{\mathrm{a},i}} = P_\mathrm{const}(k), \\ \forall i \in \{1,2,...,M_\mathrm{N} \mid k_{\mathrm{a},i} \leq k < k_{\mathrm{d},i}\}, \\ P_{\mathrm{sol},i} \geq 0, \ , \ \forall i \in \{1,2,...,M_\mathrm{N}, \} \\ \forall k \in \{1,2,...,N\}. \end{cases} \tag{4.16}$$

Of course, the case when element $P_{\mathrm{sol},i} = 0$ is understood as there is no EV with parameters $\{k_{\mathrm{a},i}, k_{\mathrm{c},i}, k_{\mathrm{r},i}, k_{\mathrm{d},i}\}$ in the population $\mathcal{EV}_2$. On the other hand, if $P_{\mathrm{sol},i} > 0$, an EV with nominal charging power $P_{\mathrm{sol},i}$, capacity C_i calculated by using (4.10), arrival and departure at time instants $k_{\mathrm{a},i}$ and $k_{\mathrm{d},i}$, respectively, is added to the reconstructed population $\mathcal{EV}_2$.

For a more compact representation, the relations (4.16) can be rewritten as:

$$\begin{aligned} A_N \boldsymbol{P}_\mathrm{sol} &= \boldsymbol{\theta}, \\ I \boldsymbol{P}_\mathrm{sol} &\geq \boldsymbol{0}, \end{aligned} \tag{4.17}$$

where $\boldsymbol{\theta} = [\boldsymbol{P}_{\mathrm{a}}^{\top}, \boldsymbol{P}_{\mathrm{c}}^{\top}, \boldsymbol{P}_{\mathrm{r}}^{\top}, \boldsymbol{P}_{\mathrm{d}}^{\top}, \boldsymbol{P}_{\mathrm{const}}^{\top}]^{\top}$ and matrix A_{N} follows from (4.16).

Finally, the individual EV data reconstruction procedure is defined with the Algorithm 5.

Algorithm 5 Reconstruction of individual EV descriptions

Require: $\mathcal{EV}_1$ described with $\boldsymbol{\theta} = [\boldsymbol{P}_{\mathrm{a}}^{\top}, \boldsymbol{P}_{\mathrm{c}}^{\top}, \boldsymbol{P}_{\mathrm{r}}^{\top}, \boldsymbol{P}_{\mathrm{d}}^{\top}, \boldsymbol{P}_{\mathrm{const}}^{\top}]^{\top}$
Ensure: $\mathcal{EV}_2$ described with tuples $(P, C, k_{\mathrm{a}}, k_{\mathrm{d}})$
  initialise $\mathcal{EV}_2 = \emptyset$
  find $\boldsymbol{P}_{\mathrm{sol}}$ as a solution of (4.17)
  for all $P_{\mathrm{sol},i} > 0$ **do**
    add $EV_i = (P_{\mathrm{sol},i}, C_i, k_{\mathrm{a},i}, k_{\mathrm{d},i})$ to $\mathcal{EV}_2$ ▷ (4.10)
  end for

Proof of Lemma 4.2.1

Proof. If a realistic EV_1 is taken for an example with attributes $\{C_1, P_{\mathrm{nom},1}, k_{\mathrm{a},1}, k_{\mathrm{d},1}\}$ the corresponding $k_{\mathrm{c},1}$, $k_{\mathrm{r},1}$ and $P_{\mathrm{rem},1}$ can be calculated using (4.1), (4.2) and (4.4). Since only one EV - EV_1 is observed, the aggregated representation vectors consist only of several non-zero elements according to (4.5)-(4.9):

$$P_{\mathrm{a}}(k_{\mathrm{a},1}) = P_{\mathrm{nom},1}, \tag{4.18}$$

$$P_{\mathrm{c}}(k_{\mathrm{c},1}) = P_{\mathrm{nom},1} - P_{\mathrm{rem},1}, \qquad P_{\mathrm{c}}(k_{\mathrm{c},1}+1) = P_{\mathrm{rem},1}, \tag{4.19}$$

$$P_{\mathrm{r}}(k_{\mathrm{r},1}) = P_{\mathrm{rem},1}, \qquad P_{\mathrm{r}}(k_{\mathrm{r},1}-1) = P_{\mathrm{nom},1} - P_{\mathrm{rem},1}, \tag{4.20}$$

$$P_{\mathrm{d}}(k_{\mathrm{d},1}) = P_{\mathrm{nom},1}, \tag{4.21}$$

$$P_{\mathrm{const}}(k) = \frac{C_1}{T(k_{\mathrm{d},1} - k_{\mathrm{a},1})\eta_{\mathrm{ch}}}, \qquad \forall k | k_{\mathrm{a},1} \leq k < k_{\mathrm{d},1}. \tag{4.22}$$

By solving relations (4.17) with vectors values from (4.22), two reconstructed EVs are obtained with attributes shown in Table 4.2. If capacities C_2 and C_3 are summed, it can be seen in (4.23) that together they are equal to the initial C_1 according to (4.4). In the second expression of (4.23) the first and the second member can be recognised as parts of the capacity C_1 which are the multiplier of $P_{\mathrm{nom},1} * T$ and the remaining part, respectively.

$$\begin{aligned} C_2 + C_3 =& (P_{\mathrm{nom},1} - P_{\mathrm{rem},1})T(k_{\mathrm{c},1} - k_{\mathrm{a},1})\eta_{\mathrm{ch}} + \\ & P_{\mathrm{rem},1}T(k_{\mathrm{c},1} - k_{\mathrm{a},1} + 1)\eta_{\mathrm{ch}} \\ =& P_{\mathrm{nom},1}T(k_{\mathrm{c},1} - k_{\mathrm{a},1})\eta_{\mathrm{ch}} + P_{\mathrm{rem},1}T\eta_{\mathrm{ch}} \\ =& C_1 \end{aligned} \tag{4.23}$$

It can be seen in Table 4.2. that $P_{\mathrm{nom},1} = P_{\mathrm{nom},2} + P_{\mathrm{nom},3}$, $k_{\mathrm{a},1} = k_{\mathrm{a},2} = k_{\mathrm{a},3}$ and $k_{\mathrm{d},1} = k_{\mathrm{d},2} = k_{\mathrm{d},3}$ which proves that the population consisting of only EV_1 is for optimisation

Table 4.2: Explicitly given parameters of the reconstructed EV_2 and EV_3

$P_{\text{nom},2}$	$P_{\text{nom},1} - P_{\text{rem},1}$	$P_{\text{nom},3}$	$P_{\text{rem},1}$
$k_{\text{a},2}$	$k_{\text{a},1}$	$k_{\text{a},3}$	$k_{\text{a},1}$
$k_{\text{c},2}$	$k_{\text{c},1}$	$k_{\text{c},3}$	$k_{\text{c},1} + 1$
$k_{\text{r},2}$	$k_{\text{r},1}$	$k_{\text{r},3}$	$k_{\text{r},1} - 1$
C_2	$(P_{\text{nom},1} - P_{\text{rem},1}) \cdot T$ $\cdot(k_{\text{c},1} - k_{\text{a},1})$	C_3	$P_{\text{rem},1} \cdot T$ $\cdot(k_{\text{c},1} - k_{\text{a},1} + 1)$
$k_{\text{d},2}$	$k_{\text{d},1}$	$k_{\text{d},3}$	$k_{\text{d},1}$

problem (2.21) analogous to the population consisting of EV_2 and EV_3.

□

Proof of Lemma 4.2.2

Proof. Aggregation in Lemma 4.2.2 is valid since all the batteries are present during the intervals $[k_{\text{a},1}, k_{\text{d},1})$. The following ratios ensure that all the batteries are empty or full at the same moment to prevent that the aggregator relies on a power contributions of already full batteries.

$$\frac{P_{\text{nom},i}}{P_{\text{nom},1}} = \frac{C_i}{C_1} = \frac{u_{\text{ch},i}(k)}{u_{\text{ch},1}(k)} = \frac{u_{\text{dch},i}(k)}{u_{\text{dch},1}(k)} = \frac{SoE_i(k)}{SoE_1(k)}, \quad \forall k \in \{1, 2, ..., N\}. \tag{4.24}$$

Since both control signals $\boldsymbol{u}_{\text{ch},i}$ and $\boldsymbol{u}_{\text{dch},i}$ and battery relative state of energy $\boldsymbol{SoE}_i$ of EV_1 and their constraints can be explicitly expressed, there is no information loss and every charging trajectory of EV_1 can be realised with $\boldsymbol{u}_{\text{ch},i}$ and $\boldsymbol{u}_{\text{dch},i}$ without any other hidden costs or energy losses.

From (4.24) follows that result of floor operator in (4.1) and (4.2) is the same for EV_1 and EV_i. Since $k_{\text{a},1} = k_{\text{a},i}$ and $k_{\text{d},1} = k_{\text{d},i}$ it is also $k_{\text{c},1} = k_{\text{c},i}$ and $k_{\text{r},1} = k_{\text{r},i}$. □

4.2.3 Robust reconstruction of individual EV data

Constrained equation system (4.17) is underdetermined and matrix A_N is rank-deficient. Dimensions of matrix A_N are $5N$ x M_N and $\text{rank}(A_N) = 4N - 3$. The sum of every N rows that belong to the one of the first four equations in (4.16) is equal to a vector of ones $\boldsymbol{I}_{M_N}[1, 1, ..., 1] \in \mathbb{R}^{M_N}$. Last N rows that belong to equation related to $\boldsymbol{P}_{\text{const}}$ are

linear combinations of other rows. Consequently, due to existing linear dependencies of rows in A_N as well as due to the requirement that all $\boldsymbol{P}_{\text{sol}}$ must be non-negative, there is a possibility that (17) has no solution.

To generalise the method and make it applicable to the proposed concept in Fig. 4.1, Algorithm 6 was designed as the robust version of Algorithm 5. Solution feasibility in Algorithm 6 is guaranteed by optimisation problem (4.25) that is derived from (4.17), with equation constraints implemented as soft constraints:

$$\begin{aligned} \boldsymbol{P}^*_{\text{sol}} &= \arg\min_{\boldsymbol{P}_{\text{sol}},\,\bar{\boldsymbol{\theta}}} |\bar{\boldsymbol{\theta}} - \boldsymbol{\theta}|, \\ \text{s.t.} \begin{cases} [A_{\text{N}} \; -I] \begin{bmatrix} \boldsymbol{P}_{\text{sol}} \\ \\ \bar{\boldsymbol{\theta}} \end{bmatrix} = 0, \\ \\ \boldsymbol{P}_{\text{sol}} \geq 0 \end{cases} \end{aligned} \tag{4.25}$$

where $|\cdot|$ denotes vector norm 1 and vector $\bar{\boldsymbol{\theta}}$ is the closest one to the input vector theta, in the norm-1 sense, for which it is possible to find $\boldsymbol{P}_{\text{sol}}$.

Finally, the robust individual EV data reconstruction procedure is defined with the Algorithm 6.

Algorithm 6 Robust reconstruction of individual EV descriptions

Require: $\mathcal{EV}_1$ described with $\boldsymbol{\theta} = [\boldsymbol{P}_{\text{a}}^\top, \boldsymbol{P}_{\text{c}}^\top, \boldsymbol{P}_{\text{r}}^\top, \boldsymbol{P}_{\text{d}}^\top, \boldsymbol{P}_{\text{const}}^\top]^\top$
Ensure: $\mathcal{EV}_2$ described with tuples $(P, C, k_{\text{a}}, k_{\text{d}})$
  initialise $\mathcal{EV}_2 = \emptyset$
  find $\boldsymbol{P}^*_{\text{sol}}$ by solving minimisation problem (4.25)
  for all $P^*_{\text{sol},i} > 0$ **do**
    add $EV_i = (P^*_{\text{sol},i}, C_i, k_{\text{a},i}, k_{\text{d},i})$ to $\mathcal{EV}_2$ ▷ (4.10)
  end for

Algorithm 6 was used to validate the proposed aggregated representation in a way that it is applied directly to the outputs of Algorithm 4 so there is at least one possible solution $\boldsymbol{P}^*_{\text{sol}}$ with $\bar{\boldsymbol{\theta}} = \boldsymbol{\theta}$ - the population that was the input to Algorithm 4.

4.2.4 Adaptation of Algorithm 6 for EVs that depart outside the observing horizon

For the full application of the aggregated representation the EVs that depart outside of the observing horizon must be included. Such EVs can have:

- only contribution to $\boldsymbol{P}_{\text{a}}$ on the horizon,

- contribution to either $\boldsymbol{P}_\mathrm{c}$ or $\boldsymbol{P}_\mathrm{r}$ on the horizon,
- both contribution to $\boldsymbol{P}_\mathrm{c}$ and $\boldsymbol{P}_\mathrm{r}$ on the horizon.

The rhombus of EV charging envelope in Fig. 4.2 is fully defined by minimally three corners. The three corners are found with respective characteristic intervals k_a, k_c, k_d or k_r and the nominal charging power $\boldsymbol{P}_\mathrm{nom}$. The essence of the reconstruction algorithm is to find $\boldsymbol{P}_\mathrm{nom}$ for all possible unique tuples of the characteristic intervals. There is indefinite number of rhombuses that have one or two corners on the observing horizon, i.e. the respective one or two characteristic intervals are $\leq N$. To keep extended set $\mathcal{K}_{N\mathrm{e}}$ of all possible tuples of the characteristic intervals finite, all unknown characteristic intervals outside the observing horizon are set as close to the end of the horizon as possible.

For the first group of EVs with only contribution to $\boldsymbol{P}_\mathrm{a}$ on the horizon (green in Fig. 4.4), missing k_c and k_r are set to $N+1$, which is the closest possible to the end of the observing horizon. For the second group (blue and purple), missing k_c or k_r is also set to $N+1$. For all three groups, including the last on (orange), missing k_d is then explicitly calculated from $k_\mathrm{d} - k_\mathrm{r} = k_\mathrm{c} - k_\mathrm{a}$. The finite set $\mathcal{K}_{N\mathrm{e}}$ of all possible tuples of the characteristic intervals is then defined as:

$$\mathcal{K}_{N\mathrm{e}} = \mathcal{K}_N \cup \left\{ (k_\mathrm{a}, k_\mathrm{c}, k_\mathrm{r}, k_\mathrm{d}) \;\middle|\; \begin{array}{c} N < k_\mathrm{d}, \\ 1 < k_\mathrm{c} \leq N+1, \\ 1 < k_\mathrm{r} \leq N+1, \\ 1 \leq k_\mathrm{a} < k_\mathrm{c} \leq k_\mathrm{d}, \\ 1 \leq k_\mathrm{a} \leq k_\mathrm{r} < k_\mathrm{d}, \\ k_\mathrm{d} - k_\mathrm{r} = k_\mathrm{c} - k_\mathrm{a} \end{array} \right\}. \tag{4.26}$$

Such approach allows to determine a charging envelope for any EV with at least one contribution on the observing horizon, as visualised in Fig. 4.4. Theoretically, in the case of two or three missing contributions, there is infinite number of possible envelopes but that does not influence the charging schedule optimisation since the part of the charging envelopes on the horizon stays the same in the introduced approach, as shown in Fig. 4.4. Dotted line denotes envelopes obtained using the introduced approach while dashed line denotes some examples of infinite possible envelopes.

The equations (4.16) and (4.25) for the robust algorithm are unchanged. Values of the vectors $\boldsymbol{P}_\mathrm{a}, \boldsymbol{P}_\mathrm{c}, \boldsymbol{P}_\mathrm{r}, \boldsymbol{P}_\mathrm{d}$ and $\boldsymbol{P}_\mathrm{const}$ behind the horizon N are free to take values that support the reconstructed EVs based on the known - predicted values of the vectors on the horizon.

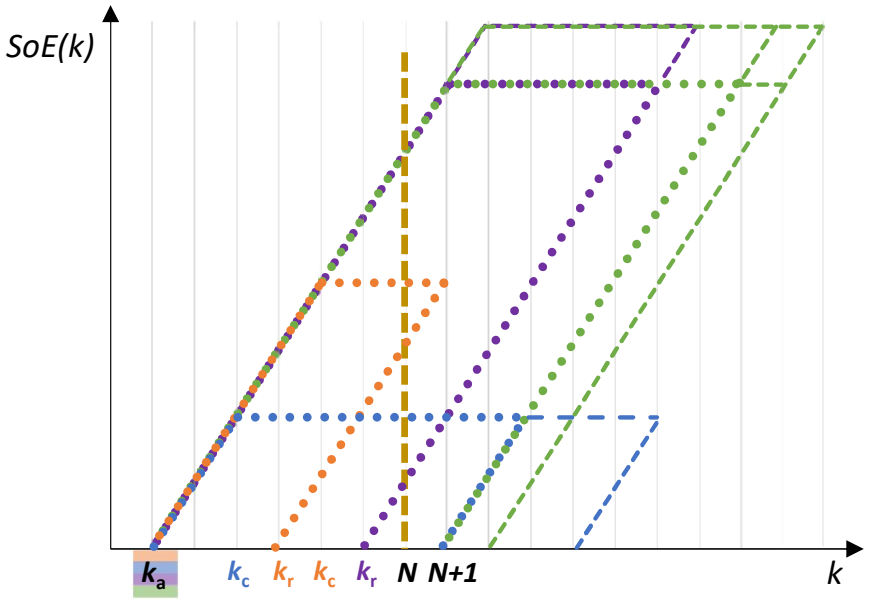

Figure 4.4: Visualisation of the explicitly missing contributions: green - only contribution to $\boldsymbol{P}_{\mathrm{a}}$, blue - contribution to $\boldsymbol{P}_{\mathrm{a}}$ and $\boldsymbol{P}_{\mathrm{c}}$, purple - contribution to $\boldsymbol{P}_{\mathrm{a}}$ and $\boldsymbol{P}_{\mathrm{c}}$, orange - contribution to $\boldsymbol{P}_{\mathrm{a}}$, $\boldsymbol{P}_{\mathrm{c}}$ and $\boldsymbol{P}_{\mathrm{r}}$.

4.2.5 Number of EVs in the reconstructed population

As a consequence of Lemma 4.2.1 and the way of the capacity C reconstruction in (4.10), one original EV will be reconstructed as two EVs. From the day-ahead scheduling perspective only cumulative electric energy consumption of the aggregator and its DR capacity are of interest for the aggregator. This fact allows the number of reconstructed EVs to be bigger than the number of CPs on the aggregator's parking lot. During the operation of MPC (real-time operation), the aggregator explicitly schedules the charging only of the known present and connected EVs. Future EVs, the ones to arrive to the parking lot along the prediction horizon, are reconstructed from the prediction in the form of the proposed five vectors. Such predicted EVs do not need to be allocated to specific physical CPs but they require a part of cumulative charging power to be scheduled and assigned to them.

4.3 Validation through optimisation for demand response

In order to validate the introduced EVs representation, worst-case optimisation is applied to schedule charging of EVs connected to the CPs of an EV aggregator that offers an active power reserve. The full optimisation problem is defined in Section 2.2 for the more convenient reading. In this section only charging point model and aggregated battery model are introduced to emphasise their key differences in capturing the demand response capacity of the EV population. The rest of the constraints concerning demand response costs are given in Section 2.1.

4.3.1 Charging point model

The 24-hours ahead scheduling problem engages n CPs, where n is equal to the maximum concurrent number of EVs in the population. In accordance with the elaboration in II.D, number n could be even higher than the physically available number of CPs on the parking lot.

A CP is modeled as a system with one state SoE_{cp} that is equal to zero when CP is not occupied. Otherwise, it is equal to the relative SoE of a connected EV, which is described as:

$$\begin{gathered} SoE_{cp}(k+1) = SoE_{cp}(k) + \eta_{\text{ch}} u_{\text{ch},cp}(k) - u_{\text{dch},cp}(k)/\eta_{\text{dch}}, \\ \forall k | k+1 \in \mathcal{O}_{cp}, \\ SoE_{cp}(k) = 0, \forall k | \begin{cases} k \in \mathcal{O}_{cp}, k-1 \in \mathcal{I}_{cp} \\ \text{or} \\ k \in \mathcal{I}_{cp} \end{cases}, \end{gathered} \tag{4.27}$$

where the index cp denotes a CP, $u_{\text{ch},cp}$ and $u_{\text{dch},cp}$ are charging and discharging energies of the CP, respectively, $\eta_{\text{ch}} = 0.9$ and $\eta_{\text{dch}} = 0.9$ are charging and discharging efficiency, respectively, $\mathcal{O}_{cp}$ is the set of time intervals in which the CP indexed with cp is occupied with an EV connected to the CP and $\mathcal{I}_{cp}$ is the set of time intervals when the CP is not occupied. It can be also seen that relative SoE is automatically initialised to zero at the arrival when the EV is connected to a CP. The value of the efficiency coefficients η_{ch} and η_{dch} are equal for all EVs since the predicted vehicle in the population is not made concrete (or personalised) and only represents a forthcoming generic charging task for the aggregator of the charging stations.

In the absence of an EV $u_{\text{ch},cp}(k)$ and $u_{\text{dch},cp}(k)$ must be zero. During an EV presence, the EV's battery charger defines power constraints:

$$\begin{cases} u_{\text{ch},cp}(k) + u_{\text{dch},cp}(k) \leq P_{\text{nom},i} T, \\ 0 \leq u_{\text{ch},cp}(k) \leq P_{\text{nom},i} T, \\ 0 \leq u_{\text{dch},cp}(k) \leq \begin{cases} 0, & \text{vehicle-to-grid disabled} \\ P_{\text{nom},i} T, & \text{vehicle-to-grid enabled} \end{cases}, \end{cases} \tag{4.28}$$

where i denotes the corresponding EV connected to the charging point cp at the k^{th}

discrete-time interval and T is discretisation time. EV relative battery capacity C_i constrains the CP state as follows:

$$0 \leq SoE_{cp}(k) \leq C_i,\ k_{\mathrm{a},i} \leq k < k_{\mathrm{d},i}, \tag{4.29}$$

$$SoE_{cp}(k_{\mathrm{d},i}-1) + \eta_{\mathrm{ch}} u_{\mathrm{ch},cp}(k_{\mathrm{d},i}-1) - u_{\mathrm{ch},cp}(k_{\mathrm{d},i}-1)/\eta_{\mathrm{dch}} = C_i. \tag{4.30}$$

Constraint (4.30) ensures that EV_i leaves the parking lot with the battery charged to the required level.

4.3.2 Aggregated battery model

To emphasise the necessity for the introduced EV population representation method and its corresponding conversion algorithms, the optimisation was also carried out with using an aggregated battery model similar to [28, 29, 30].

Instead with (4.27)-(4.30), the dynamics of all EVs' batteries is modeled with only one state and one pair of control signals:

$$\begin{aligned} SoE_{\mathrm{agg}}(k+1) =& SoE_{\mathrm{agg}}(k) + \eta_{\mathrm{ch}} u_{\mathrm{ch,agg}}(k) \\ & - u_{\mathrm{dch,agg}}(k)/\eta_{\mathrm{dch}}, \\ SoE_{\mathrm{agg}}(0) =& 0. \end{aligned} \tag{4.31}$$

Aggregated relative state of energy is constrained with:

$$R_{\mathrm{agg}}(k) \leq SoE_{\mathrm{agg}}(k) \leq C_{\mathrm{agg}}(k), \tag{4.32}$$

where $\boldsymbol{R}_{\mathrm{agg}} \in \mathbb{R}^N$ is a vector of aggregated energy requests and it is derived from $\boldsymbol{P}_{\mathrm{r}}$ and $\boldsymbol{P}_{\mathrm{d}}$. Visually, it is the sum of all constraints on individual EVs, marked red in Fig. 4.2. Similarly, $\boldsymbol{C}_{\mathrm{agg}} \in \mathbb{R}^N$ is derived from $\boldsymbol{P}_{\mathrm{a}}$ and $\boldsymbol{P}_{\mathrm{c}}$:

$$R_{\mathrm{agg}}(k) = T \sum_{j=1}^{k} \sum_{l=1}^{j} \left(P_{\mathrm{r}}(l) - P_{\mathrm{d}}(l) \right), \tag{4.33}$$

$$C_{\mathrm{agg}}(k) = T \sum_{j=1}^{k} \sum_{l=1}^{j} \left(P_{\mathrm{a}}(l) - P_{\mathrm{c}}(l) \right). \tag{4.34}$$

Aggregated battery charging energy is constrained with:

$$0 \leq u_{\mathrm{ch,agg}}(k) \leq P_{\max}(k) T, \tag{4.35}$$

$$0 \leq u_{\mathrm{dch,agg}}(k) \leq P_{\min}(k) T, \tag{4.36}$$

$$P_{\max}(k) = \sum_{j=1}^{k} \left(P_{\mathrm{a}}(j) - P_{\mathrm{d}}(j) \right), \tag{4.37}$$

$$P_{\min}(k) = \begin{cases} 0, & \text{vehicle-to-grid disabled} \\ P_{\max}, & \text{vehicle-to-grid enabled} \end{cases}. \tag{4.38}$$

Vector $\boldsymbol{P}_{\max} \in \mathbb{R}^N$ can also be defined as a sum of nominal powers of all EVs power converters connected to CPs at a specific moment.

At first sight constraint (4.32) guarantees that every EV will be fully charged but that is not the case as will be shown in Section 4.4.3 by a counter-example.

4.4 Experimental validation

The proposed method was validated by optimising the charging schedule for an EV population using first the original data and then using reconstructed population data obtained by reconstruction of the proposed aggregated representation of the same original population (Fig. 4.5). Two measures are used for comparison of the two populations: the reserved frequency regulation power and the calculated total optimisation cost. Results were also compared with optimisation results based on the aggregated EV battery model of the original population, to emphasise the ability of the proposed aggregated representation to capture a correct demand response capacity of the population. For the optimisation with the original and with the reconstructed data was used optimisation problem (2.21) defined in Section 2.2, while for the optimisation with aggregated EV battery model equations (4.27)-(4.30) were replaced with (4.31)-(4.38).

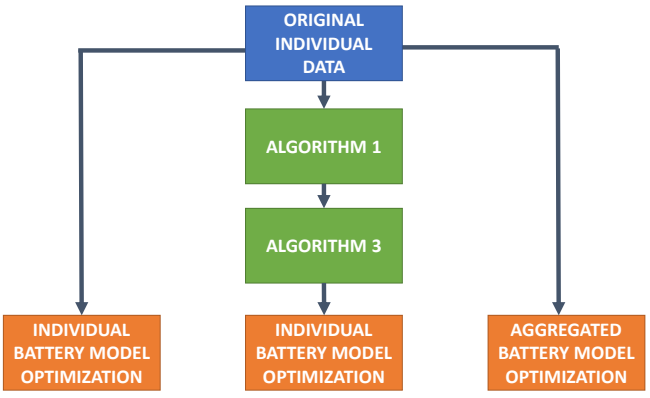

Figure 4.5: Validation procedure of the proposed representation method.[13]

4.4.1 Experimental data

The method is tested on real historical data provided by ACN-Data [16] that include two datasets from parking lots of the California Institute of Technology (CalTech) and the Jet Propulsion Laboratory (JPL). The datasets contain 1057 and 928 days, respectively. The original data consist of:

- Connection time when an EV was plugged in (t_{con});
- Done-charging time when the last non-zero current draw recorded (t_{full});
- Departure time when the EV was disconnected (t_{d});
- Delivered energy to the EV ($E_{\text{delivered}}$).

In order to represent an EV charging session as shown in Fig. 4.2 and Table 4.1., the data is preprocessed to obtain EV power P and capacity C that are not contained in the data. Power is determined using conservative assumption that EV was being charged full time between the connection time t_{con} and the done-charging time t_{full}:

$$P = \frac{E_{\text{delivered}}}{t_{\text{full}} - t_{\text{con}}}. \tag{4.39}$$

After discretisation of t_{con} and t_{d} into k_{a} and k_{d}, it is possible that charging session becomes infeasible. For that reason, with the assumption that the EV was fully charged or was being charged during the whole connection period, the relative capacity C is determined by using:

$$C = \min\left(P * T(k_{\text{d}} - k_{\text{a}} - 1)\eta_{\text{ch}},\ E_{\text{delivered}}\eta_{\text{ch}}\right). \tag{4.40}$$

Since the data is gathered from the CPs side there is no information about EVs that left without being charged due to no available CP. Such information is however irrelevant from the microgrid and DR point of view.

Values of the electrical prices used in the optimisation problem (2.21) are as follows: $c_{\text{pp}} = 0.116$ €/kW, $c_{\text{res}} = -0.0162$ €/kW, $c_{\text{act}} = 0.065$ €/kWh, $c_{\text{batt}} = 0.226$ €/kWh. Vector of day-ahead prices $\boldsymbol{c}_{\text{da}}$ is shown in Fig. 4.6. Discretisation time is $T = 15$ min and recuperation period is $T_{\text{r}} = 24$ h.

4.4.2 Computational requirements

Linear optimisation problem (LP) (4.25) was set up in Python [24] using Numpy [25] and Scipy [26] modules and as a solver IBM Cplex [27] was used. The construction of the matrix A_N in (4.17) lasts for 5 minutes for $N = 96$ while loading the prepared matrix from the memory lasts for 20 s. LP solving times are given in Table 4.3. The size and

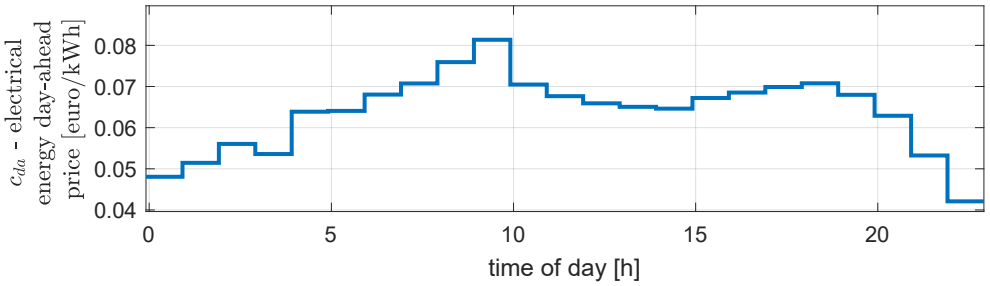

Figure 4.6: Day-ahead electrical energy price profile. [13]

the computational time of the optimisation problem (2.21) depend on the number of EVs in the population, as shown in Fig. 4.7. For every point on the x axis a single EV population was used such that it is possible that for a specific case larger number of EVs gives a smaller computation time, but still the growing trend is visible. The bigger number of EVs in the reconstructed population is discussed in Subsection 4.2.5. Computations were run on a Linux server with processor AMD Epyc 7351 CPU @ 2.4 GHz (16 cores) and 64 GB RAM.

Table 4.3: Computational times of the reconstruction algorithm

mean	10.82 s
standard deviation	0.89 s
minimum value	8.92 s
maximum value	15.56 s

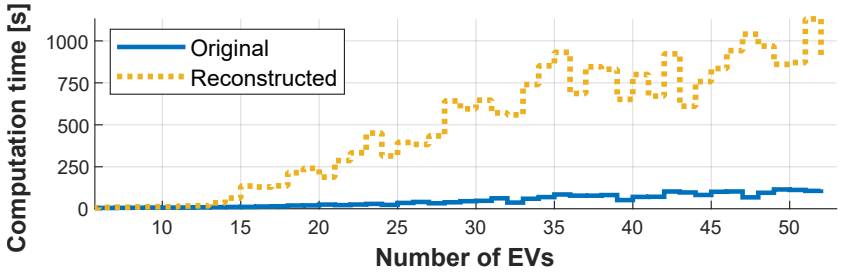

Figure 4.7: Computational times of the optimisation problem (2.21) for the original and the reconstructed EV population. [13]

4.4.3 Analysis of results

Simulation results are compared by using the optimised daily cost and reserved regulation power. Those values are used as deviation measures between the populations since they are the data of interest for the aggregator's cost analysis and DR contracting with the power grid. Cost deviation can be seen in Fig. 4.8. A small deviation was expected

since the reconstructed EV population is generally not identical to the original one due to the underdetermined reconstruction problem (4.17) that has multiple solutions. Daily operation costs of the reconstructed populations are mostly higher than the ones of the original populations which corresponds with mostly lower flexibility power shown in Fig. 4.9.

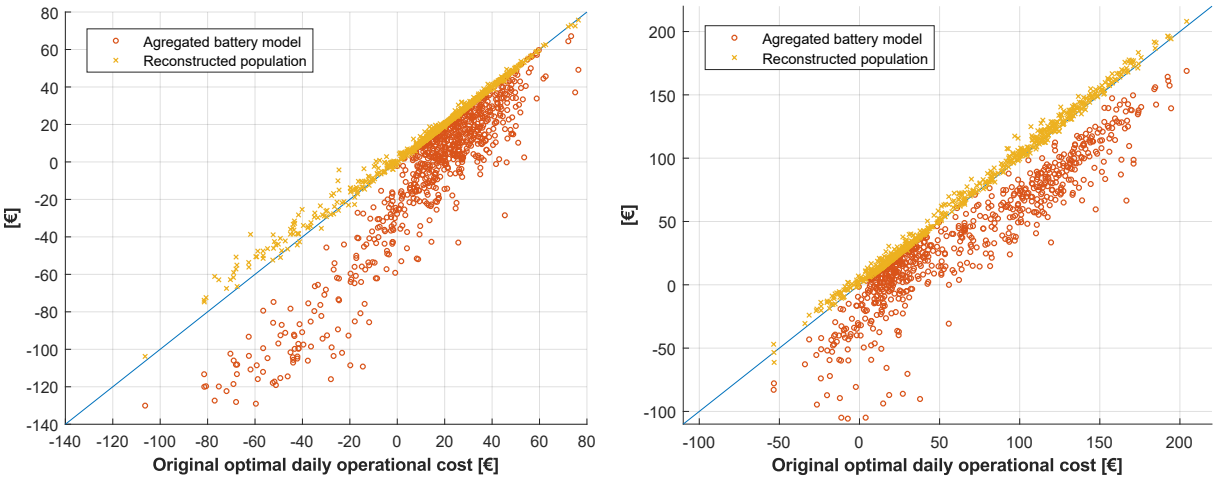

Figure 4.8: Comparison of optimal daily operation cost for one-day populations from datasets a) CalTech, b) JPL. [13]

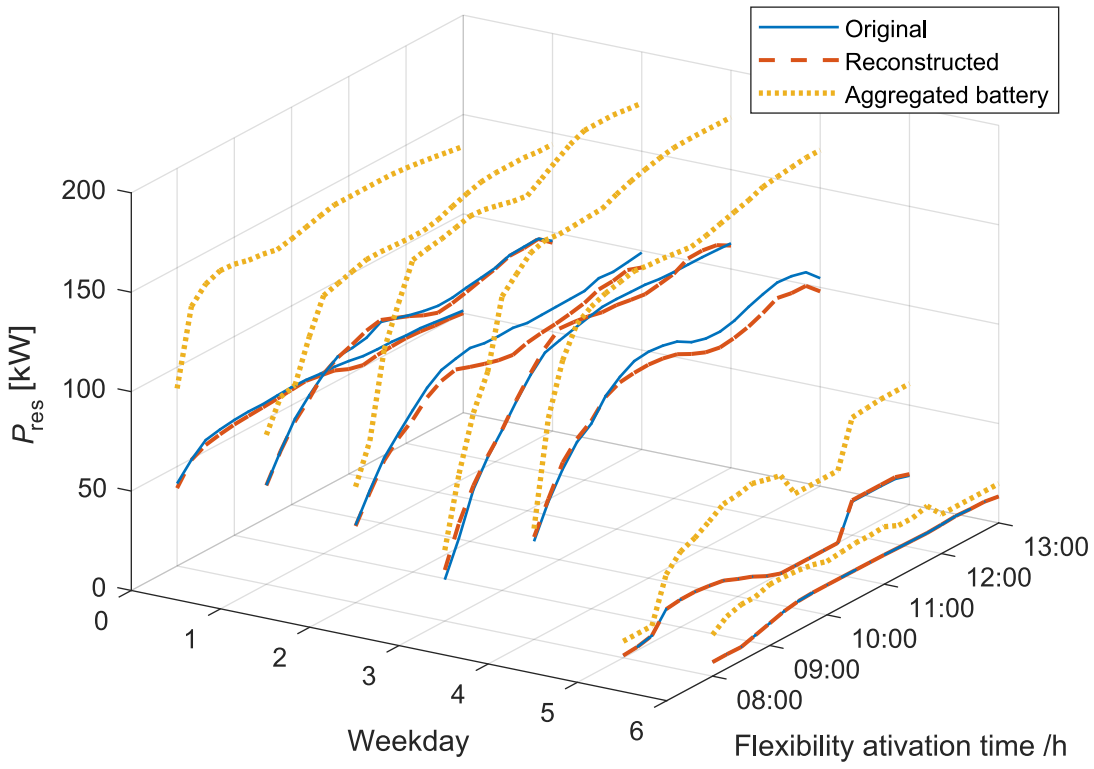

Figure 4.9: Reserved regulation power for the considered time intervals per day in one week. [13]

An example explaining too optimistic results of the aggregated battery model is given in Fig. 4.10. Two different populations (Fig. 4.10a and 4.10b) with the same aggregated battery model (Fig. 4.10c) are compared. An aggregated charging trajectory is given for the case of higher energy prices between intervals $k = 5$ and $k = 9$ when charging is avoided. If the original population consists of EV_1 and EV_2 then both of EVs are fully charged and the aggregated charging trajectory corresponds to the sum of their individual trajectories. For the mentioned case of energy prices, EV_1 will be charged as soon as possible, while EV_2 will be charged as late as possible. In the case of population in Fig. 4.10b EV_3 can be charged only during the mentioned period with high prices. To satisfy the chosen aggregated charging trajectory EV_4 must be discharged at the same time and of course pre-charged before and charged again after the high price period. Such case does not take into account battery degradation cost and energy losses due to EV_4 charging, discharging and charging again. Consequently the aggregated battery model operational cost is seemingly lower than the real operational cost. This effect is even more emphasised when the aggregator participates in DR when in the specific intervals all charging must be reduced to obtain reward from the power grid. The proposed aggregated representation method distinguishes the two populations with vector P_{const}, as shown in Fig. 4.10d. Applying the reconstruction Algorithm 5 to the discrete-time signals in Fig. 4.10d will result with populations identical to the original ones.

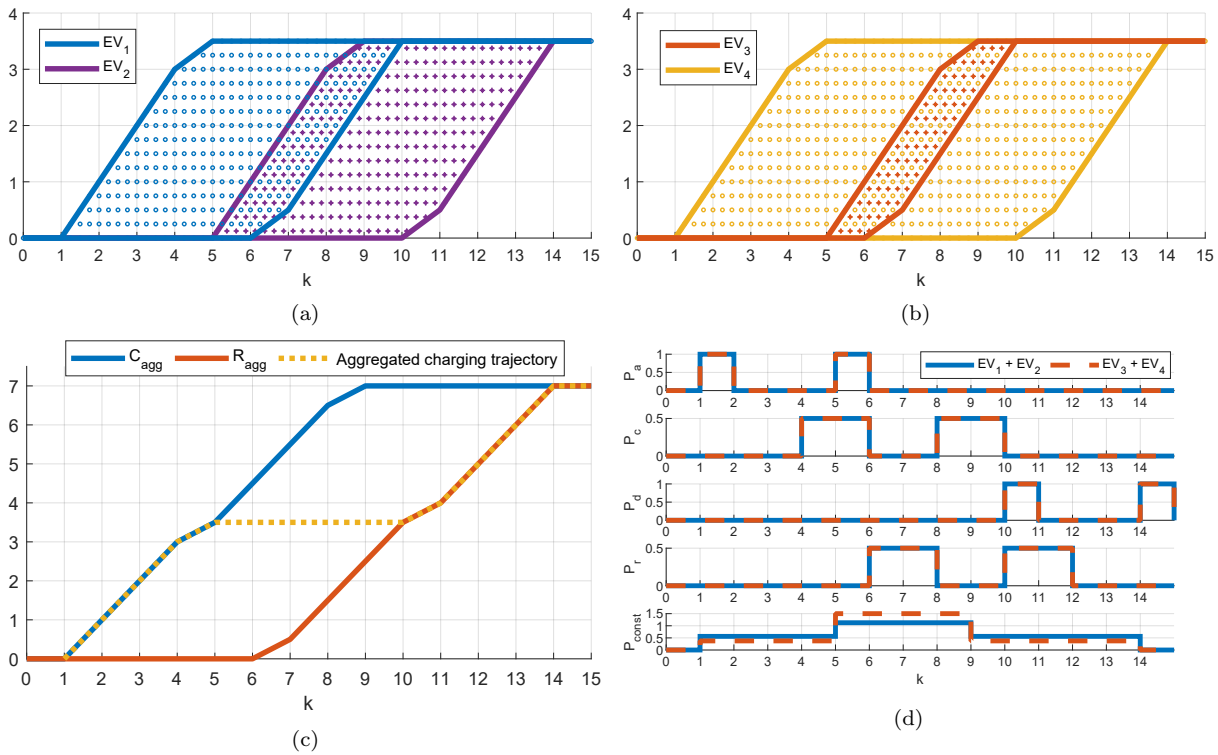

Figure 4.10: A qualitative example of two populations (a), (b), with the same representation using the aggregated battery model (c) and the proposed method with vectors $\boldsymbol{P}_{\text{a}}, \boldsymbol{P}_{\text{c}}, \boldsymbol{P}_{\text{r}}$, $\boldsymbol{P}_{\text{d}}$ and $\boldsymbol{P}_{\text{const}}$ (d). [13]

Empirical results showed that for big enough EV populations in which more EVs are present at the same time, the reconstructed number of EVs is up to five times bigger than the original number of EVs. To better explore this effect, the proposed reconstruction algorithm was iteratively applied on the population which was stacked with one EV every iteration. The EVs which were stacked belonged to the original population of one working day from the dataset. The order of the EVs stacking was according to their arrivals. The results of the experiment are shown in Fig. 4.11. It can be seen that for the initial small number of EVs, the number of the reconstructed EVs is two times bigger than the original number, which matches the effect mentioned in 4.2.5 and that is a consequence of Lemma 4.2.1. For the larger number of EVs, the ratio can even be five to one. That is a consequence of underdetermination of the system (4.17). The influence of a larger number of the reconstructed EVs to the error of the optimal daily cost is acceptable, as evidenced in Fig. 4.11.

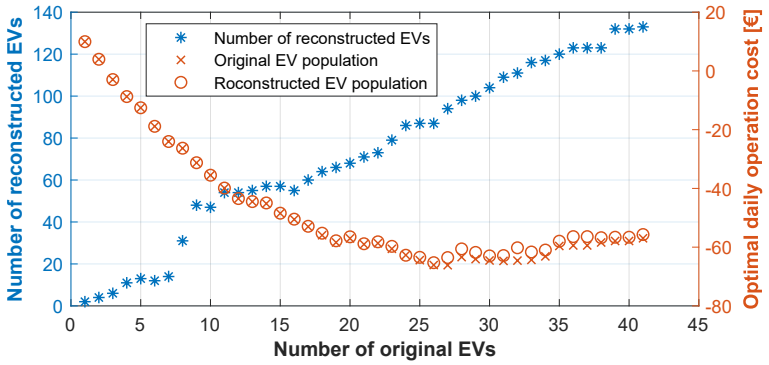

Figure 4.11: Comparison of the original and the reconstructed population sizes. [13]

Since the charging fee is not included in the daily optimisation cost J, negative values in Fig. 4.8. and Table 4.4a denote that the aggregator can obtain profit already by participating in DR. The DR participation and profit possibilities obviously rise with the number of EVs in the population. With some tolerance chosen using statistical data from Table 4.4a and 4.4b, reconstructed results could be used to contract day-ahead frequency regulation power. Finally, the experimental proof of the main hypothesis can be seen in Fig. 4.8., Fig 4.9. and Table 4.4 altogether.

Table 4.4: Statistical comparison of the reconstructed and the original population, where $\bar{\cdot}$ and $\sigma(\cdot)$ denote mean value and standard deviation: a) the reconstructed J and the original J' and b) the reconstructed P_{res} and the original P'_{res}. [13]

(a)

dataset	CalTech	JPL
	[€]	[€]
$\max(J)$	76.40	204.20
$\min(J)$	-103.80	-53.57
$\overline{\lvert J - J' \rvert}$	0.91	2.22
$\overline{J - J'}$	0.77	2.04
$\sigma(J - J')$	2.41	3.22
$\min(J - J')$	-4.72	-8.01
$\max(J - J')$	23.24	20.54
$\frac{\sqrt{\overline{(J-J')^2}}}{\overline{J'}}$	0.16	0.07

(b)

dataset	CalTech	JPL
	[kW]	[kW]
$\max(P_{\text{res}})$	210.11	257.81
$\min(P_{\text{res}})$	0	0
$\overline{\lvert P_{\text{res}} - P'_{\text{res}} \rvert}$	0.76	1.42
$\overline{P_{\text{res}} - P'_{\text{res}}}$	-0.55	-1.10
$\sigma(P_{\text{res}} - P'_{\text{res}})$	2.55	2.69
$\min(P_{\text{res}} - P'_{\text{res}})$	-26.18	-23.67
$\max(P_{\text{res}} - P'_{\text{res}})$	6.45	15.65
$\frac{\sqrt{\overline{(P_{\text{res}}-P'_{\text{res}})^2}}}{\overline{P'_{\text{res}}}}$	0.09	0.07

4.5 Conclusion

This chapter introduced a method of representing an EV population connected to a set of charging points that are managed by an aggregator. The method preserves the information valuable for EV charging scheduling in order for the aggregator to participate in tertiary frequency regulation, peak power shaving and volatile prices market. It consists of creating five vectors from which an equivalent population can be reconstructed. The simulation was run using real world data and charging scheduling was optimised for both the original population and the reconstructed one. The daily cost and the optimal reserved power of the reconstructed population matches to the optimisation result of the original population with acceptable deviation. The proposed method for EV population representation can be used in prediction of the EV population using machine learning.

Chapter 5

Prediction of aggregated EV representation using XGBoost and LightGBM

5.1 Introduction

Most research focuses on prediction of the aggregated load profile [11, 12, 31, 32, 33, 34, 35, 36, 37, 38]. For the coordinated EV scheduling it is necessary to have charging requests and the mentioned load predictions are useful only for the grid operator to plan system balancing. Approach suitable for EV charging scheduling is to predict future quantities of certain EVs types [39, 40, 41, 42, 43]. The EV types are distinguished by state of charge at the arrival as well as by arrival and departure times. The downside of the approach is limitation to finite number of types. To avoid that obstacle, in this chapter the goal is to predict the aggregated representation of future EVs, introduced in the previous chapter. The aggregated representation of future EVs captures demand response capacity and allows every EV to have a unique charging task [13]. The new approach is proven to very well capture the demand response potential of a group of EV charging points, and here is introduced the prediction procedure for the aggregated representation.

For EV load profile prediction different methods are used such as linear regression, decision trees, support vector machine, k-nearest neighbours and several deep learning methods [43]. Several researches have shown that extreme gradient boosting ensembles (XGBoost) outperform other compared models in different similar applications connected to EVs [33, 36, 44]. Furthermore, together with XGBoost other gradient boosting models, like light gradient boosting machine (LightGBM), are chosen as the most promising [45].

In this chapter Adaptive Charging Network (ACN) dataset [16] is transformed to the aggregated representation using Algorithm 4. The obtained data is the focus of time-

series feature engineering procedure and is used to train two gradient boosting models XGBoost and LightGBM. The models are validated by comparing their accuracy with two baselines.

The Chapter is organised as follows. Forecasting problem and extensive data analysis are introduced in Section 5.2. Evaluation of the obtained forecasting models is given in Section 5.3 and conclusion is given in Section 5.4.

5.2 Forecasting problem definition and dataset

The final goal is to predict future EV charging tasks in order to apply individual battery optimisation scheduling algorithm such as [10, 13, 46] or the ones proposed in Chapters 2 and 3. The forecasting problem, marked dashed orange, described in this chapter is only one part of the concept proposed in this thesis. The full pipeline of optimisation for EVs charging and demand response is again given in Fig. 5.1. The proposed method does forecasting in aggregated representation domain that consists of five discrete-time vectors related to envelopes of feasible charging powers and charging states for the EV population. Collecting historical data and EV charging schedule optimisation are done in individual EV data domain. Transformation between two domains is reversible without almost any information loss [13].

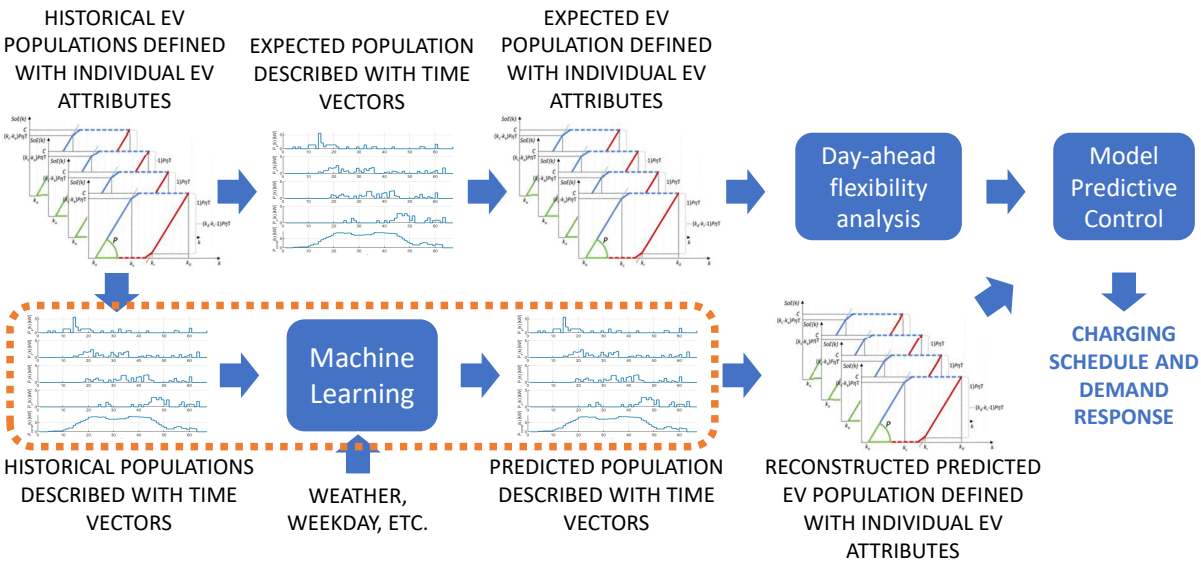

Figure 5.1: The proposed concept of aggregated population prediction using machine learning and charging scheduling of individual electric vehicles [13].

ACN dataset [16] is well used in various EV load prediction papers [34, 35, 36, 47]. It includes two datasets from parking lots of California Institute of Technology and the Jet Propulsion Laboratory. In this article only the first one is used. The dataset contains

charging sessions of 54 charging points through 1057 days (2018/04/25 - 2020/08/29). All available historical data of EV arrivals, transformed to $\boldsymbol{P}_{\mathrm{a}}$, $\boldsymbol{P}_{\mathrm{c}}$, $\boldsymbol{P}_{\mathrm{d}}$, $\boldsymbol{P}_{\mathrm{r}}$ and $\boldsymbol{P}_{\mathrm{con}}$ using Algorithm 4, is used for model training. Based on the current and recent past signal values, obtained model is used to predict values of these signals on the horizon of 2 hours to enable EV charging scheduling.

5.2.1 Aggregated representation data analysis

An exploratory data analysis of the available historical data is conducted to appropriately choose adequate inputs to model. Historical aggregated data signals $\boldsymbol{P}_{\mathrm{a}}$, $\boldsymbol{P}_{\mathrm{c}}$, $\boldsymbol{P}_{\mathrm{d}}$, $\boldsymbol{P}_{\mathrm{r}}$ and $\boldsymbol{P}_{\mathrm{con}}$ are analyzed to find patterns and correlation. Daily mean values, sigma and 3-sigma limits for all five signals, separated for working and non-working days are given in Fig. 5.2. Visualisation in Fig. 5.2. gives insight in peak values of $\boldsymbol{P}_{\mathrm{a}}$ during morning and of $\boldsymbol{P}_{\mathrm{d}}$

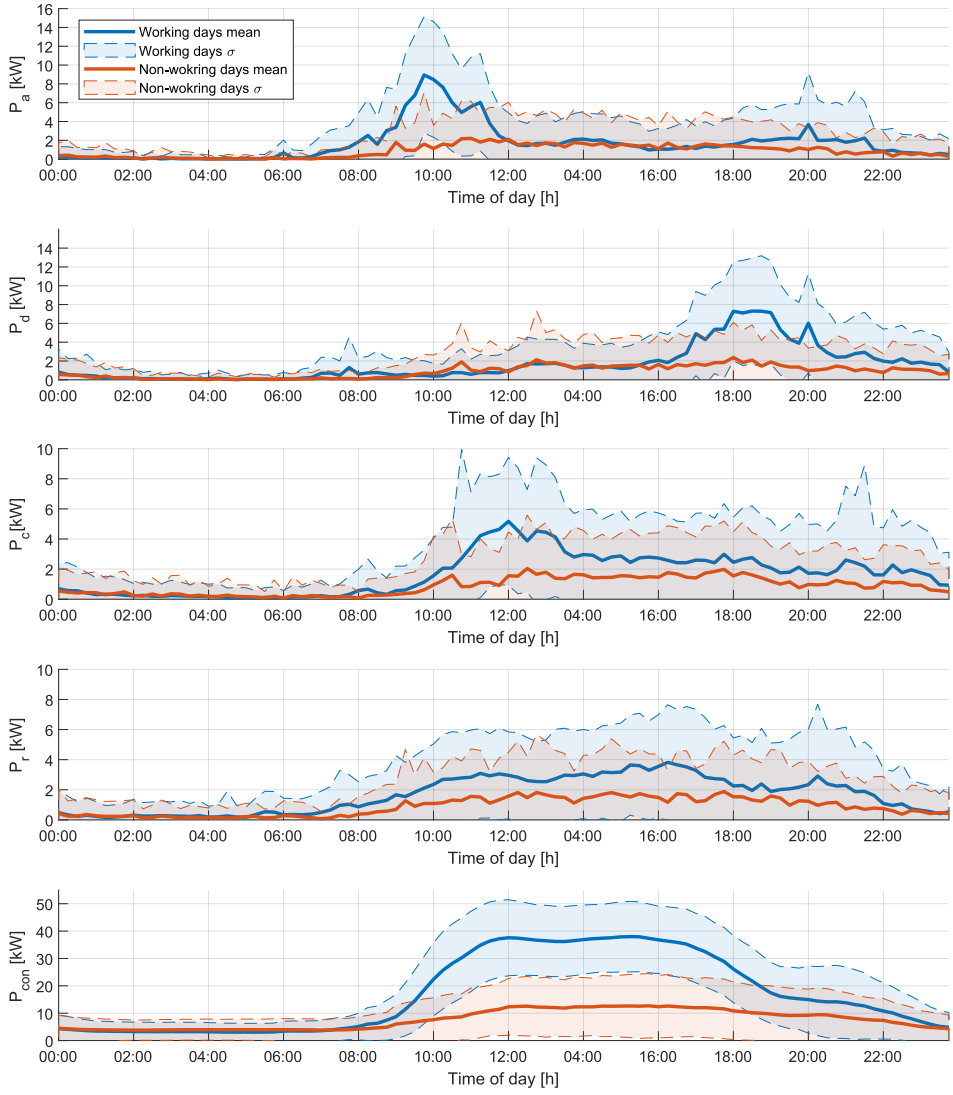

Figure 5.2: Daily mean values and 3-sigma limits for time-vectors $\boldsymbol{P}_{\mathrm{a}}$, $\boldsymbol{P}_{\mathrm{d}}$, $\boldsymbol{P}_{\mathrm{c}}$, $\boldsymbol{P}_{\mathrm{r}}$ and $\boldsymbol{P}_{\mathrm{con}}$, separated for working and non-working days.[48]

during afternoon and evening which is quite expected since $\boldsymbol{P}_{\mathrm{a}}$ and $\boldsymbol{P}_{\mathrm{d}}$ are sum of arrived and departed nominal EV charging powers, respectively. It can be seen in Fig. 5.2 and especially in Fig. 5.3 that $\boldsymbol{P}_{\mathrm{a}}$ is significant amount of time close or equal to zero, as it is the case with $\boldsymbol{P}_{\mathrm{c}}$, $\boldsymbol{P}_{\mathrm{d}}$, $\boldsymbol{P}_{\mathrm{r}}$. The nature of the signals derives from (4.1)-(4.9) where the signals are built from zero vector by adding contributions of EVs that are temporally scattered. Every EV contribution is a discrete impulse and the signals are superposition of them. That is not the case with $\boldsymbol{P}_{\mathrm{con}}$ where an EV contributes to the signal through all time intervals while being connected to a specific charging point. Qualitative comparison of $\boldsymbol{P}_{\mathrm{a}}$, $\boldsymbol{P}_{\mathrm{d}}$ and $\boldsymbol{P}_{\mathrm{con}}$ in Fig. 5.2 and signals definition (4.1)-(4.9) show dynamic characteristic between the signals: $P_{\mathrm{con}}(k) \approx \sum_{j=0}^{k} P_{\mathrm{a}}(j) - P_{\mathrm{d}}(j)$.

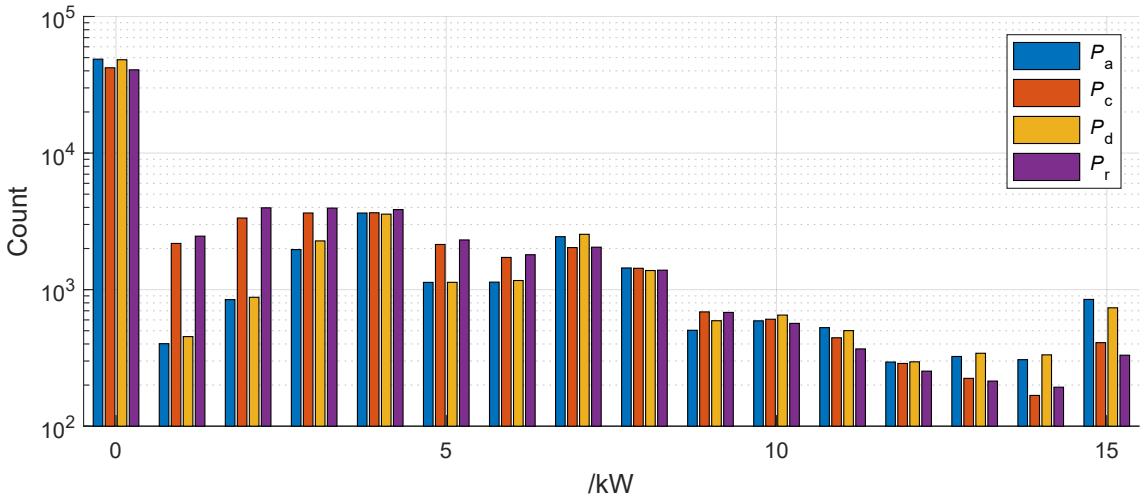

Figure 5.3: Histogram of $\boldsymbol{P}_{\mathrm{a}}$, $\boldsymbol{P}_{\mathrm{d}}$, $\boldsymbol{P}_{\mathrm{c}}$, $\boldsymbol{P}_{\mathrm{r}}$ and $\boldsymbol{P}_{\mathrm{con}}$

At first sight to a selected week period in Fig. 5.4. one can spot that there is an obvious daily and weekly pattern which is further confirmed with autocorrelation analysis shown in Fig 5.5. Smaller amplitude is expectedly seen during Saturday and Sunday. Through visual analyses of data plotted on weekly interval it was easy to notice smaller amplitude on national holidays.

5.2.2 Model inputs

Values of $\boldsymbol{P}_{\mathrm{a}}$ are input to all five models since contribution of an EV to the $\boldsymbol{P}_{\mathrm{a}}$ precedes contributions to the other four signals as it can be seen combining Fig. 4.2 and (4.1)-(4.9). In a similar way, contributions of $\boldsymbol{P}_{\mathrm{c}}$ and $\boldsymbol{P}_{\mathrm{r}}$ precede to contribution to $\boldsymbol{P}_{\mathrm{d}}$ which is the last "trace" of an EV in the aggregated representation. Furthermore, every EV must contribute to $\boldsymbol{P}_{\mathrm{d}}$, $\boldsymbol{P}_{\mathrm{c}}$ and $\boldsymbol{P}_{\mathrm{r}}$ after it arrived and thus three inputs are derived. The first input $\boldsymbol{P}_{\mathrm{d,to}} = \sum_{j=0}^{k} P_{\mathrm{a}}(j) - P_{\mathrm{d}}(j)$ represents the cumulative power of present EVs at time instant k that are about to depart. Analogly the inputs $\boldsymbol{P}_{\mathrm{c,to}}$ and $\boldsymbol{P}_{\mathrm{r,to}}$ are derived as still expecting contributions to signals $\boldsymbol{P}_{\mathrm{c}}$ and $\boldsymbol{P}_{\mathrm{r}}$, respectively.

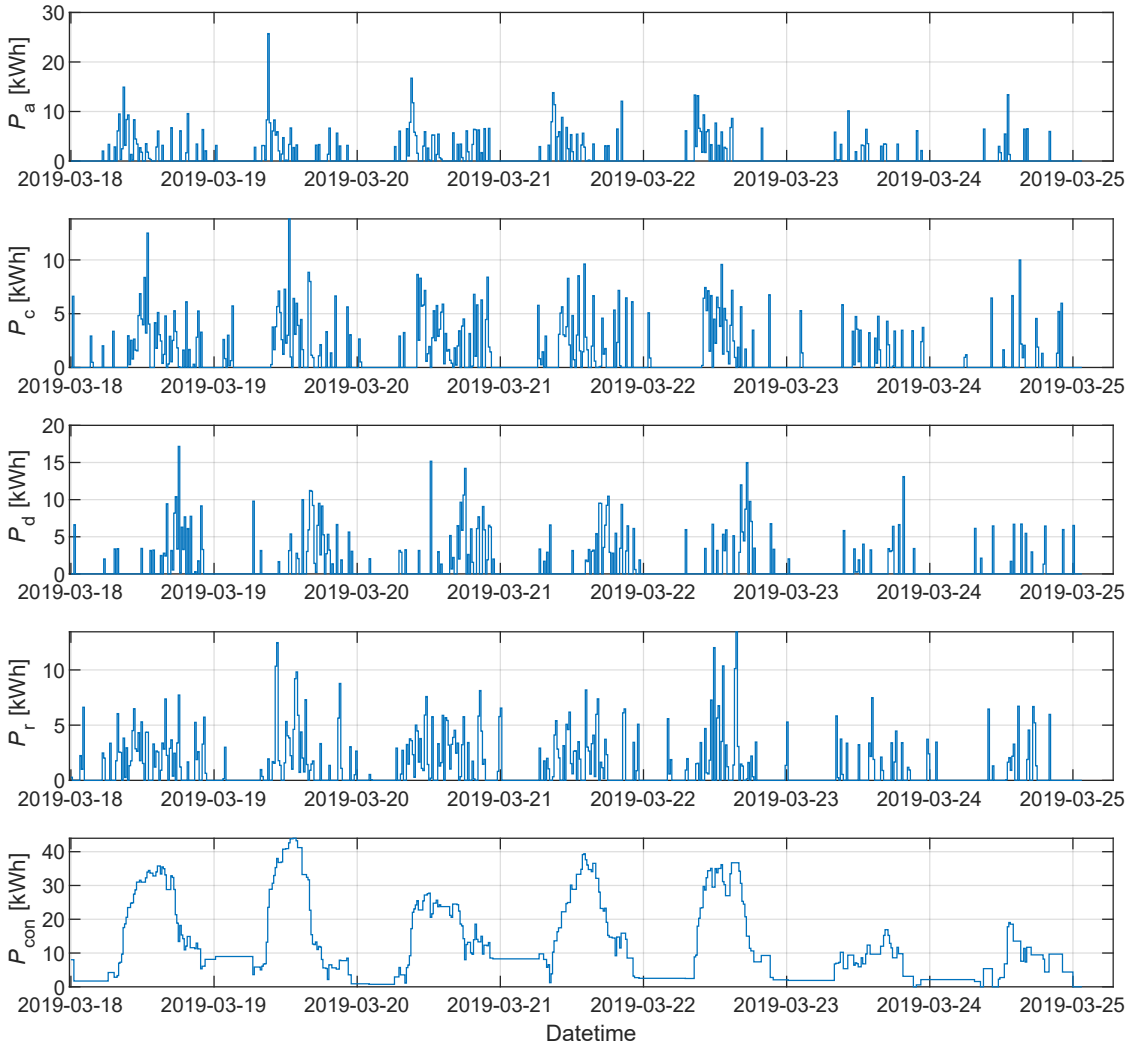

Figure 5.4: Time series $\boldsymbol{P}_{\mathrm{a}}$, $\boldsymbol{P}_{\mathrm{c}}$, $\boldsymbol{P}_{\mathrm{d}}$, $\boldsymbol{P}_{\mathrm{r}}$ and $\boldsymbol{P}_{\mathrm{con}}$ for a selected week period.

As mentioned before, the observed parking lot can be seen as a dynamic system where its state consists of all present EVs with their current phase in charging cycle visualised in Fig. 4.2. It is then reasonable to look for integrative characteristics of all the five signals. The integration interval should not be longer than about 8 hours because it would include EVs that maybe already departed. Integration (summing) intervals of the last 3, 6, 10 and 20 steps (45, 90, 150, 300 min) are proposed to capture different "system dynamics". Furthermore, probability of a departure of any EV and thus capturing it in $\boldsymbol{P}_{\mathrm{d}}$ depends on the number of present EVs. Both number of the present EVs and number of free charging points are used as inputs.

Harmonic and categorical time indices are chosen as inputs for all five models because of noticed daily and weekly patterns as can be seen in Fig. 5.2. The spikes in autocorrelation function in Fig. 5.5. makes justified to include values of certain signal delayed for

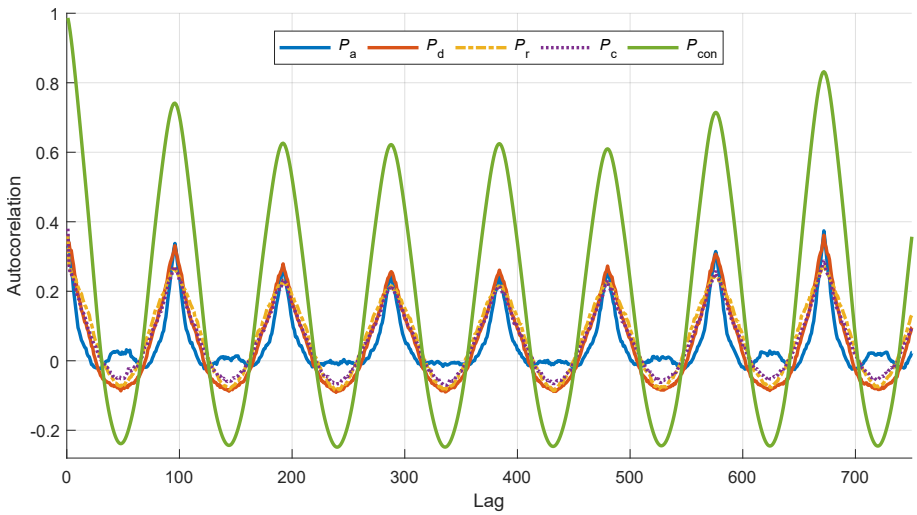

Figure 5.5: Autocorrelation analysis of $\boldsymbol{P}_{\mathrm{a}}$, $\boldsymbol{P}_{\mathrm{f}}$, $\boldsymbol{P}_{\mathrm{c}}$, $\boldsymbol{P}_{\mathrm{r}}$ and $\boldsymbol{P}_{\mathrm{con}}$

one, two and three weeks, as follows:

$$y(k-d), \;\; d \in \left\{ \begin{array}{c} 670, \; \ldots, 674, \\ 1342, \; \ldots, 1346, \\ 2014, \; \ldots, 2018 \end{array} \right\}, \tag{5.1}$$

where y is value of one of the five signals, k is current discrete time instant and d denotes the number of 15 minute time instants used for lagging. Working day indicator is used to more strongly distinguish Saturday and Sunday and to distinguish national holidays at the same time.

Model inputs chosen according to conducted exploratory analysis of the historical data set are shown in Table 5.1.

5.2.3 Baseline

Nature of signal $\boldsymbol{P}_{\mathrm{con}}$ is significantly different than the rest of the signals. It lacks sudden changes and spikes which are frequent in other signals. Two basic statistical methods are chosen as baseline because of the mentioned different natures of the signals. The first baseline is simple persistence that shows better results for $\boldsymbol{P}_{\mathrm{con}}$. The second baseline is time-of-day average of the respective day of week. Under the assumption that EV owners have mostly stable routines for certain days of week and that deviations of arrival and departure times are white noise, the proposed average represents the expectation of the signals.

Table 5.1: List of all model inputs

Input name	Description	$\boldsymbol{P}_{\mathrm{a}}$	$\boldsymbol{P}_{\mathrm{c}}$	$\boldsymbol{P}_{\mathrm{d}}$	$\boldsymbol{P}_{\mathrm{r}}$	$\boldsymbol{P}_{\mathrm{con}}$
Current values of all five signals		✓	✓	✓	✓	✓
Values of $\boldsymbol{P}_{\mathrm{a}}$ for the last day		✓	✓	✓	✓	✓
Values of $\boldsymbol{P}_{\mathrm{c}}$ for the last day			✓	✓		
Values of $\boldsymbol{P}_{\mathrm{d}}$ for the last day				✓		
Values of $\boldsymbol{P}_{\mathrm{r}}$ for the last day				✓	✓	
Values of $\boldsymbol{P}_{\mathrm{con}}$ for the last day						✓
$\boldsymbol{P}_{\mathrm{d,to}}$, $\boldsymbol{P}_{\mathrm{c,to}}$, $\boldsymbol{P}_{\mathrm{r,to}}$	Derived from historical data		✓	✓	✓	✓
Rolling travel time statistics	Maximum, minimum, median and average value of the last 2, 4 and 8 steps. Average of the last 10 working/not-working days	✓	✓	✓	✓	✓
Rolling sum	Sum of the last 3, 6, 10 and 20 values	✓	✓	✓	✓	✓
Delayed values	Values of the same day-of-week and time-of-day for last 3 weeks.	✓	✓	✓	✓	✓
Parking lot status	Number of present EVs and free charging points	✓	✓	✓	✓	✓
Harmonic time indices	Sine and cosine functions of time-of-day, day-of-week, day-of-year	✓	✓	✓	✓	✓
Categorical time indices	Integer variables denoting time-of-day, day-of-week and day-of-year	✓	✓	✓	✓	✓
Working day indicator	Boolean variable denoting if day is weekend or national holiday	✓	✓	✓	✓	✓

5.2.4 Machine learning approaches

Training of models was implemented in Python using the XGBoost [49] and LightGBM libraries [50]. The historical dataset was divided into three parts of which 80% was used as a training set, 10% for hyperparameters validation and 10% as a test set for final prediction performance metrics calculation. Tuning of hyperparameters was conducted using Optuna framework [51]. Optuna is based on Tree-Structured Parzen Estimator (TPE) algorithm [52] that is an iterative process that uses history of evaluated hyperparameters to create probabilistic model, which is used to suggest next set of hyperparameters to evaluate. In comparison with grid search TPE is less time-consuming and is better in finding minimum than randomised search since TPE searches in *informed manner*. All

considered hyperparameters are shown in Table 5.2. while the rest was left at default values.

Table 5.2: Hyperparameter searching space of the XGBoost and LightGBM models.

	Range			Range	
Hyperparameter	XGBoost	LightGBM	Hyperparameter	XGBoost	LightGBM
γ	[0, 10]	/	Column sample by level	[0.5, 1]	/
Max depth	[5, 15]	[0, ∞]	Column sample by node	[0.5, 1]	/
Estimator number	[50, 5000]	[10, $*10^4$]	Regularisation λ	[0.5, 1]	[0, 10]
Min. child weight	[0, 10000]	$[10^{-3}, 50]$	Max number of bins	/	128
Subsample	[0.7, 1]	[0.6, 1]	Column sample by tree	[0.5, 1]	[0.6, 1]
Max. δ step	[0, 1]	/	Number of leaves	/	[2, 32768]
η	[0, 0.3]	/	Min child samples	/	[5, 50]
α	[0, 0.5]	[0, 10]			

As a first step of hyperparameters tuning for the XGBoost, max depth, minimal child weight and η, as the three parameters with strongest influence on model performance [49], were tuned by using simple iterative grid search and intuition. In every iteration grid search had defined 5 different values per parameter. Between two performance dependency on parameters was examined and new 5 values for every parameter were chosen. Per one signal there were between three to five iterations until the parameters were evaluated as final. Then Optuna framework was used to run 100 trials per signal to tune 12 parameters in Table 5.2 with cold start. It is interesting that Optuna's best performances for all the five signals were about 1-2% worse than what eventually was found as final performance. On the other hand, the hyperparameter space with 12 dimensions requires far more than 100 trials. Finally another 50 trials were ran warm started with the parameters values previously found. Optuna then found the final best result, which was expected since it continued to very fine tune all 12 parameters around the new point found. Ten LightGBM hyperparameters were tuned only using Optuna with 100 trials. At first, the upper limit for parameter number of leaves was set to maximum 65536 but it was reduced to a half due to too large memory consumption (16 GB of RAM installed).

Models for prediction on horizons up to 8 steps (2 hours) were also tuned and trained, separate model per every signal and prediction step on the horizon. The inputs of the models are the same for all horizon lengths. The horizon of 2 hours is chosen as appropriate one for the mid-term EV charging schedule optimisation.

Similar utilisation of inputs-features for both models can be seen in Fig. 5.6.

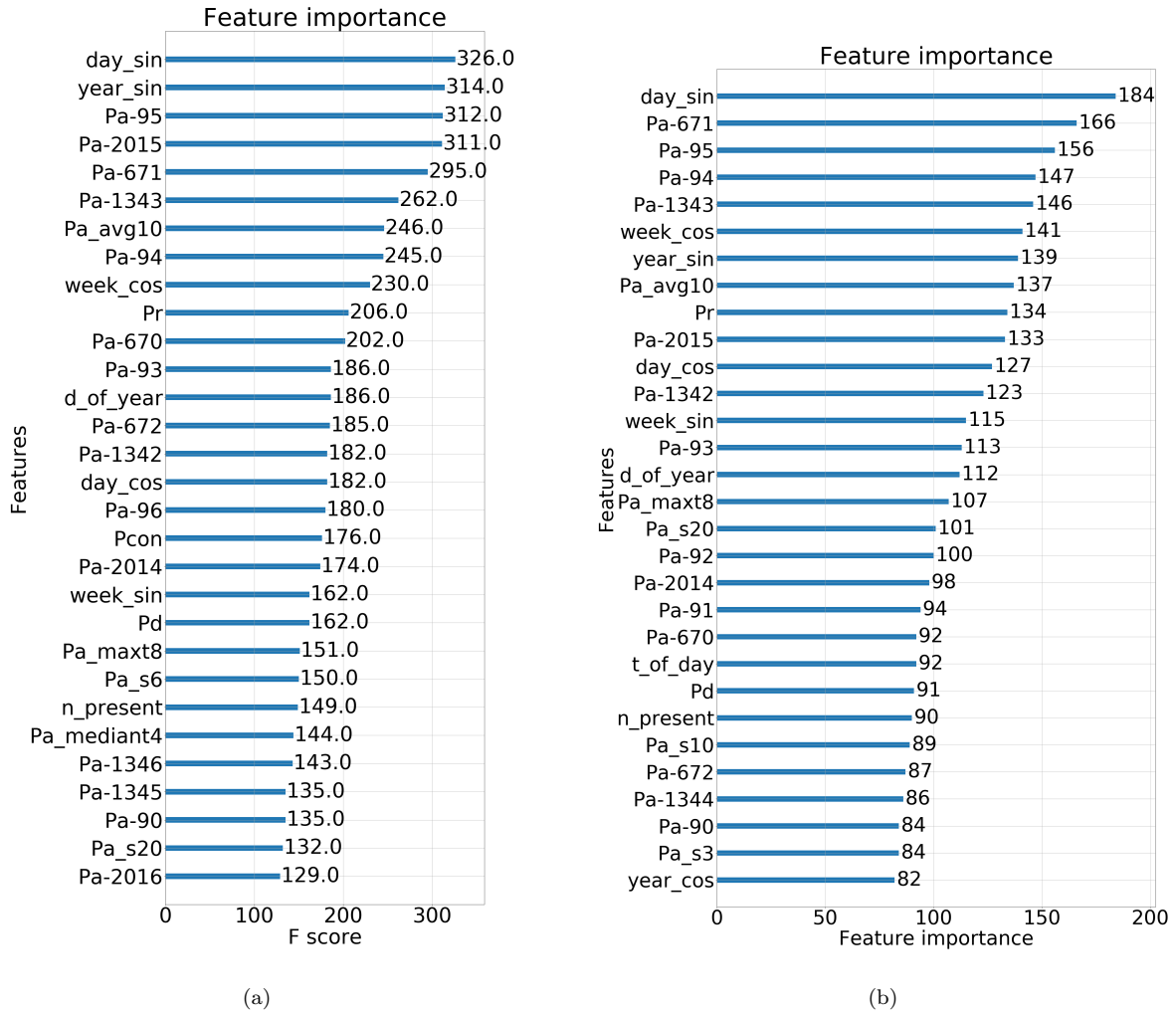

(a) (b)

Figure 5.6: Feature importance of models for $\boldsymbol{P}_{\mathrm{a}}$ one step ahead a) XGBoost, b) LightGBM . [48]

5.3 Evaluation of the obtained forecasting models

5.3.1 Metrics and validation environment

Baseline and forecasting models are compared using mean absolute error (MAE) and root mean square error (RMSE) as the two most commonly used metrics:

$$MAE = \frac{1}{N}\sum_{k=1}^{N}|y_k - \hat{y}_k|, \tag{5.2}$$

$$RMSE = \sqrt{\frac{1}{N}\sum_{k=1}^{N}(y_k - \hat{y}_k)^2}, \tag{5.3}$$

where y_k and $\hat{y}_k$ are true and forecasted values, respectively and N is the number of samples for which the metric is calculated. Mean absolute percentage error (MAPE) cannot be used due to big number of zero elements in the true data which would lead to big relative

errors that would be hard to interpret. Instead a symmetric mean absolute percentage error (SMPAE) is used as follows:

$$SMAPE = \frac{1}{N}\sum_{k=1}^{N}\begin{cases}\frac{|y_k-\hat{y}_k|}{(|y_k|+|\hat{y}_k|)/2}, & if\ |y_k|+|\hat{y}|_k > 0,\\ 0, & otherwise.\end{cases} \tag{5.4}$$

RMSE was used for fitting of all prediction models, with intention to focus on forecasting peak values.

5.3.2 Forecasting results

Final metrics were calculated on predictions made on the test dataset. One step ahead models are compared with both baseline methods in Table 5.3. The worst performance for $\boldsymbol{P}_{\mathrm{a}}$ is expected since it is "truly independent" variable while other signals follow it. Different values of MAE and RMSE of both baselines indicate specific nature of $\boldsymbol{P}_{\mathrm{con}}$. For very short prediction, which is the case in Table 5.3., it is reasonable that persistence performs better than weekday average. Errors of weekday average for $\boldsymbol{P}_{\mathrm{con}}$ are extremely high since the signal is static between arrivals and departures of EVs. The other four signals are "event-based" and thus some error is present around that specific time instant, while one day with more EVs with empty batteries cause grater deviations of $\boldsymbol{P}_{\mathrm{con}}$ from weekday average than from persistence along the whole day.

The performance of $\boldsymbol{P}_{\mathrm{con}}$ significantly decreases along the horizon (Fig. 5.7.), which means it is also focused on persisting the current value of the signal. On the other hand, the performance of the other four signals is quite stable indicating it uses lagged values. In Table 5.3. it can be seen that LightGBM generally outperforms XGBoost.

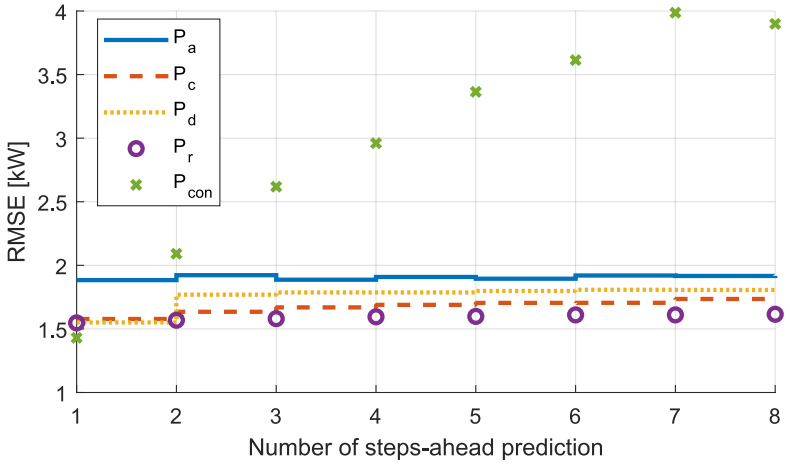

Figure 5.7: RMSE of all LightGBM models.[48]

Table 5.3: 15 minutes (one step) ahead forecast model metric calculated on test dataset.[48]

		Weekday average	Persistence	XGBoost	LightGBM
$\boldsymbol{P}_{\mathrm{a}}$	MAE	1.375	1.120	1.021	**0.976**
	RMSE	2.197	2.785	1.983	**1.88**
	SMAPE	0.426	**0.104**	0.454	0.455
$\boldsymbol{P}_{\mathrm{d}}$	MAE	1.336	1.160	**0.723**	0.975
	RMSE	2.113	2.774	1.613	**1.551**
	SMAPE	0.435	**0.113**	0.428	0.269
$\boldsymbol{P}_{\mathrm{c}}$	MAE	1.318	1.021	0.765	**0.721**
	RMSE	1.955	2.365	1.586	**1.578**
	SMAPE	0.426	**0.117**	0.419	0.281
$\boldsymbol{P}_{\mathrm{r}}$	MAE	1.334	1.063	0.917	**0.879**
	RMSE	1.912	2.316	1.648	**1.547**
	SMAPE	0.418	**0.136**	0.421	0.284
$\boldsymbol{P}_{\mathrm{con}}$	MAE	6.503	0.809	0.807	**0.756**
	RMSE	8.983	1.953	1.557	**1.420**
	SMAPE	0.267	**0.031**	0.163	0.273

5.4 Conclusion

This chapter outlines the application of two state-of-the-art machine learning models, light gradient boosting machine (LightGBM) and extreme gradient boosting machine (XGBoost), for forecasting time-series providing a recently introduced aggregate representation of electrical vehicles present on a parking lot. Prediction horizon is 2 hours with a 15 minute time step. Obtained predictions are compared with week-of-day average and persistence with three different metrics. Both models outperformed the baselines and LightGBM has slightly better results than XGBoost. The introduced predictions are a necessary precondition for application of model predictive control to charging scheduling and demand response for a group of EV chargers on a parking lot.

Chapter 6

General conclusions and future research opportunities

Optimisation of EV charging schedule is a must for the power system today. With volatile production of renewable sources, the demand side of the system should take part in system regulation. Although participation of EVs in demand response is already well explored, this thesis proposed the concept of charging scheduling of an EV population, connected to a set of charging points that are managed by an aggregator, based on innovative aggregated representation of EV population (set). Aggregated representation allows to represent a set of vehicles using five discrete-time vectors that are suitable for prediction using machine learning models for time series prediction. Also, the aggregated representation allows the EV population with a large number of vehicles to be reduced to a smaller one, exactly as it was used for the day-ahead flexibility analysis. The key feature of the aggregated representation is that it preserves information about the flexibility capacity of the population, which was empirically proven in the Chapter 4, showing the daily cost and the optimal reserved power of the reconstructed population match to the optimisation result of the original population with acceptable deviation. Furthermore, the EV population can consist of EVs with any nominal charging power, relative capacity, discrete-time arrival and departure intervals.

Due to a weekly pattern of EV arrivals in the used dataset, the day-ahead analysis of the EV aggregator's demand response capacity was conducted separately for every weekday. Large number of EVs in the expected daily EV population, obtained by summing all EVs in a certain weekday and dividing them with the number of days in data sample, is avoided by applying the aggregated representation to the population which resulted in the reconstructed expected EV population of only 150 EVs. The reasonable number of EVs in the expected daily population is crucial due to computational and memory requirements of the optimisation problem used. The conducted day-ahead flexibility analysis is based

on stochastic worst-case optimisation and offers control over the possible financial loss if the flexibility is not contracted with the power grid operator on day-ahead frequency regulation market. To enable the aggregator can influence the certainty of fulfilling contracted flexibility, chance-constraints and statistical analysis of real-world historical data are applied. The performed analysis showed flexibility capacity of 80 kW for the expected EV population on Monday on a parking lot equipped with 52 EV charging points. During validation of MPC, in which the obtained results were used as the contracted flexibility, it is shown that the aggregator can fulfil flexibility without jeopardising the flexibility contract with the power grid operator.

As the future works remains to transform uncertainty of the aggregated representation of EV population to the uncertainty of the individual EV data. Such transformation would enable the application of the stochastic optimisation methods directly to the individual constraints on EV's state of energy and charging power.

The introduced model predictive control for the charging scheduling of EVs, that are operated by an aggregator, relies on the contracted flexibility from the day-ahead analysis and on individual EV data of the already present EVs and of the predicted ones. The proposed MPC is based on linear stochastic optimisation. Validation conducted both for deterministic and stochastic MPC showed that even with the optimisation horizon of 2 hours the aggregator succeeds to fulfil the contracted flexibility, thus obtaining economical benefits. MPC handles predicted EVs as virtual - without the assigned charging points. After MPC is solved, at the beginning of the next discrete-time interval total charging energy of the predicted EVs is assigned to the EVs arrived during the current interval in which MPC is being solved.

That feature enables usage of predicted EV population reconstructed from predicted aggregated representation that can contain of more EVs than there are free charging points. The prediction of the future EV population in domain of the aggregated representation is obtained using two state-of-the-art machine learning models, light gradient boosting machine (LightGBM) and extreme gradient boosting machine (XGBoost), introduced in Chapter 5. Prediction horizon is 2 hours with a 15 minute time step which correspond to the shortest optimisation horizon of the proposed MPC. Obtained predictions are compared with week-of-day average and persistence with three different metrics. Both models outperformed the baselines and thus can contribute to mitigate uncertainty of the stochastic MPC. In comparison of the two analysed machine learning models, LightGBM has slightly better results than XGBoost.

Every step of the proposed charging scheduling concept is validated on real-world ACN dataset [16] and as the future work it remains to reach further in testing the proposed scheduling concept on other datasets, especially the datasets with other charging point

configurations. Including private household charging points could prolong the interval in which the aggregator offers flexibility. While the used ACN dataset is consistent and EV arrivals are aligned with working hours of the faculty building, different dataset will require further analysis and upgrade of the machine learning models since there are other possible data that influence EV arrivals, such as weather or traffic.

Bibliography

[1]Hadley, S. W., Tsvetkova, A. A., "Potential impacts of plug-in hybrid electric vehicles on regional power generation", The Electricity Journal, Vol. 22, 2009, pp. 56–68, url: https://www.sciencedirect.com/science/article/pii/S104061900900267X

[2]Azadfar, E., Sreeram, V., Harries, D., "The investigation of the major factors influencing plug-in electric vehicle driving patterns and charging behaviour", Renewable and Sustainable Energy Reviews, Vol. 42, 2015, pp. 1065-1076, url: https://www.sciencedirect.com/science/article/pii/S1364032114008831

[3]Babrowski, S., Heinrichs, H., Jochem, P., Fichtner, W., "Load shift potential of electric vehicles in europe", Journal of Power Sources, Vol. 255, 2014, pp. 283–293, url: https://www.sciencedirect.com/science/article/pii/S0378775314000342

[4]Soares, J., Morais, H., Sousa, T., Vale, Z., Faria, P., "Day-ahead resource scheduling including demand response for electric vehicles", IEEE Transactions on Smart Grid, Vol. 4, 2013, pp. 596–605.

[5]Flammini, M. G., Prettico, G., Julea, A., Fulli, G., Mazza, A., Chicco, G., "Statistical characterisation of the real transaction data gathered from electric vehicle charging stations", Electric Power Systems Research, Vol. 166, 2019, pp. 136–150, url: https://www.sciencedirect.com/science/article/pii/S037877961830316X

[6]Borray, A. F. C., Merino, J., Torres, E., Mazón, J., "A review of the population-based and individual-based approaches for electric vehicles in network energy studies", Electric Power Systems Research, Vol. 189, 2020, pp. 106785, url: https://www.sciencedirect.com/science/article/pii/S0378779620305885

[7]Develder, C., Sadeghianpourhamami, N., Strobbe, M., Refa, N., "Quantifying flexibility in ev charging as dr potential: Analysis of two real-world data sets", in 2016 IEEE International Conference on Smart Grid Communications (SmartGridComm). 2016 IEEE International Conference on Smart Grid Communications (SmartGridComm), 2016, pp. 600–605.

[8]Sadeghianpourhamami, N., Refa, N., Strobbe, M., Develder, C., "Quantitive analysis of electric vehicle flexibility: A data-driven approach", International Journal of Electrical Power & Energy Systems, Vol. 95, 2018, pp. 451–462, url: https://www.sciencedirect.com/science/article/pii/S0142061516323687

[9]Gerritsma, M. K., AlSkaif, T. A., Fidder, H. A., van Sark, W. G. J. H. M., "Flexibility of electric vehicle demand: Analysis of measured charging data and simulation for the future", World Electric Vehicle Journal, Vol. 10, 2019, url: https://www.mdpi.com/2032-6653/10/1/14

[10]Alinia, B., Hajiesmaili, M. H., Crespi, N., "Online ev charging scheduling with on-arrival commitment", IEEE Transactions on Intelligent Transportation Systems, Vol. 20, 2019, pp. 4524–4537.

[11]Li, Y., Huang, Y., Zhang, M., "Short-term load forecasting for electric vehicle charging station based on niche immunity lion algorithm and convolutional neural network", Energies, Vol. 11, 2018, url: https://www.mdpi.com/1996-1073/11/5/1253

[12]Zhu, J., Yang, Z., Guo, Y., Zhang, J., Yang, H., "Short-term load forecasting for electric vehicle charging stations based on deep learning approaches", Applied Sciences, Vol. 9, 2019, url: https://www.mdpi.com/2076-3417/9/9/1723

[13]Kovačević, M., Vašak, M., "Aggregated representation of electric vehicles population on charging points for demand response scheduling", IEEE Transactions on Intelligent Transportation Systems, Vol. 24, No. 10, 2023, pp. 10 869-10 880.

[14]Shapiro, A., Dentcheva, D., Ruszczynski, A., Lectures on stochastic programming: modeling and theory. SIAM, 2014.

[15]Kleywegt, A., Shapiro, A., De-Mello, T. H., "The sample average approximation method for stochastic discrete optimization", SIAM Journal on Optimization, Vol. 12, Jan. 2001, pp. 479 -.

[16]Lee, Z. J., Li, Low, S. H., "Acn-data: Analysis and applications of an open ev charging dataset", in Proceedings of the Tenth International Conference on Future Energy Systems, ser. e-Energy '19. Proceedings of the Tenth International Conference on Future Energy Systems, Jun. 2019.

[17]Kovačević, M., Brkić, B., Vašak, M., "Worst-case optimal scheduling and real-time control of a microgrid offering active power reserve", in 2021 23rd International Conference on Process Control (PC). 2021 23rd International Conference on Process Control (PC), 2021, pp. 66–71.

[18](2020) Distribution system tariff, url: https://zakon.poslovna.hr/public/tarifni-sustav-za-distribuciju-elektricne-energije%2C-bez-visine-tarifnih-stavki/409408/zakoni.aspx

[19](2020) Distribution system prices, url: https://www.hep.hr/ods/kupci/poduzetnistvo/tarifne-stavke-cijene-161/161#

[20]Rukavina, F., Vašak, M., "Optimal parameterization of a pv and a battery system add-on for a consumer", in 2020 IEEE 11th International Symposium on Power Electronics for Distributed Generation Systems (PEDG). 2020 IEEE 11th International Symposium on Power Electronics for Distributed Generation Systems (PEDG), 2020, pp. 621–626.

[21]Murphy, J., "Benders, nested benders and stochastic programming: An intuitive introduction", url: https://arxiv.org/abs/1312.3158v1 2013.

[22]Parzen, E., "On Estimation of a Probability Density Function and Mode", The Annals of Mathematical Statistics, Vol. 33, No. 3, 1962, pp. 1065 – 1076, url: https://doi.org/10.1214/aoms/1177704472

[23]Scott, D. W., Multivariate Density Estimation: Theory, Practice, and Visualization, 2nd Edition. John Wiley & Sons, New York, Chicester, 1992.

[24]Python Software Foundation, Python 3.6., 2021, url: https://docs.python.org/3.6/

[25]Numpy 1.22., 2022, url: https://numpy.org/doc/stable/reference/index.html

[26]Scipy 1.8., 2022, url: https://docs.scipy.org/doc/scipy/reference/index.html

[27]IBM Corp., IBM ILOG CPLEX V12.8., 2017, url: https://www.ibm.com/support/pages/cplex-optimization-studio-v128

[28]Zhang, H., Hu, Z., Xu, Z., Song, Y., "Evaluation of achievable vehicle-to-grid capacity using aggregate PEV model", IEEE Transactions on Power Systems, Vol. 32, No. 1, 2017, pp. 784-794.

[29]Cortés Borray, A. F., Merino, J., Torres, E., Garcés, A., Mazón, J., "Centralised coordination of EVs charging and PV active power curtailment over multiple aggregators in low voltage networks", Sustainable Energy, Grids and Networks, Vol. 27, 2021, pp. 100470.

[30]López, K. L., Gagné, C., Gardner, M.-A., "Demand-side management using deep learning for smart charging of electric vehicles", IEEE Transactions on Smart Grid, Vol. 10, No. 3, 2019, pp. 2683-2691.

[31]Amini, M. H., Kargarian, A., Karabasoglu, O., "Arima-based decoupled time series forecasting of electric vehicle charging demand for stochastic power system operation", Electric Power Systems Research, Vol. 140, 2016, pp. 378-390.

[32]Buzna, L., De Falco, P., Ferruzzi, G., Khormali, S., Proto, D., Refa, N., Straka, M., van der Poel, G., "An ensemble methodology for hierarchical probabilistic electric vehicle load forecasting at regular charging stations", Applied Energy, Vol. 283, 2021, pp. 116337.

[33]Frendo, O., Graf, J., Gaertner, N., Stuckenschmidt, H., "Data-driven smart charging for heterogeneous electric vehicle fleets", Energy and AI, Vol. 1, 2020, pp. 100007.

[34]Cadete, E., Alva, R., Zhang, A., Ding, C., Xie, M., Ahmed, S., Jin, Y., "Deep learning tackles temporal predictions on charging loads of electric vehicles", in 2022 IEEE Energy Conversion Congress and Exposition (ECCE), 2022, pp. 1-6.

[35]P Sasidharan, M., Kinattingal, S., Simon, S. P., "Comparative analysis of deep learning models for electric vehicle charging load forecasting", Journal of The Institution of Engineers (India): Series B, Vol. 104, No. 1, Feb 2023, pp. 105-113.

[36]Rathore, H., Meena, H. K., Jain, P., "Prediction of ev energy consumption using random forest and xgboost", in 2023 International Conference on Power Electronics and Energy (ICPEE), 2023, pp. 1-6.

[37]Orzechowski, A., Lugosch, L., Shu, H., Yang, R., Li, W., Meyer, B. H., "A data-driven framework for medium-term electric vehicle charging demand forecasting", Energy and AI, Vol. 14, 2023, pp. 100267.

[38]Zhu, J., Yang, Z., Mourshed, M., Guo, Y., Zhou, Y., Chang, Y., Wei, Y., Feng, S., "Electric vehicle charging load forecasting: A comparative study of deep learning approaches", Energies, Vol. 12, 2019, url: https://www.mdpi.com/1996-1073/12/14/2692

[39]Chung, Y.-W., Khaki, B., Li, T., Chu, C., Gadh, R., "Ensemble machine learning-based algorithm for electric vehicle user behavior prediction", Applied Energy, Vol. 254, 2019, pp. 113732.

[40]Maurici, M. C., Frigola, J. M., "Electric vehicle user profiles for aggregated flexibility planning", in 2021 IEEE PES Innovative Smart Grid Technologies Europe (ISGT Europe), 2021, pp. 1-5.

[41]Helmus, J. R., Lees, M. H., van den Hoed, R., “A data driven typology of electric vehicle user types and charging sessions”, Transportation Research Part C: Emerging Technologies, Vol. 115, 2020, pp. 102637.

[42]Hu, L., Dong, J., Lin, Z., “Modeling charging behavior of battery electric vehicle drivers: A cumulative prospect theory based approach”, Transportation Research Part C: Emerging Technologies, Vol. 102, 2019, pp. 474-489.

[43]Shahriar, S., Al-Ali, A. R., Osman, A. H., Dhou, S., Nijim, M., “Machine learning approaches for EV charging behavior: A review”, IEEE Access, Vol. 8, 2020, pp. 168 980-168 993.

[44]Frendo, O., Gaertner, N., Stuckenschmidt, H., “Improving smart charging prioritization by predicting electric vehicle departure time”, IEEE Transactions on Intelligent Transportation Systems, Vol. 22, No. 10, 2021, pp. 6646-6653.

[45]Shwartz-Ziv, R., Armon, A., “Tabular data: Deep learning is not all you need”, Information Fusion, Vol. 81, 2022, pp. 84-90.

[46]Sortomme, E., El-Sharkawi, M. A., “Optimal scheduling of vehicle-to-grid energy and ancillary services”, IEEE Transactions on Smart Grid, Vol. 3, 2012, pp. 351–359.

[47]Li, Y., He, S., Li, Y., Ge, L., Lou, S., Zeng, Z., “Probabilistic charging power forecast of evcs: Reinforcement learning assisted deep learning approach”, IEEE Transactions on Intelligent Vehicles, Vol. 8, No. 1, 2023, pp. 344-357.

[48]Kovačević, M., Novak, H., Vašak, M., “Prediction of aggregated ev representation using xgboost and lightgbm”, in 58th International Universities Power Engineering Conference (UPEC23). 58th International Universities Power Engineering Conference (UPEC23), 2023.

[49]“XGBoost Documentation”, url: https://xgboost.readthedocs.io/en/stable/index.html# (Date last accessed 18-May-2023).

[50]“LightGBM Documentation”, url: https:https://lightgbm.readthedocs.io/en/v3.3.2/ (Date last accessed 2-June-2023).

[51]Akiba, T., Sano, S., Yanase, T., Ohta, T., Koyama, M., “Optuna: A next-generation hyperparameter optimization framework”, in Proceedings of the 25th ACM SIGKDD International Conference on Knowledge Discovery and Data Mining, 2019.

[52]Watanabe, S., “Tree-structured parzen estimator: Understanding its algorithm components and their roles for better empirical performance”, arXiv, 2023, doi: 10.1109/TITS.2023.3286012.

Biography

Marko Kovačević was born in 1994 in Zagreb, Croatia. In 2013 he enrolled in Electrical Engineering and Information Technology study programme at University of Zagreb Faculty of Electrical Engineering and Computing (UNIZGFER). He finished his bachelor's degree in Control Engineering and Automation in 2016. In 2019 he obtained master's degree in the same field under the supervision of Prof. Zdenko Kovačić. In 2018 he starts to work at ABB Ltd in Zagreb. In 2019 he starts to work at UNIZGFER as a research assistant within the Department of Control and Computer Engineering and starts his PhD studies under the supervision of Prof. Mario Vašak, as part of Young Researchers' Career Development Project – Training New Doctoral Students, financed by the Croatian Science Foundation (HRZZ). At same time he was part of UNIZGFER team working on the project Development of a System for Predictive Control and Autonomous Trading of Energy in Buildings (PC-ATE Buildings) focused on production and commercialisation of services for predictive control of energy in buildings connected to energy grids and subject to dynamic energy market conditions.

He is a member of the Laboratory for Renewable Energy Systems (LARES). He has 4 years of research and development experience in the smart microgrid energy and building management via predictive control which resulted in 7 research articles in international scientific journals and on international scientific conferences.

List of publications

Journal papers

1.Kovačević, M., Vašak, M., "Aggregated Representation of Electric Vehicles Population on Charging Points for Demand Response Scheduling", *IEEE transactions on intelligent transportation systems*, Vol. 24, No. 10, 2023, pp. 10869-10880, doi: 10.1109/tits.2023.3286012

2.Vašak, M., Banjac, A., Hure, N., Novak, H., Kovačević, M., "Predictive control based assessment of building demand flexibility in fixed time windows",*Applied energy*, 329 (2023) 120244, 17 .doi: 10.1016/j.apenergy.2022.120244

Conference papers

1.Kovačević, M., Novak. H, Vašak, M., "Prediction of aggregated EV representation using XGBoost and LightGBM", *Proceedings of the 58th International Universities Power Engineering Conference*, 2023.

2.Vašak, M., Hure, N., Kovačević, M., "Optimal day-ahead operation scheduling of a one-pipe heating system", *Proceedings of the 8th International Conference on Control, Decision and Information Technologies*, 2022., pp. 443-450, doi:10.1109/CoDIT55151.2022.9803885

3.Kovačević, M., Kovačić, Z., "A Method of Positioning a Humanoid Robot Relative to the Center of a Group of People—Analysis and Implementation" , *Proceedings of KES International Symposium on Agent and Multi-Agent Systems: Technologies and Applications*, Springer Nature, 2023., pp. 27-39, doi:10.1007/978-981-99-3068-5_3

4.Kovačević, M., Brkić, B., Vašak, M., "Worst-case optimal scheduling and real-time control of a microgrid offering active power reserve", *Proceedings of the 23rd IEEE International Conference on Process Control (PC)*, 2021., pp. 66-71, doi:10.1109/PC52310.2021.9447502

5.Kovačević, M., Marušić, D., Vašak, M., "Price-optimal Electrical and Thermal Energy Flow Control within Microgrid – Smart Grid Interaction", *Proceedings of the 11th IEEE International Symposium on Power Electronics for Distributed Generation Systems (PEDG)*, 2020., pp. 247-252, doi:10.1109/PEDG48541.2020.9244397

Životopis

Marko Kovačević rođen je 1994. godine u Zagrebu, Hrvatska. Godine 2013. upisuje studij Elektrotehnike i informacijskih tehnologija na Fakultetu elektrotehnike i računarstva Sveučilišta u Zagrebu (UNIZGFER). Završio je prvostupnički studij 2016. godine te magistrirao u istom području pod mentorstvom prof. dr. sc. Zdenka Kovačića. Zapošljava u ABB d.o.o. u Zagrebu 2018. godine. Godine 2019. zapošljava se na UNIZGFER-u kao asistent u okviru Zavoda za automatiku i računalno inženjerstvo te započinje doktorski studij pod mentorstvom prof. dr. sc. Marija Vašaka, u sklopu Projekta razvoja karijera mladih istraživača - izobrazba novih doktora znanosti, financiran od strane Hrvatske zaklade za znanost (HRZZ). Istovremeno je bio dio tima UNIZGFER-a koji je radio na projektu Razvoj sustava za prediktivno upravljanje i autonomno trgovanje energijom u zgradi (PC-ATE Buildings) usmjerenom na proizvodnju i komercijalizaciju usluga prediktivnog upravljanja energijom u zgradama priključenim na energetski sustav podložnima dinamičnim uvjetima tržišta energije.

Član je Laboratorija za sustave obnovljivih izvora energije (LARES). Kroz istraživački rad sakupio je 4 godine iskustva u istraživanju i razvoju pametne električne mikromreže i upravljanja zgradama putem prediktivnih algoritama što je rezultiralo sa 7 istraživačkih članaka u međunarodnim znanstvenim časopisima i na međunarodnim znanstvenim konferencijama.